ISSUED
2006/04/28

PC-000529
Revision 0

ADVANCED GAS REACTOR FUEL DEVELOPMENT AND QUALIFICATION PROGRAM

HFR-B1 FINAL SUMMARY REPORT

Prepared under
Idaho Operations Office
Contract No. DE-AC07-03ID14488
For the U.S. Department of Energy

Project 30192

GENERAL ATOMICS

GENERAL ATOMICS

GA 2175 (1199E)

PROJECT CONTROL ISSUE SUMMARY

	DOC. CODE	PROJECT	DOCUMENT NO.	REV.
	TPN	30192	PC-000529	0

TITLE: HFR-B1 Final Summary Report

CM APPROVAL/ DATE	REV.	PREPARED BY	APPROVALS		REVISION DESCRIPTION/ W.O. NO.
			RESOURCE/ SUPPORT	PROJECT	
7 ISSUED APR 2 8 2006	0	D. L. Hanson D Hanson	J. J. Saurwein V. Nicolayeff	A. S. Shenoy A. S. Shenoy	Initial Issue 30192.006..25000

* SEE LIST OF EFFECTIVE PAGES

☐ GA PROPRIETARY INFORMATION

☒ NO GA PROPRIETARY INFORMATION

LIST OF EFFECTIVE PAGES

Page Number	Number of Pages	Revision
i through ix	9	0
1 through 120	123	0
Back Cover	1	
Total No. of Pages:	133	

TABLE OF CONTENTS

LIST OF FIGURES

LIST OF TABLES

ACRONYMS AND ABBREVIATIONS

ACRONYMS AND ABBREVIATIONS

AGR	Advanced Gas Reactor [He-cooled]
AGRFDQP	Advanced Gas Reactor Fuel Development and Qualification Program
AVR	Arbeitsgemeinschaft Versuchs Reactor
BEST	Brennelementsegment
DDN	Design Data Need
DOE	[U.S.] Department of Energy
Dtf	designed-to-fail
ECN	Energieonderzoek Centrum Nederland [Energy Research Centre, Netherlands]
EFPD	effective full power days
EOL	end-of-life
FIMA	fissions per initial metal atom (a measure of burnup in nuclear fuel)
FP	fission product
FRG	Federal Republic of Germany
FZJ	Forschungszentrum Juelich [German national laboratory; formerly KFA]
GA	General Atomics
GC	gas chromatograph
GCR	gas-cooled reactor
GT-MHR	Gas Turbine-Modular Helium Reactor
HFIR	High Flux Isotope Reactor
HFR	High Flux Reactor [Petten]
HTGR	High-Temperature Gas-Cooled Reactor
HTR	high-temperature reactor
IAEA	International Atomic Energy Agency
JRC	Joint Research Center [Petten]
KFA	Kernforschungsanlage Juelich [former German national laboratory, now FZJ]
LEU	low enriched uranium [<20% U-235]
MCA	multichannel analysis
MHTGR	Modular High-Temperature Gas-Cooled Reactor
NE	Nuclear Energy

ORNL	Oak Ridge National Laboratory
PIE	postirradiation examination
QA	quality assurance
QC	quality control
R/B	release rate-to-birth rate ratio
RN	radionuclide
SPN	self-powered neutron [detector]
TC	thermocouple
TRISO	TRi-ISOtropic coated-fuel particle design with three materials in coating system (low-density PyC, high-density PyC, and SiC)
UCO	a mixture of UO_2 and UC_2
VDU	vertical displacement unit
VHTR	Very High Temperature Reactor

1 SUMMARY

The Advanced Gas Reactor (AGR) fuel development program work scope includes reexamination of previously generated experimental data to determine their further utility for meeting certain fuel and fission product Design Data Needs (DDNs). A leading candidate for further evaluation and use is the High Flux Reactor (HFR)-B1 experiment. Because of this interest, the AGR program has funded the preparation of this final summary report for the HFR-B1 test.

In addition to supplying experimental data that could partially satisfy certain fission product transport DDNs, the HFR-B1 experiment can provide valuable "lessons learned" to guide in the design of several planned AGR irradiation experiments that have test objectives closely related to those for HFR-B1.

The HFR-B1 test was irradiated in HFR Petten in the Netherlands under the former U.S./Federal Republic of Germany (FRG) Umbrella Agreement for Cooperation in Gas-Cooled Reactor Development. The test contained three independent "capsules," each with different test objectives. HFR-B1 produced a wealth of data about fission product release from low enriched uranium (LEU) UCO fuel particles under both dry and hydrolyzing conditions. The primary source of data for the Capsules 2 and 3 experiments was the online fission gas release measurements that were made during the irradiation phase of the experiment. In contrast, the primary source of data for the Capsule 1 experiment was the planned postirradiation examination.

The HFR-B1 test was technically complex, programmatically challenging, excessively time-consuming, and largely successful. The time from its initial conception in 1983 to the last data evaluation completed in 1995 spanned more than a decade (and, unfortunately, included prolonged periods of inactivity that led to data loss). The actual timeline for the HFR-B1 test program is summarized in Table 1-1. Because of these factors, at least 40 formal documents regarding the HFR-B1 test have been issued by various participating organizations, and these documents, both programmatic and technical, cite dozens of additional subordinate documents. Given the value of the experimental data and the diffuse nature of the test documentation, it was judged prudent to prepare this summary report that describes the HFR-B1 test and the essential results and provides a comprehensive bibliography in the anticipation that ongoing High-Temperature Gas-Cooled Reactor (HTGR) programs could benefit from further evaluation and utilization of these data.

The test rig consisted of three capsules; each was individually monitored and temperature-controlled throughout the test. Each capsule contained 12 fuel compacts housed in an H-451 graphite body. The fuel particle types were TRISO-coated LEU UCO fissile and TRISO ThO_2 fertile in both compacts and unbonded form. A known percentage (8.9%) of "designed-to-fail"

(dtf) UCO particles (thin PyC seal coat on a UCO kernel) was incorporated into each fuel compact to provide a well-defined source of released fission products during irradiation. One capsule had timed injections of moisture at several points during irradiation so that graphite oxidation and fuel hydrolysis and its effect on fission gas release could be measured. Piggyback samples included in the fuel bodies consisted of unbonded fuel particles from the same batches of particles used in the compacts, encapsulated intact and laser-failed particle assemblies, and various non-fueled samples.

The purpose of the Capsule 1 experiment was to obtain information about the transport of metallic fission products (Ag-110m, Cs-134/-137, Sr-90, etc.) in 20%-enriched UCO fuel particles contained in a prismatic fuel element. Consequently, the primary data source for the Capsule 1 experiment was necessarily the postirradiation examination (PIE) because the transport of these condensable radionuclides (RNs) can not be measured online during the irradiation.

The online, fission gas release measurements made during the irradiation provided a wealth of data about the effects of water vapor and temperature changes on the fission gas release rates from failed LEU UCO particles. Water vapor will react with exposed UCO kernels and cause a significant transient increase in the fission gas release rates, including the release rates of radiologically important iodine isotopes. The effect of hydrolysis on fission gas release from exposed kernels is largely reversible after the water is eliminated. Large temperature increases under dry conditions also result in a transient release of stored fission gases, which has been termed an “enhanced” release. After a period of time, this enhanced release diminishes, and a new steady-state release rate is established.

The fuel hydrolysis data from Capsule 3 have been extensively analyzed and used for model development. However, the fission gas release data from Capsules 1 and 2 have not been quantitatively assessed. These data were evaluated in preparing this report and judged to have substantial value for development of improved fission gas release models. Consequently, the data from Capsule 1 (burnup effects) and Capsule 2 (temperature effects) should be further analyzed; this analysis would include a quantitative comparison of the predicted gas release with the reference release models for the as-run test conditions to the measured gas release data. These results, in combination with the other existing UCO gas release data, should be used to upgrade the reference gas release models for LEU UCO particles as appropriate.

A postirradiation examination of Capsule 1 was initiated in the KFA Juelich (now FZJ) hot cells in 1993 under subcontract from Oak Ridge National Laboratory (ORNL) but was not completed as a consequence of the U.S. HTGR program being cancelled in August 1995. An effort was made in 2004 to recover all of the available PIE data, and a determination was made that a number of critical PIE tasks had not been completed. In addition, all potential Ag-110m data had been lost because of the protracted delay between the end of the irradiation and the start of

the PIE. Based upon that assessment, further evaluation of the partial PIE data about fission metal release from Capsule 1 does not appear justified.

The HFR-B1 experiment has provided the following major "lessons learned" that should be factored into the design of the planned AGR-3, AGR-4, and AGR-8 irradiation experiments which have test objectives closely related to those for HFR-B1.

- A well-defined fission product source is essential to characterize fission product transport in core materials. "Designed-to-fail" particles serve that purpose well.
- A complete mass balance for each capsule is essential to characterize fission product transport in core materials.
- A simple, one-dimensional test geometry is needed to characterize the transport of volatile fission metals in core materials.
- A timely, well-planned PIE will be essential for the success of the AGR fission product release experiments.

TABLE 1-1
TIMELINE FOR HFR-B1 TEST PROGRAM

Activity	Date
Discussions of possible test of U.S. fuel in HFR Petten	1982-1983
HFR-B1 test specification (initial issue) issued	May 1984
Formal proposal for HFR-B1 test issued	October 1984
HFR-B1 preirradiation report issued	August 1985
HFR-B1 test specification (final revision) issued	September 1986
Irradiation in HFR Petten begins	April 1987
HFR-B1 PIE plan (initial issue) issued	March 1989
Irradiation in HFR Petten complete	July 1989
German HTR program cancelled	Summer 1989
Capsules prepared for shipment to KFA	November, 1989
Capsules 1, 2 and 3 received at KFA for PIE	December, 1990
PIE plan for Capsules 1, 2, and 3 (ORNL revision) issued	November 1991
Decision made to perform Capsule 1 PIE at KFA	Early 1993
Plan for Capsule 1 PIE at FZJ issued	November 1993
HFR-B1 operating history report issued	September 1994
Capsules 2 and 3 PIE status report issued	September 1994
Closeout of U.S. HTGR program initiated	August 1995
Last test evaluation report issued (ORNL)	September 1995
Last Capsule 1 PIE progress report issued by FZJ	October 1995
Data recovery and evaluation of Capsule 1 PIE	May 2004
Final summary report issued (this document)	April 2006

2 INTRODUCTION AND BACKGROUND

There is a need to validate the design methods used to predict fission product (FP) source terms for HTGRs during normal operation and postulated accidents. To that end, various technology development programs have been conducted internationally during the past three decades to generate test data that can be used to assess the predictive accuracy of these design methods. Such work scope is included in the ongoing, Department of Energy (DOE)-sponsored, Advanced Gas Reactor Fuel Development and Qualification Program (AGRFDQP 2005).

The primary emphasis of the AGRFDQP is to develop new experimental data. However, in recognition of the considerable time and expense required to conduct nuclear research and development (R&D), the program work scope also includes reexamination of previously generated experimental data to determine their further utility for meeting certain fuel and fission product DDNs. A leading candidate for further evaluation and use is the HFR-B1 experiment. Because of this interest, the AGRFDQP has funded the preparation of this final summary report for the test.

In addition to supplying experimental data that satisfy certain FP transport DDNs, the HFR-B1 experiment can provide valuable "lessons learned" to guide in the design of several planned Advanced Gas Reactor (AGR) irradiation experiments (*viz*., AGR-3, AGR-4, and AGR-8) that have test objectives closely related to those for HFR-B1 (Hanson 2005).

2.1 Purpose

The purpose of this report is to summarize the extensive fission product transport data generated by the HFR-B1 test. HFR-B1 was an in-pile test that was irradiated in HFR Petten in the Netherlands under the former U.S./FRG Umbrella Agreement for Cooperation in Gas-Cooled Reactor Development. The overall objective of the test was to characterize fission product release from HTGR cores under normal operating conditions and postulated core heat-up accidents. The HFR-B1 test contained three independent "capsules,"[1] each with specific test objectives. The test yielded a wealth of data about fission product release from LEU, TRISO-coated UCO fuel particles under conditions representative of a modular HTGR core with prismatic fuel elements.

[1] In previous U.S. HTGR fuel irradiation tests, the term "cell" was traditionally used instead of "capsule" because the latter was used to refer to the overall experimental assembly that typically contained one or more "cells." However, since all of the extensive HFR-B1 literature uses the term "capsule" to refer to the three individual units within the overall experimental rig, "capsule" is used exclusively herein. In any case, the AGRFDQP has also chosen to use the term "capsule" instead of the traditional "cell" for the individual units within a "test train" for the planned AGR irradiation experiments.

The HFR-B1 test was technically complex, programmatically challenging, excessively time-consuming, and largely successful. The time from its initial conception in 1983 to the last data evaluation completed in 1995 spanned more than a decade (and, unfortunately, included prolonged periods of inactivity that led to data loss). Because of these factors, at least 40 formal documents regarding the HFR-B1 test have been issued by the various participating organizations, and these documents, both programmatic and technical, cite dozens of additional subordinate documents. Given the value of the experimental data and the diffuse nature of the test documentation, it was judged prudent to prepare a summary report describing the HFR-B1 test and essential results and providing a comprehensive bibliography in the anticipation that ongoing HTGR programs will benefit from further evaluation and utilization of these data.

2.2 Radionuclide Release from HTGR Cores

There is a renewed international interest in AGR designs, based upon HTGR technology, to contribute to the resolution of key national and international issues. For example, among the Generation IV concepts, the helium-cooled Very High Temperature Reactor (VHTR) is the nearest-term system (estimated to be deployable before 2020) capable of producing nuclear hydrogen and/or high-efficiency electricity (Gen-IV 2002). The direct-cycle Gas Turbine-Modular Helium Reactor (GT-MHR) is already being developed under a joint U.S. DOE/MINATOM program for the purpose of destroying surplus Russian weapons plutonium (GT-MHR 1997). Moreover, the GT-MHR with a modified core design is also being evaluated as an efficient burner of transuranic materials. The primary benefit of the so-called Deep-Burn MHR would be to significantly reduce the long-term storage requirements for high-level waste generated by the currently operating light-water reactors around the world (Venneri 2001).

For each of these applications, suitable design methods for predicting radionuclide source terms used for reactor design and licensing must be developed and ultimately validated. The following section provides a summary description of the context in which the HFR-B1 test data have been and will be utilized for that purpose.

2.2.1 Radionuclide Release from HTGR Cores

A fundamental requirement in the design of any nuclear power plant is the containment and control of the radionuclides produced by the nuclear reactions during normal plant operation and a broad spectrum of postulated accidents. In response, different radionuclide containment systems have been designed and employed for different reactor designs. For modular HTGR designs, a hallmark philosophy has been adopted since the early 1980s to design the plant such that the radionuclides would be retained in the core during normal operation and postulated accidents (PSID 1992). The key to achieving this safety goal is the reliance upon ceramic-coated fuel particles for primary fission product containment at their source, along with

passive cooling to assure that the integrity of the coated particles is maintained even if the normal cooling systems were permanently disrupted.

2.2.2 Radionuclide Containment System

The radionuclide containment system for an HTGR is comprised of multiple barriers to limit radionuclide release from the core to the environment to insignificant levels during normal operation and a spectrum of postulated accidents (PSID 1992). As shown schematically in Fig. 2-1, the five principal release barriers are: (1) the fuel kernel; (2) the particle coatings, particularly the SiC coating; (3) the fuel element structural graphite; (4) the primary coolant pressure boundary; and (5) the reactor building/containment structure. The effectiveness of these individual barriers in containing radionuclides depends upon a number of fundamental factors, including the chemistry and half-lives of the various radionuclides, the service conditions, and irradiation effects. The effectiveness of these release barriers is also event-specific. The performance of the first three barriers is addressed in the HFR-B1 test, and they are described in greater detail below.

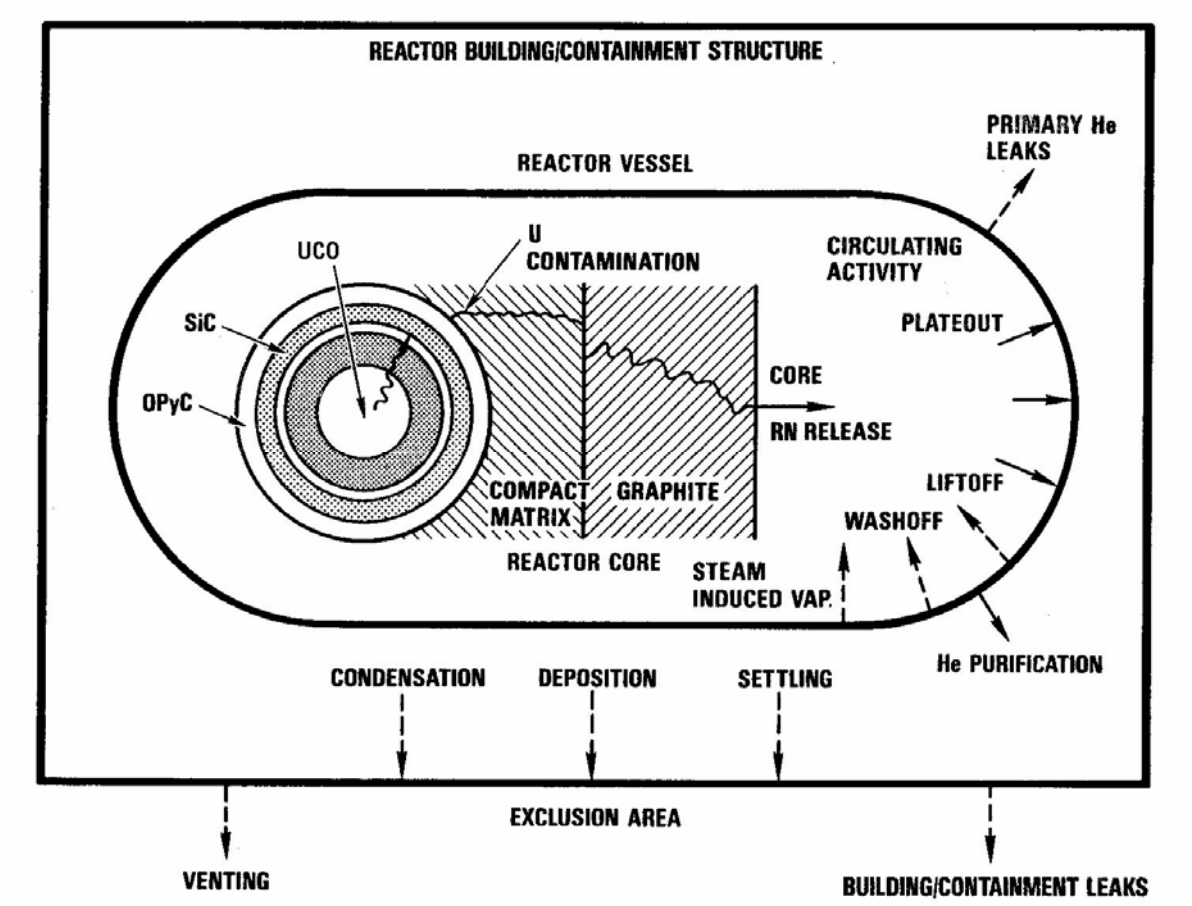

Fig. 2-1. MHR radionuclide containment system

The first barrier to fission product release is the fuel kernel itself. Under normal operating conditions, the kernel retains >95% of the radiologically important, short-lived fission gases such as Kr-88 and I-131. However, the effectiveness of a UCO kernel for retaining gases can be reduced at elevated temperatures or if an exposed kernel is hydrolyzed by reaction with trace amounts of water vapor that may be present in the helium coolant (a major topic addressed in HFR-B1). The retentivity of oxidic fuel kernels for long-lived, volatile fission metals such as Cs, Ag, and Sr is strongly dependent upon the temperature and the burnup.

The second and most important barrier to fission product release from the core is the silicon carbide (SiC) and pyrocarbon (PyC) coatings of each fuel particle. Both the SiC and PyC coatings provide a barrier to the release of fission gases. The SiC coating acts as the primary barrier to the release of metallic fission products because of the low solubilities and diffusion coefficients of fission metals in SiC. The PyC coatings are partially retentive of Cs at lower temperatures but provide little holdup of Ag and Sr.

With a prismatic core, the fuel-compact matrix and the graphite fuel block collectively are the third release barrier. The fuel-compact matrix is relatively porous and provides little holdup of the fission gases that are released from the fuel particles. However, the matrix is a composite material that has a high content of amorphous carbon, and this constituent of the matrix is highly sorptive of metallic fission products, especially Sr. While the matrix is highly sorptive of metals, it provides little diffusional resistance to the release of fission metals because of its high interconnected porosity.

The fuel element graphite, which is denser and has a more ordered structure than the fuel-compact matrix, is somewhat less sorptive of the fission metals than the matrix, but it is much more effective as a diffusion barrier than the latter. The effectiveness of the graphite as a release barrier decreases as the temperature increases. Under typical core conditions, the fuel element graphite attenuates the release of Cs from the core by an order of magnitude, and Sr and the actinides are essentially completely retained. The extent to which the graphite attenuates Ag release is not well characterized, and there is some evidence that the retention of Ag by graphite increases as the total system pressure increases (implying gas-phase transport through the interconnected pore structure of the graphite).

Typically, the two dominant sources of fission product release from the core are as-manufactured, heavy-metal contamination (i.e., heavy metal outside the coated particles), and particles whose coatings are defective or fail in service. In addition, the volatile metals (e.g., Cs, Ag, Sr) can, at sufficiently high temperatures for sufficiently long times, diffuse through the SiC coating and be released from intact TRISO particles; however, diffusive release from intact particles during normal operation is only significant compared with other sources for silver release. Fission products resulting from fissions in heavy-metal contamination outside of the particles are obviously not attenuated by the kernels or coatings, nor are the fission products

produced in the kernels of failed particles appreciably attenuated by the failed coatings. In these cases, the fission product release must be controlled by limiting the respective sources and by the fuel element graphite in the case of the fission metals and actinides.

2.3 Design Methods for Predicting Radionuclide Release

A number of different phenomenological models and associated computer codes have been developed internationally to predict fuel performance and radionuclide release from HTGR cores. Typically, the utility of the more sophisticated models has been limited by unavailability and/or unreliability of the material property data required as input to these codes. The HFR-B1 test was designed to provide material property data and the technological basis for developing improved component models for those computer codes that predict fission product release from prismatic cores. The U.S. computer codes used for that purpose are listed below.

2.3.1 Computer Codes

SURVEY (Pfremmer 2002): An analytical/finite-difference, core-survey code that calculates the steady state, full-core, fuel particle failure, and the full-core fission gas releases rates. An automatic interface with the core physics codes provides burnup, fast fluence, and temperature distributions. Similarly, the temperature and fuel failure distributions calculated by SURVEY are passed on to the metallic release code TRAFIC.

SURVEY/HYDROBURN (Pfremmer 2002): An optional subroutine in SURVEY that calculates the corrosion of fuel element graphite and the hydrolysis of failed fuel particles by coolant impurities, particularly water vapor. Transport of water vapor through the graphite web of the fuel element is modeled as a combination of diffusion and convection due to cross-block pressure gradients. The effects of catalysts and burnoff on the graphite corrosion kinetics are modeled.

TRAFIC-FD (Tzung 1992a): A core-survey code for calculating the full-core release of metallic fission products and actinides. TRAFIC is a finite-difference solution to the transient diffusion equation for multi-hole fuel element geometry with a convective boundary condition at the coolant hole surface. The effect of fluence on graphite sorptivity is modeled explicitly. The temperature and failure distributions required as input are supplied by an automatic interface with the SURVEY code.

COPAR-FD (Tzung 1992b): A stand-alone code as well as a subroutine in the TRAFIC-FD code that calculates the transient fission product release from failed and intact coated particles with burnup-dependent kernel diffusivities. COPAR-FD is a finite-difference solution to the transient diffusion equation for multi-region spherical geometry and with arbitrary temperature and failure histories.

SORS (Cadwallader 1993): A core-survey code for calculating the transient releases of gaseous and metallic fission products. The code is used extensively for the analysis of core conduction cooldown transients. The transient core temperature distributions required as input are supplied by an automatic interface with a suitable, transient thermal analysis code, such as SINDA/FLUENT. SORS uses the same material property correlations that are used by the SURVEY code for normal operation but uses a fuel performance model that was specifically developed for core conduction cooldown conditions.

2.3.2 Phenomenological Models and Material Property Data

The phenomenological models and attendant material property data used in calculating fuel performance and radionuclide release from HTGR cores have been catalogued by several different authors. The most recent and comprehensive compilation is IAEA TECDOC-978 (1997). The primary strength of TECDOC-978 is its comprehensiveness under one cover, including an impressive bibliography. Its principal weakness is that it is fundamentally a data compilation report with little evaluation and few recommendations.

The models used at GA to describe fuel performance and fission product transport are contained and controlled in the Fuel Design Data Manual, Issue F (FDDM/F) (Myers 1987). FDDM/F is a GA proprietary document, but the transport models and material property correlations contained therein are readily available in the review report prepared by Martin (1993) at ORNL.

2.4 Utilization of the Data from HFR-B1

Despite four decades of international development, the current design methods for predicting HTGR source terms are characterized by excessively large uncertainties. Consequently, additional technology development will be necessary to reduce these uncertainties to prescribed limits for a given design application. On the DOE-funded MHTGR program in the mid-1980s, a formal methodology was developed for identifying technology development needs. Historically on U.S. HTGR programs, these technology development needs have been referred to as “Design Data Needs” (DDNs) (GT-MHR DDNs 1996). A number of these DDNs are related to fission product release from the core. In general, two types of tests are needed to satisfy these FP transport DDNs: (1) single-effects tests to generate differential data for deriving improved component models and material property data correlations to upgrade the current design methods and (2) independent integral tests to confirm the validity of the upgraded design methods.

The HFR-B1 test was designed to be a single-effects test to generate differential data for deriving improved component models for predicting fission product release from prismatic HTGR cores. The test was designed to address the FP release DDNs identified at the time (late

1980s) for the steam-cycle MHTGR. The FP transport DDNs are largely generic, especially for core designs that utilize LEU UCO fissile fuel particles. Consequently, the HFR-B1 test was also responsive to the most recently defined set of FP transport DDNs, *viz*., those for the commercial GT-MHR (DDNs 1996), and it is anticipated that it will also be largely responsive to the FP release DDNs ultimately defined for the very high temperature reactor (VHTR) as well. The GT-MHR DDNs addressed by the HFR-B1 are summarized in Table 2-1.

2.5 Report Organization

This report is intended to be a stand-alone document as well as a roadmap. It is organized as follows:

- Section 2: Provides introductory and background information
- Section 3: Describes the HFR-B1 experiment, including the physical configuration and test articles

The next sections describe the major phases of the test in chronological order:

- Section 4: Describes the Preirradiation phase
- Section 5: Describes the Irradiation phase
- Section 6: Describes the Postirradiation phase
- Section 7: Summarizes evaluations of the HFR-B1 conducted to date
- Section 8: Provides conclusions and recommendations
- Section 9: Provides a comprehensive bibliography (The serious reader is strongly encouraged to acquire the key references that are identified throughout this report.)

TABLE 2-1
FP RELEASE DDNS ADDRESSED BY HFR-B1

DDN No.	DDN Title	Work Scope
C.07.03.01	Fission Gas Release from Core Materials	Measurement of the fission gas release rates (Kr, Xe, I, and Te) from heavy-metal contamination and from failed reference LEU UCO/Nat. UCO fuel particles as a function of temperature, half-life, burnup, and flux under irradiation and under dry and wet core conduction cooldown conditions. In addition, the effect of hydrolysis on gas release must be quantified for steady-state irradiation and for transient wet core conduction cooldown conditions. The assumption that I and Te isotopes behave like Xe isotopes under irradiation must also be confirmed. The releases of I-131 from exposed LEU UCO and Nat. UCO kernels must be measured directly. Sufficient data are needed to develop and refine gas release models with uncertainties <4x at 95% confidence.
C.07.03.02	Fission Metal Diffusivities in Fuel Kernels	Correlations are needed for the effective diffusivities of key fission metals (Cs, Ag and Sr) and Pu isotopes in LEU UCO/Nat. UCO fuel kernels as a function of temperature, burnup and, if appropriate, neutron flux for normal operation and dry and wet core conduction cooldown conditions. The tentative observation that the metal diffusivities in the kernels of intact particles are significantly lower than in the kernels of failed particles also needs to be confirmed and quantified. Sufficient data are needed to develop and refine diffusivity correlations with uncertainties <10x at 95% confidence level.
C.07.03.03	Fission Product Diffusivities in Particle Coatings	The effective diffusivities of key radionuclides in particle coatings are needed as a function of temperature and, as required, of fluence, irradiation temperature, and as-manufactured coating attributes for normal operation and for core conduction cooldown conditions. Specifically, the effective diffusivities of the volatile fission metals (Ag, Cs, and Sr) in SiC coatings are needed as are the diffusivities of key fission gases (I, Te, Xe and Kr) in pyrocarbon (PyC) coatings. Sufficient data are needed to develop and refine effective diffusivity correlations with uncertainties <10x at 95% confidence level.
C.07.03.04	Fission Product Diffusivities/ Sorptivities in Graphite	Correlations/models for the diffusivities and sorptivities of Cs, Sr, Ag, and Pu in fuel-compact matrix and core graphites as a function of temperature, fast fluence, and, as appropriate, coolant impurities, system pressure (for Ag), and the extent of graphite oxidation under normal operating and dry and wet core conduction cooldown conditions. Sufficient data are needed to develop and refine diffusivity and sorptivity correlations with uncertainties <10x at 95% confidence.

3 HFR-B1 EXPERIMENT DESCRIPTION

The HFR-B1 test was performed in the High Flux Reactor (HFR) at the Joint Research Centre (JRC), the Petten Establishment of the Commission of European Communities in the Netherlands, in collaboration with the Forschungszentrum Juelich (FZJ)[2] and GA under the U.S./FRG Umbrella Agreement for Cooperation in Gas-Cooled Reactor Development.

The HFR-B1 test (designated experiment D214.01 within the JRC) was designed to provide for measurement of fission gas release and metallic fission product transport in simulated, prismatic core, fuel elements over the range of normal operating conditions and in the presence of significant quantities of water vapor. The Petten staff designed and assembled the irradiation rig using fuel elements and other samples fabricated by GA. The overall management of the test program was the responsibility of the KFA; the supervision and conduct of the test were the responsibility of the JRC.

The irradiation phase began in April 1987 and ended in July 1989, during which time 444 effective full-power days (EFPD) of exposure were accumulated. The U.S. DOE gas-cooled reactor program incurred no irradiation charges for the HFR-B1 irradiation. The irradiation was performed under the U.S./FRG Umbrella Agreement instead of an obligated German irradiation in HFR Petten under a EURATOM agreement that KFA chose not to perform (Myers 1984, Ketterer 1985a). After the irradiation was completed, the test rig was disassembled and the contents sent to KFA in December 1990 (some 17 months after the completion of the irradiation with attendant loss of data). A partial postirradiation examination (PIE) was conducted at the KFA under a DOE subcontract that was administered through ORNL. Test evaluations were subsequently performed by GA and ORNL under DOE/NE contracts for HTGR development.

3.1 Test Objectives

The HFR-B1 experiment was conducted to address several DDNs (Table 2-1) involving the FP transport in fuel elements under conditions simulating those of an HTGR prismatic core in the presence and absence of water vapor. These single-effects experiments were conducted in three separate capsules contained within the test rig. Each capsule had a specific purpose as shown in Fig. 3-1. The temperature range was between 820 and 1,230 ^{o}C, and in Capsule 3 water vapor was injected at partial pressures between 18 and 1,060 Pa. The main objectives of the HFR-B1 test were as follows (Ketterer 1985a, Burnette 1994):

1. Measurement of the transport and distribution of condensable fission products in a prismatic fuel element representative of the HTGR

[2] Forschungszentrum Juelich (FZJ) was formerly known as Kernforschungsanlage (KFA) Juelich; within this report KFA and FZJ are used interchangeably.

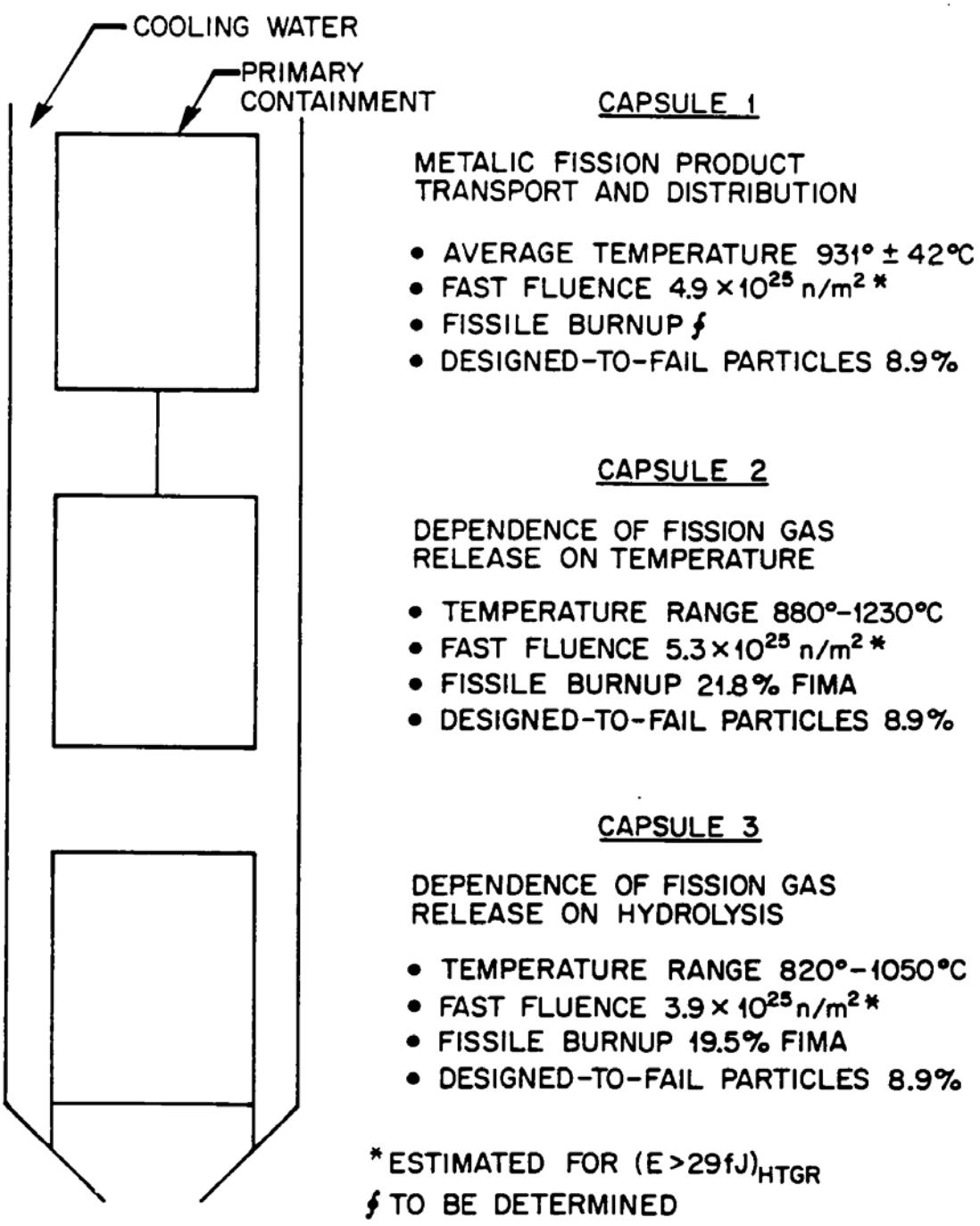

Fig. 3-1. General description and test objectives of HFR-B1 experiment

2. Measurement of the release of fission gases at temperatures near and above the upper limit of HTGR normal operating temperatures
3. Measurement of the effect of hydrolysis on coated fuel particles with exposed uranium oxycarbide (UCO) kernels and on the surrounding fuel compact matrix material and graphite
4. Measurement of fission product release from and distribution in coated fuel particles with different artificial defects encapsulated under a controlled atmosphere
5. Provision of irradiated fuel compacts for use in postirradiation heating tests simulating accident conditions and of unbonded, coated fuel particles for postirradiation tests
6. Measurement of the irradiation response of grades H-451 and H-451I graphite and SiC samples and of inert compacts fired in alumina and silicon carbide molds
7. Measurement of the fractional release of iodine isotopes whose decay products could be detected (I-133 and I-135) and of the amount of iodine released in volatile form[3]

The relation between the capsules and the objectives was as follows: Capsule 1 was devoted to meeting objective 1; Capsule 2 to objectives 2 and 6; and Capsule 3 to objectives 3, 4, and 6. All capsules were devoted to meeting objectives 5 and 7.

3.2 Test Description

The test rig consisted of three capsules. Each was individually monitored and temperature-controlled throughout the test (see Section 4). Each capsule contained 12 fuel compacts housed in an H-451 graphite body. The fuel particle types were TRISO-coated LEU $UC_{0.5}O_{1.5}$ fissile and TRISO ThO_2 fertile in both compacts and unbonded form. A known percentage (8.9%) of dtf UCO particles (thin PyC seal coat on UCO kernel) incorporated into each fuel compact to provide a well-defined source of released fission products during irradiation. One capsule had timed injections of moisture at several points during irradiation so that graphite oxidation and fuel hydrolysis and its effect on fission gas release could be measured. Piggyback samples included in the fuel bodies consisted of unbonded fuel particles of the same batches used in the compacts, encapsulated intact and laser-failed particle assemblies, and various non-fueled samples.

The test objective and design philosophy for each capsule is described in the following subsections. The mechanical design of each capsule is described in greater detail in Sections 4 and 5.

3.2.1 Capsule 1, Fission Metal Transport in Core Materials

The objective of the Capsule 1 experiment was to characterize metallic fission product transport, especially Cs-134/-137 and Ag-110m transport, in each material region of a prismatic core: (1) UCO kernels; (2) TRISO-particle coatings, especially the SiC coating; (3) fuel-compact

[3] This last objective was added after the beginning of the irradiation.

matrix; and (4) fuel-element graphite. To accomplish this objective, a relatively complicated capsule design was developed as described below.

As shown in Fig. 3-2, the graphite body in Capsule 1 consisted of six wedges that were confined by outer and inner graphite annuli (Ketterer 1985a, Ketterer 1986). As shown in Fig. 3-3, three of the wedges had holes filled with a column of four fuel compacts. The other three wedges served as sinks for fission products. These sink wedges were impregnated with resin and carbonized to increase their sorptivity for condensable fission products. One of the wedges containing fuel compacts was oxidized to about 1% burnoff to determine the effect of burnoff on fission product transport in graphite. Each fuel compact contained 1,396 normally configured fuel particles and 87 dtf[4] particles to provide a well-defined fission product source. The release of fission products from the intact particles is expected to be negligible by comparison with the dtf particles. The major test parameters for HFR-B1 are summarized in Table 3-1.

Transport of metallic fission products from the dtf UCO particles in the fuel compacts of this capsule proceeded through the matrix, across the compact-graphite gap, through reference H-451 graphite, across a graphite sink gap and into impregnated graphite sinks. The presence of the sinks, which are many times more sorptive than H-451, was intended to simulate the removal of fission products by the flowing coolant in an HTGR core. The graphite surrounding one fuel hole oxidized to about 1 wt.% burnoff prior to irradiation to simulate fuel exposed to in-core oxidants.

With this arrangement, (a) transport phenomena occurring in an HTGR core with failed particles was to be simulated, and (b) it was expected that the following data for metallic fission products could be extracted: (1) fractional release from UCO kernels, (2) diffusion coefficients in fuel compact matrix material and in H-451 graphite at a high neutron fluence and for the combination of oxidation and neutron irradiation, (3) distribution between fuel compact matrix material and H-451 graphite at a high neutron irradiation, (4) coolant hole surface release fluxes, and (5) effect of mixed species. Effective diffusion coefficients for fission metal transport in particle coating would be determined by postirradiation heating of intact TRISO particles contained in piggyback samples irradiated in the graphite body.

3.2.2 Capsule 2, Temperature Dependence of Fission Gas Release

The objective of the Capsule 2 experiment was to characterize the temperature dependence of fission gas release from failed UCO particles, including the effect of so-called “enhanced” fission gas release (Montgomery 1982, Myers 1982). This enhanced fission gas release, which has been attributed to release of stored fission gases as a result of kernel restructuring, was expected to occur between 1,000 and 1,500 °C only in the presence of a neutron flux.

[4] The “designed-to-fail” particles were standard 350-µm LEU UCO kernels with a 23-µm PyC seal coat.

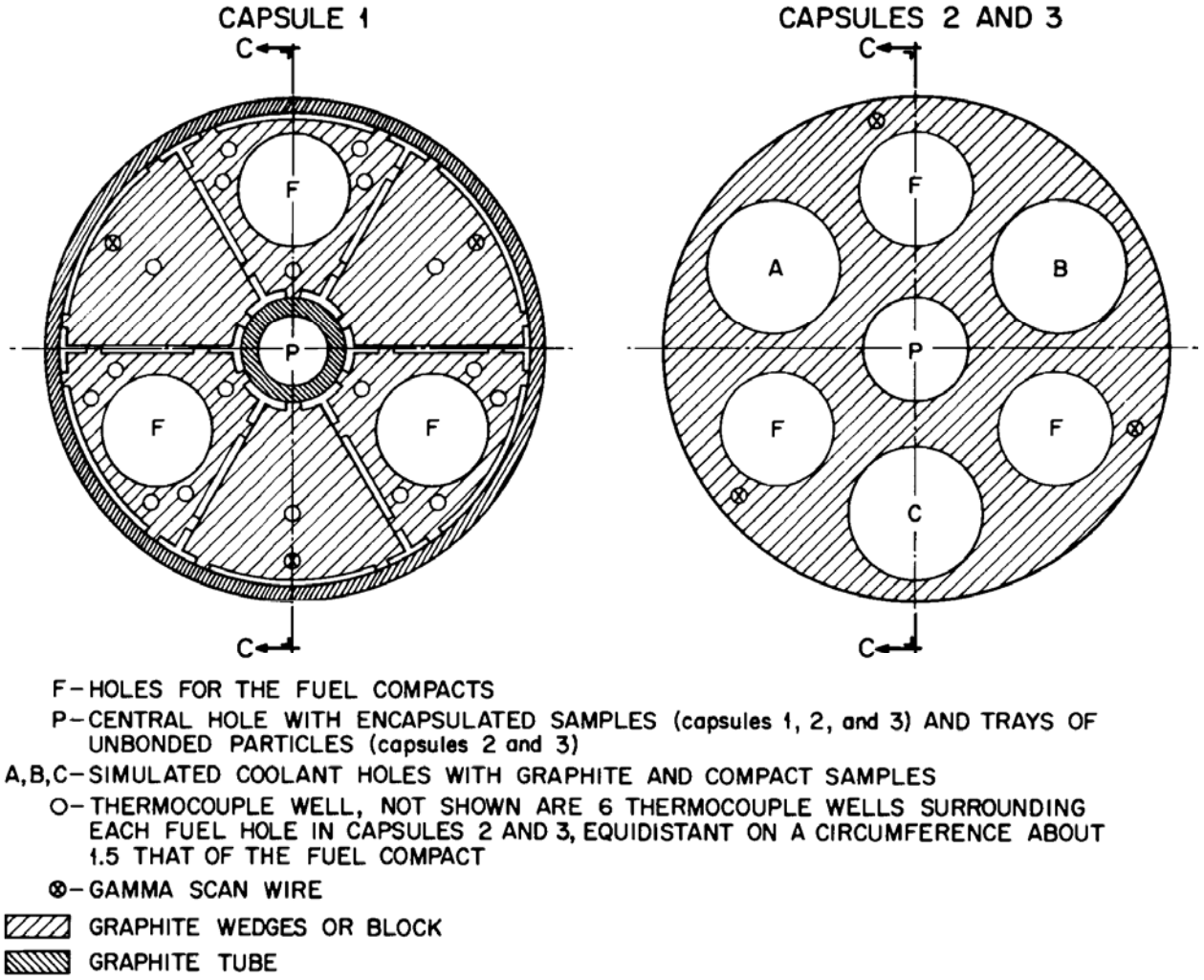

Fig. 3-2. Plan views of HFR-B1 Capsules

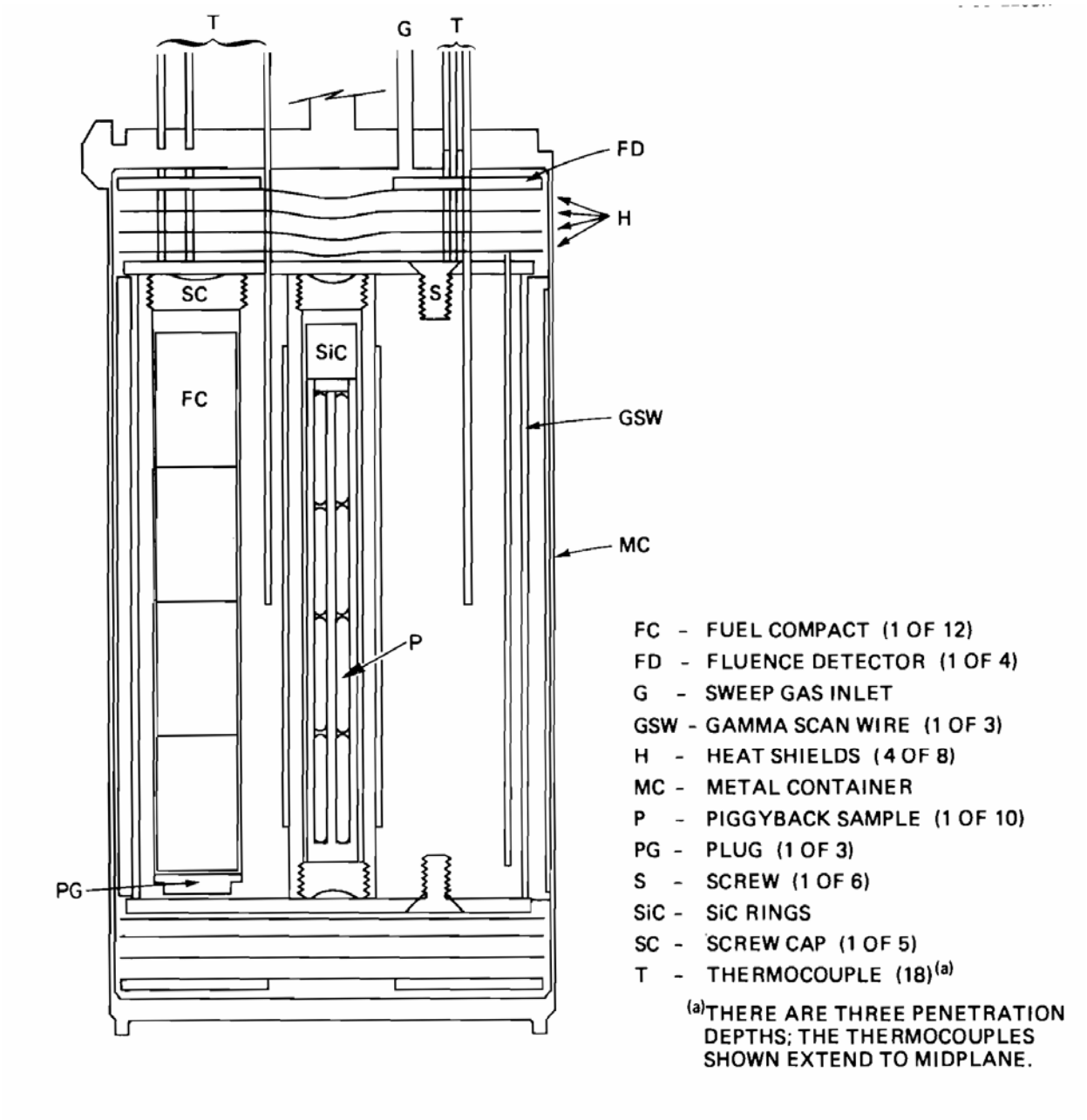

Fig. 3-3. Elevation view of Capsule 1

TABLE 3-1
HFR-B1 TEST PARAMETERS

Parameter	Value
Capsule Design	
Fuel form	Coated fuel particles in cylindrical compacts (12 compacts)
Fuel body configuration	Capsule 1: 6 segmented graphite wedges Capsules 2 and 3: solid graphite body
Driver fuel kernels	19.8% enriched, 350-µm UCO fissile kernels 450-µm ThO_2 fertile kernels
Coatings	Conventional TRISO coating system
Compact matrix	Petroleum pitch
Graphite type	H-451
Fission product source	"dtf" particles (8.9% of UCO fissile particles)
Special features	Flux wires, piggyback samples
Irradiation time (EFPD)	444
Capsule 1 Irradiation Conditions (As-operated)	
Burnup (% FIMA)	21.5
Fast Fluence (n/m^2)	4.9×10^{25}
Temperature (^oC)	931 ± 42
Capsule 2 Irradiation Conditions (As-operated)	
Burnup (% FIMA)	21.8
Fast Fluence (n/m^2)	5.3×10^{25}
Temperature (^oC)	880 - 1230
Capsule 3 Irradiation Conditions (As-operated)	
Burnup (% FIMA)	19.5
Fast Fluence (n/m^2)	3.9×10^{25}
Temperature (^oC)	820 - 1050

As shown in Figs. 3-2 and 3-4, the test geometry for Capsule 2 was similar to Capsule 1 except that the graphite body in Capsule 2 was a solid piece of H-451 graphite containing fuel compacts with standard UCO/ThO_2 particles and dtf UCO fuel particles. The Capsule 2 body also had simulated coolant holes located where the sink wedges were located in Capsule 1. During irradiation, the released fission gas, swept from the cell by the carrier gas, was continuously monitored. In the beginning of the irradiation, the temperature was held at 950 °C. At selected times, corresponding to progressively higher burnups, the temperature dependence

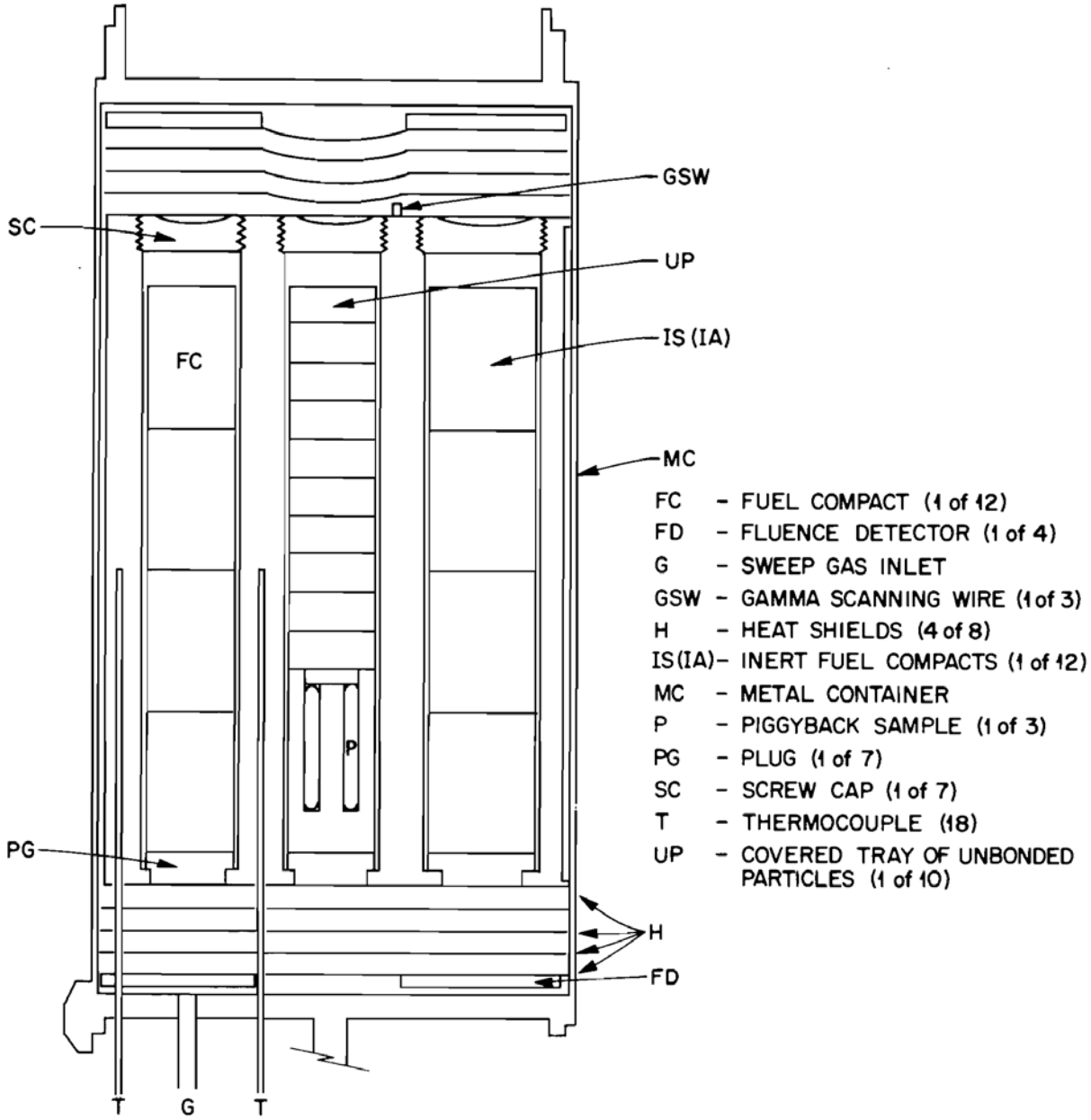

Fig. 3-4. Elevation view of Capsules 2 and 3

of fission gas release was determined by varying the temperature within the range 950 to 1,200 °C. In the later stage of the irradiation, the temperature was again raised to 1200 °C. The stored fission gas release was measured and the temperature held constant until the fission gas release became steady. The fission gas release was measured for various isotopes of Kr and Xe. The fractional releases of I isotopes with radioactive Xe daughters were determined by measuring their daughters between selected irradiation cycles and at end-of-life.

3.2.3 Capsule 3, Effect of Water on Fission Product Release

The objective of the Capsule 3 experiment was to characterize effect of water on fission product transport, especially the effect of hydrolysis on the fission gas release rates from failed UCO particles. The test geometry for Capsule 3 was the same as Capsule 2: a solid H-451 graphite body containing fuel compacts with standard UCO/ThO_2 particles and dtf UCO fuel particles. The unique feature of the Capsule 3 experiment was the periodic addition of controlled amounts of water vapor to the capsule sweep gas.

The experiment began at a relatively high temperature where the water vapor content of the sweep gas was expected to be depleted by oxidation of the graphite so that the exposed kernels would not significantly hydrolyze. The temperature was continuously lowered, past the point where the reaction of water with graphite would become slow enough to permit the water to reach the exposed fuel kernels and initiate hydrolysis. During the course of the temperature changes, the fission gas release was measured. The onset of hydrolysis resulted in a significant release of fission gas. At this point, the sweep gas was freed of water vapor and the hydrolyzed kernels were allowed to anneal. The release of fission gas was expected to decrease as the annealing proceeds. When the steady state of fission gas release was again reached, the temperature was varied to determine the dependence of release on temperature. Thereafter, water vapor was again introduced into the sweep gas and the above procedure repeated.

The results of this experiment were intended to permit the determination under neutron irradiation of (a) the rates of graphite oxidation and fuel hydrolysis; (b) the transport behavior of water in graphite and fuel-compact matrix material; (c) the effect of annealing on the fission gas release from the kernel; (d) the temperature dependence of graphite oxidation, of fuel hydrolysis and of fission gas release from hydrolyzed fuel; and (e) the fission gas release from a hydrolyzed, annealed kernel after further interaction with water.

3.3 Test Control

Established program management procedures and quality assurance (QA) protocols at GA and JRC Petten were used to control the conduct of the HFR-B1 test program. These QA protocols require the preparation of specific documents to control the planning, execution, and evaluation

of experimental test programs: test specifications, test plans/procedures, data compilation reports, and test evaluation reports. In simplified (and idealized) terms, the following sequence applies: (1) the cognizant design organization issues a Test Specification; (2) the testing organization prepares Test Plans/Test Procedures that are responsive to the Test Specification; (3) the testing organization performs the subject tests and documents the results in a Data Compilation Report; and (4) the design organization evaluates the test data, including the design implications, and documents the results in a Test Evaluation Report. On the HFR-B1 program, the test specifications were prepared by GA (e.g., Ketterer 1985a); the test plans by ORNL, JRC, and KFA (e.g., Myers 1991); the data compilation reports by JRC and KFA (e.g., Burnette 1994), and the test evaluation reports by ORNL and GA (e.g., Myers 1995).

3.3.1 QA at General Atomics

At GA, the provisions set forth in GA's Quality Assurance Manual (QAM 1993) and Program Resource Procedures Manual (PRPM 2001) as they apply to irradiation test capsules were applied to all phases of the HFR-B1 experiment. Furthermore, documentation in the form of approved and released reports of the various phases of this test were incorporated into GA's Engineering Database.

The fuel particles and fuel compacts for capsule HFR-B1 were fabricated to design specifications contained in the GA document "FMB-3 Fuel Specification for Irradiation Experiments," (Miller 1992). The construction, dimensions, and other details of the piggyback samples and graphite fuel bodies were documented in the Preirradiation Report (Ketterer 1985a). All fuel samples and graphite bodies underwent QA inspection at GA to verify their conformance to specifications and drawings, QA releases on these items prior to their shipment to JRC Petten for inclusion in the irradiation rig,

3.3.2 QA at JRC Petten

There are two QA departments at Petten, one in the HFR division and another in the JRC (de Zaaijer 1989). The main function of the QA department at JRC Petten is to inspect and approve all experiments that are inserted in the HFR. The HFR QA department provides the final inspections for all in-reactor tests. In addition, there is a separate department that performs calibration of instruments at the request of the HFR, with particular emphasis on safety.

Once the experiment is accepted and installed in the HFR, the lead engineer of the experiment becomes responsible for calibrations and other QA functions. In the case of the HFR-B1 experiment, the lead engineer was supported by the technical review function performed by the experiment cosponsors, KFA and GA. KFA and GA essentially functioned as independent reviewers and required that the tests be conducted in accordance with their QA systems. Prior to the conduct of the HFR-B1, the QA program in place at HFR Petten was judged as being in

compliance with the intent of 10 CFR 50, Appendix B, criteria 5, 6, 11, and 12.[5] A document defining the QA protocols for the HFR-B1 experiment was jointly prepared by JRC, KFA, and GA (Burnette 1990).

3.3.3 QA at KFA

A plan for the PIE of the three capsules in the HFR-B1 test at KFA was prepared by ORNL (Myers 1991b), and the PIE of Capsules 2 and 3 was performed in accordance with that plan (Myers 1994).

Capsule 1, which focused on fission metal transport in core materials, was different from Capsules 2 and 3 in that the bulk of the experimental data for Capsule 1 was to be obtained during PIE whereas the bulk of the data for Capsules 2 and 3 was from online fission gas release measurements. As a result, the planned PIE of Capsule 1 was much more extensive as well as much more expensive. Consequently, U.S. DOE contracted with KFA to provide supplemental funds for the PIE of Capsule 1 with ORNL as the contract administrator.

As part of the contract, a separate PIE plan for Capsule 1 was prepared by ORNL (Myers 1991b) and that plan invoked the following QA requirements: "The PIE at KFA shall be governed by the respective quality assurance (QA) requirements of this organization. These requirements, at the least, shall be in compliance with the intent of 10 Code of Federal Regulations (CFR) 50, Appendix B, Criteria 5, 6, 11, and 12. These criteria address, respectively, instructions, procedures, and drawings; document control; test control; and measuring and test equipment."

Contrary to programmatic protocols, the ORNL PIE plan for Capsule 1 (Myers 1991b) was actually issued well before the GA PIE specification of Capsule 1 (Medwid 1994) was issued; however, the plan is generally responsive to the specification.

The PIE of HFR-B1 at KFA was partially completed, and the results were documented in a series of progress reports; no final report on the Capsule 1 PIE could be located at either KFA or ORNL when a search of their databases and libraries was made in 2004 (Hanson 2004b).

[5] Criteria 5: Instructions, Procedures, and Drawings
Criteria 6: Document Control
Criteria 11: Test Control
Criteria 12: Control of Measuring and Test Equipment

4 PREIRRADIATION PHASE

The planned HFR-B1 test program and the test articles fabricated by GA, including the fuel particles, fuel compacts, and graphite bodies, are described in the preirradiation report (Ketterer 1985a). The test rig assembly and the actual conduct of the test at JRC Petten (Section 5) are described in the operating history report (Burnette 1994). Those two key documents are excerpted in this section. The summary information in the tables and the figures is from the pre-irradiation report (Ketterer 1985a).

4.1 Design of Experiment

As introduced in Section 3, the HFR-B1 experiment consists of three separately enclosed capsules, each with specific objectives and different control requirements during irradiation. Figure 3-1 shows a schematic layout of the cells numbered vertically from top to bottom within the test rig. Cooling during irradiation was provided by water flow within the stainless steel outer rig tube. Separate temperature control for each capsule was achieved with variable mixtures of inert gases (He/Ne) in the sweep gas and monitored with numerous in-capsule thermocouples. A special feature of the experimental assembly is that vertical and rotational movement within the reactor can be made during the irradiation. Rotation of the rig at set intervals smoothes out fluence gradients and provides for radial symmetry of burnup and material property changes.

Figures 4-1, 4-2, and 4-3 show details of the three capsules in the HFR-B1 test rig. Each consists of a graphite fuel body within a sealed, stainless steel containment. The fuel bodies are centered axially by a set of heat shields and radially by standoff pads on the graphite bodies. Eighteen thermocouples penetrate each capsule, entering from the top end in Capsule 1 and from the bottom in Capsules 2 and 3. Sweep gas is directed into the bottom of each cell and out the top ends through stainless steel tubes. Timed moisture injections at specified ppm H_20 levels were introduced into the sweep gas in Capsule 3. Other instrumentation in each capsule consisted of fluence detectors, gamma-scan wires, and self-powered neutron detectors.

The graphite bodies contain the primary fuel samples, the fuel compacts (discussed in this section), and numerous piggyback samples (detailed in Section 5) that occupy otherwise unused space within the capsule. Each body contains a total of 12 compacts in three axial holes positioned symmetrically at 120^o intervals. Piggybacks are contained in the central holes of each body and in the simulated coolant holes of bodies 2 and 3. A schematic of the complete in-core portion of the irradiation rig is shown in Fig. 4-4.

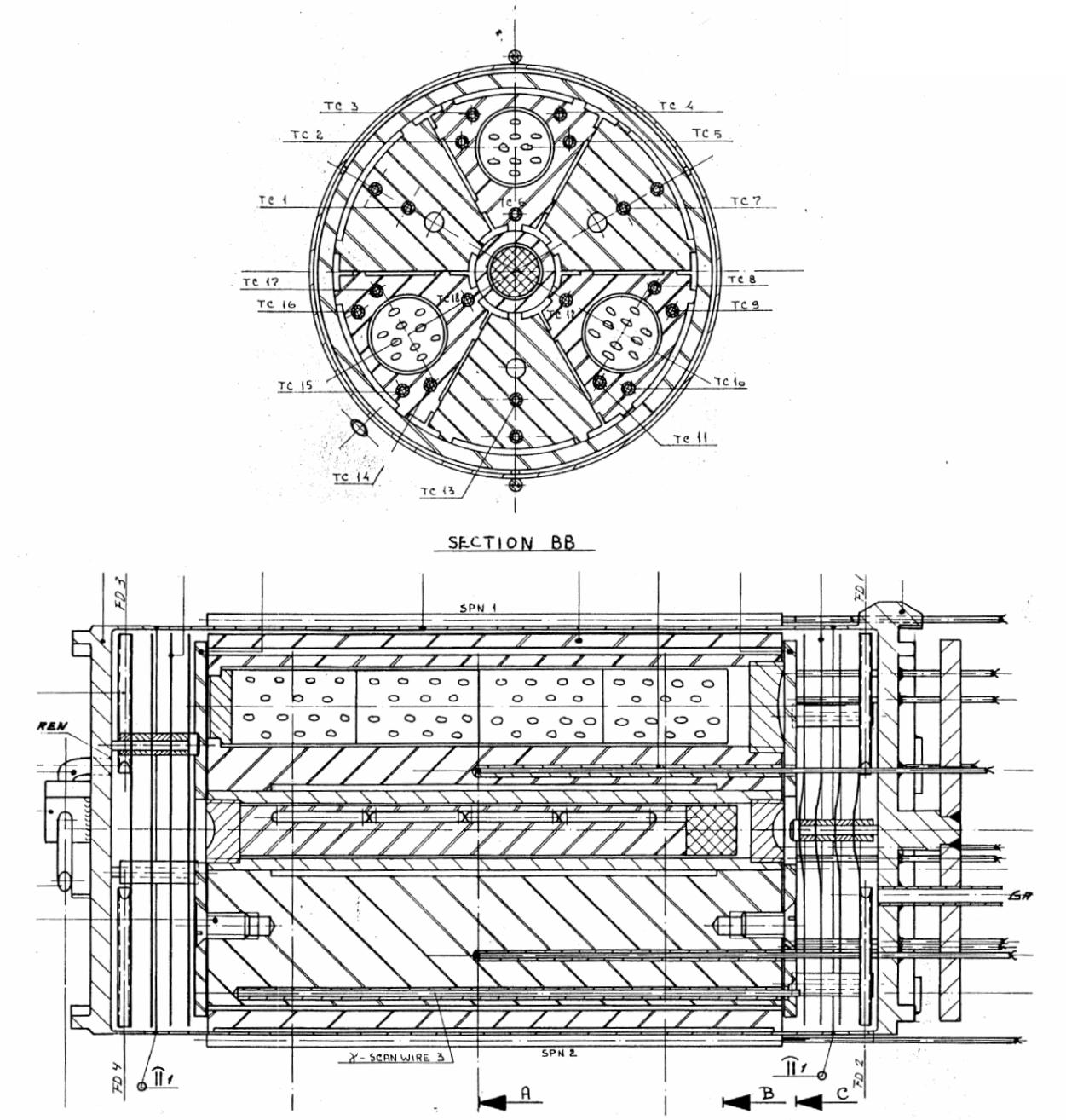

Fig. 4-1. Capsule 1 schematic

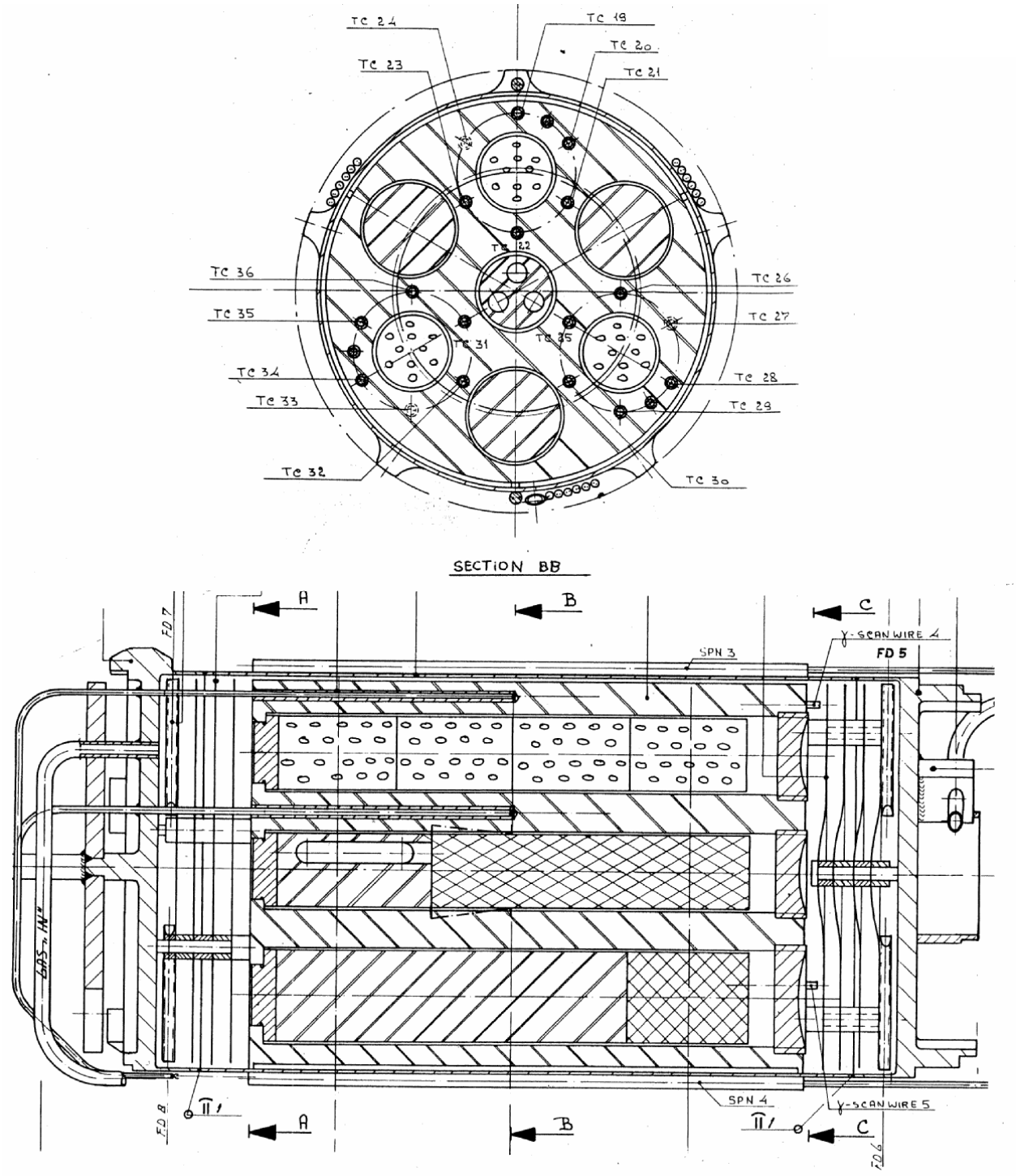

Fig. 4-2. Capsule 2 schematic

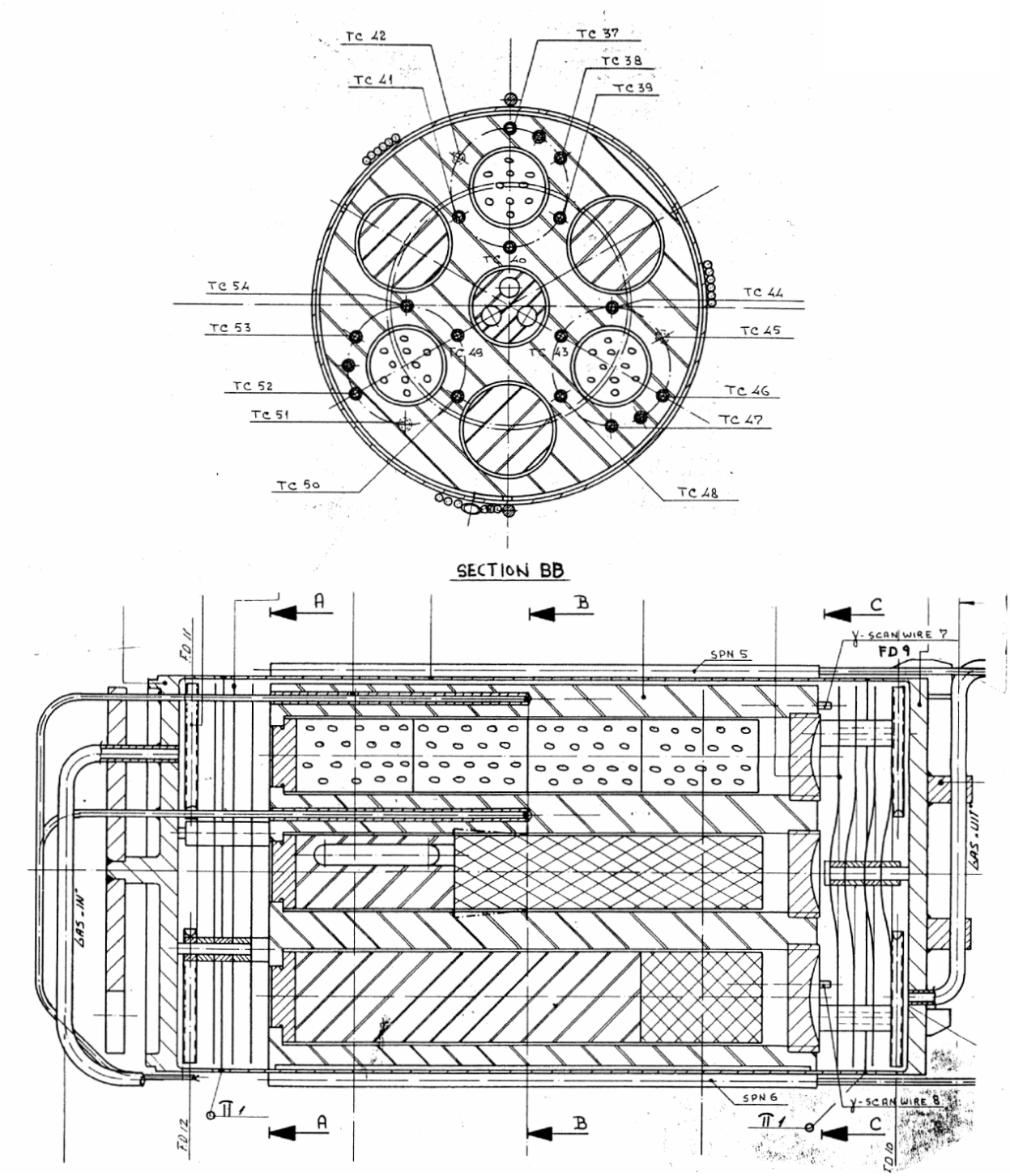

Fig. 4-3. Capsule 3 schematic

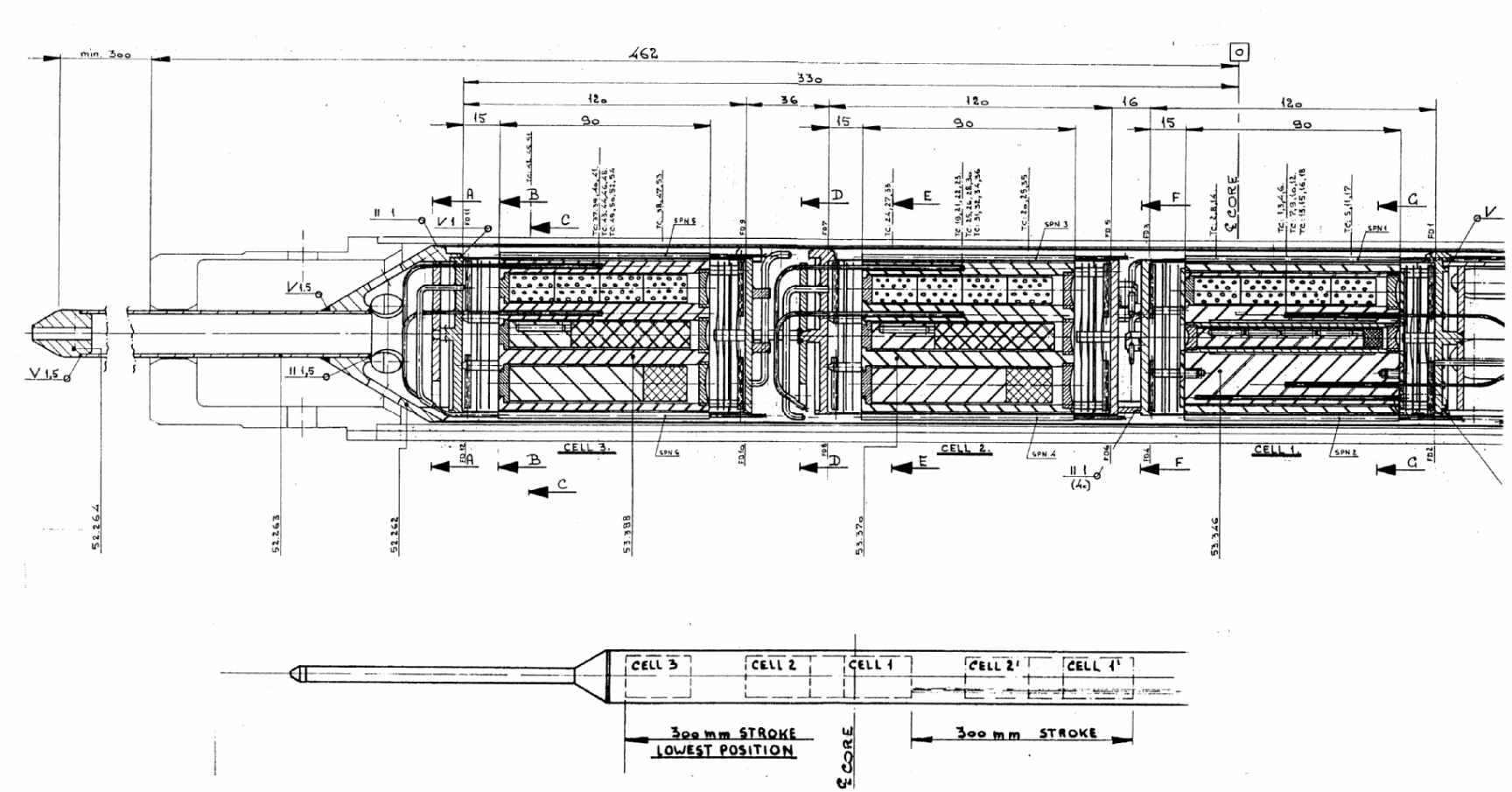

Fig. 4-4. HFR-B1 test rig, lower in-core portion

Eighteen thermocouples per capsule provided extensive monitoring of temperatures during the irradiation. Since all thermocouples were placed within the graphite bodies, fuel compact centerline temperatures were calculated rather than measured directly during the irradiation. All thermocouples in Capsules 1 and 3, and six in Capsule 2 were type K chromel/alumel sheathed in stainless steel. However, because of the higher operating temperatures in Capsule 2, twelve of the thermocouples there were type KN Nicrosil/Nisil with Inconel sheathing, which have higher temperature capabilities than the type K. In all cases, niobium protection tubes of 1.1 mm I.D. and 1.6 mm O.D. were placed in the thermocouple holes of the graphite bodies to accept the 1.0 mm diameter thermocouples.

All nuclear and thermal analyses in support of the test design were performed at JRC Petten to identify an experimental design that would achieve the operating requirements for each capsule defined in the test specification/procedures (Ketterer 1986). The resulting heavy-metal loading requirements for the fuel compacts were supplied to GA by JRC Petten.

4.2 Test Articles

The test articles were fabricated from reference U.S. HTGR core materials of construction, and they were characterized and qualified using standard coated-particle fuel quality control QC/QA techniques. The fuel particles and fuel compacts for capsule HFR-B1 were fabricated to design specifications contained in the GA document "FMB-3 Fuel Specification for Irradiation Experiments" (Miller 1992). The construction, dimensions, and other details of the piggyback samples and graphite fuel bodies were documented in the Preirradiation Report (Ketterer 1985a), which is excerpted in the following subsections. All fuel samples and graphite bodies underwent QA inspection at GA to verify their conformance to specifications and drawings, QA releases on these items prior to their shipment to JRC Petten.

4.2.1 Fuel Particles

The driver, LEU fissile particles used in capsule HFR-B1 were TRISO-coated $UC_{0.5}O_{1.5}$ particles of approximately 824 pm total diameter, with a 353 µm kernel diameter. These particles (Batch No. 6157-11-010) were fabricated in GA's 240 mm production coater and have shown good overall performance in the previous near-real-time R2-KI3 irradiation (Acharya 1987).

The "dtf" fissile particles (Batch 6450-00-010) had an LEU $UC_{0.4}O_{1.6}$ kernel, but had only a single pyrocarbon coating that failed after only a slight fast fluence exposure. These particles provided a well-defined fission product source during irradiation. The kernels were near the reference LEU fissile kernel size (346 µm vs. 350 specified) and have a ~23 µm dense pyrocarbon coating.

The microstructure of both of these UCO kernels (Figs. 4-5 and 4-6) shows that they consist of a mixture of UC_2 (light phase) and $U0_2$ (darker phase). As typically occurs during coating application, a small amount of the $U0_2$ at the surface of the kernels underwent conversion to carbide as evidenced by the thin ring of the light carbide phase. The anisotropy of the pyrocarbon coat is made evident by the alternating light and dark regions of PyC in the polarized light photo in Fig. 4-6.

A single fertile particle batch (6252-12COMP) was used in the HFR-B1 fuel samples. These particles have near reference-size 450 µm $Th0_2$ kernels and the TRISO coatings were applied in the production-size 240-mm coater.

The key property data for each of the three batches of particles used in HFR-B1 are summarized in Table 4-1. Additional characterization data are contained in the preirradiation report (Ketterer 1985a).

4.2.2 Fuel Compacts

Thirty six identical fuel compacts were irradiated in HFR-B1 in three fuel bodies containing twelve compacts each. Each compact contained ~900 driver fissile UCO particles, ~530 fertile $Th0_2$ particles, and exactly 87 dtf UCO particles. The resulting heavy-metal loadings are 0.1879 g total uranium, 0.0368g U-235, and 0.2114g thorium per compact.[6] In addition to fuel particles, the compacts had -40 vol.% of unimpregnated H-451 shim particles; no inert particles were used in these compacts. The carbonaceous matrix consisted of a mixture of graphite filler flakes in a petroleum-based pitch binder and a small amount of additives. Figure 4-7 shows the typical preirradiation appearance of the HFR-B1fuel compacts. Sections of composite photos (Fig. 4-8) show the different particle types.

The compacts were fabricated according to FMB-3 procedures (Miller 1992) that specified the weights and types of all fuel and other materials as well as all pertinent process conditions. Because of the small size of the dtf UCO particles, they were counted under a stereo microscope rather than weighed, and thus an exact number (87) of these particles was provided for each compact. The four particle charges for each compact, driver fissile, dtf fissile, fertile, and shim were blended and then loaded into one of the cavities in GA's prototype

[6] The preirradiation report (Ketterer 1985a) states that the required heavy-metal loadings for the HFR-B1 fuel compacts were specified in the FMB-3 procedures (Miller 1992). This statement appears to be incorrect. The FMB-3 procedures are generic fuel fabrication procedures and do not provide heavy-metal loading requirements for a specific irradiation test. The heavy-metal loading requirements would logically be specified by the JRC Petten staff based upon their nuclear and thermal analyses. It is believed that was in fact the case for HFR-B1 and that the loading requirements are specified in the JRC citations in the HFR-B1 irradiation proposal (Ketterer 1985b). In this regard, the test documentation is less than satisfactory. In any case, the test was conducted, and the desired test conditions were achieved.

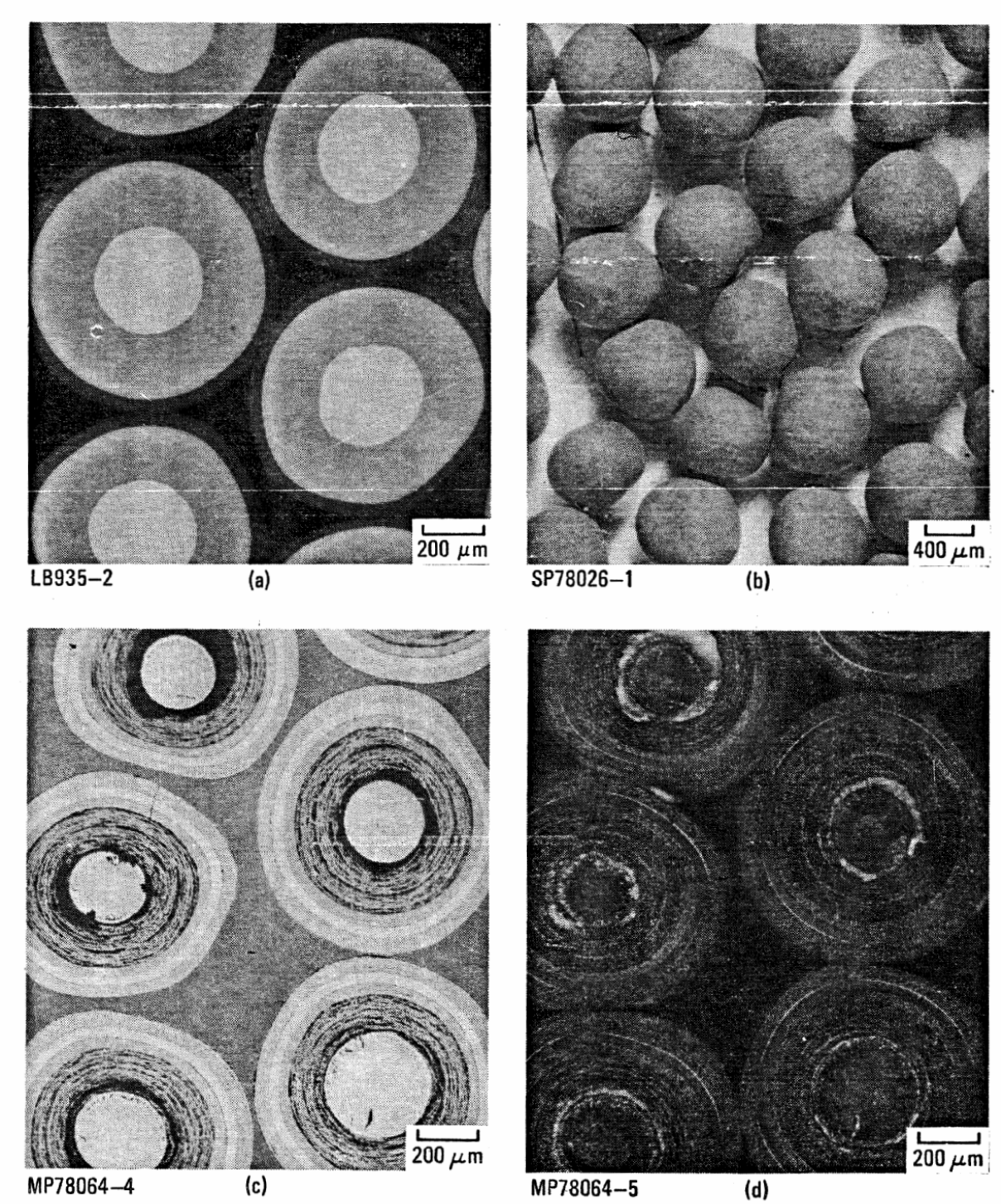

Fig. 4-5. Photomicrographs of TRISO LEU $U_{0.5}O_{1.5}$ particles for HFR-B1

(a) radiograph, (b) stereo view, (c) bright field, (d) polarized light

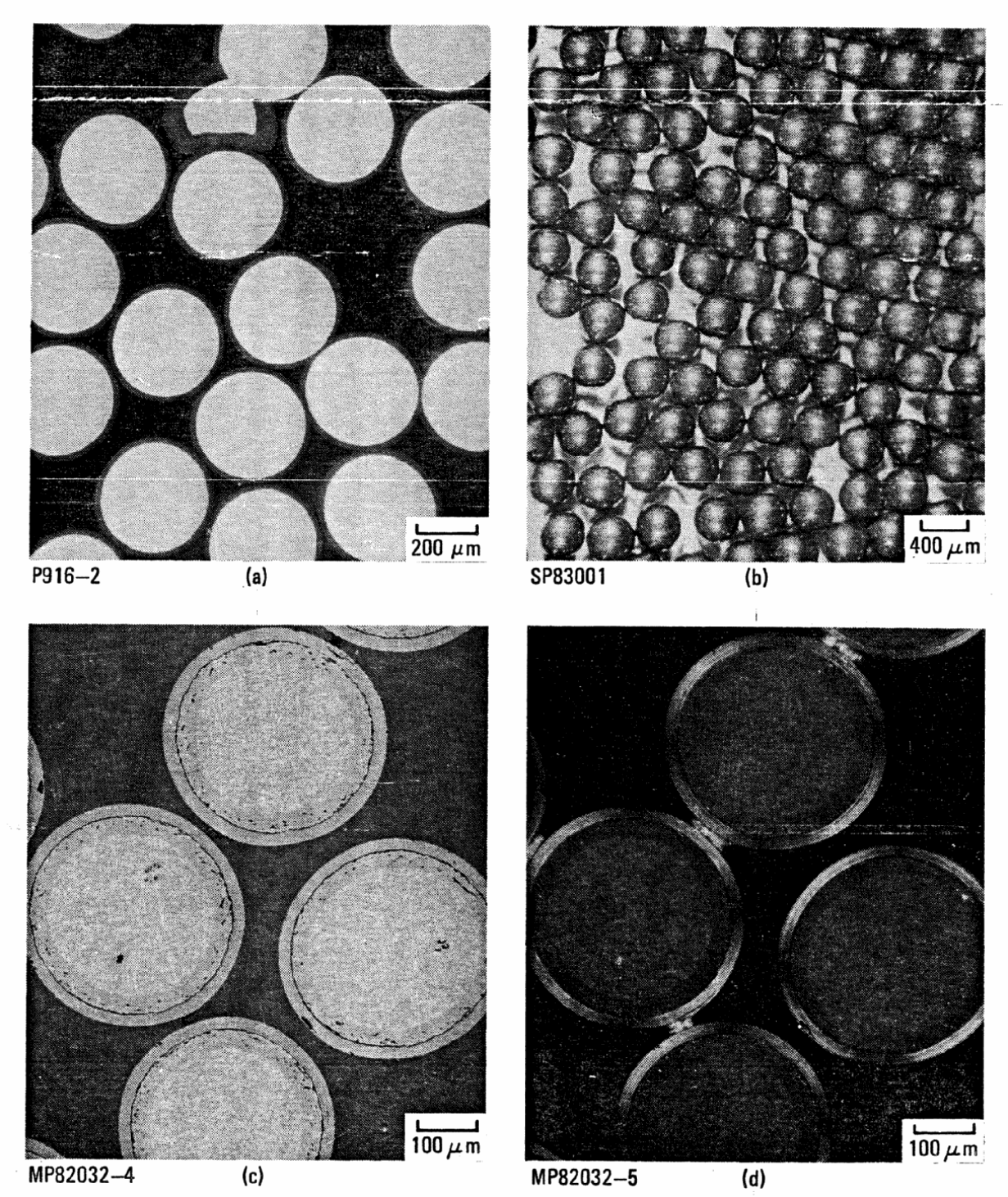

Fig. 4-6. Photomicrographs of seal-coated LEU $U_{0.4}O_{1.6}$ particles for HFR-B1

(a) radiograph, (b) stereo view, (c) bright field, (d) polarized light

TABLE 4-1
KEY ATTRIBUTES OF COATED PARTICLES USED IN HFR-B1

Attribute	Particle		
	Fissile Driver	DTF Fissile	Fertile
GA Batch Number	6157-11-010	6450-00-010	6252-12COMP
Kernel Composition	$UC_{0.5}O_{1.5}$	$UC_{0.4}O_{1.6}$	ThO_2
Kernel Diameter (µm)	353	347	452
Kernel Density (g/cm^3)	11.1	10.5	9.88
Buffer Thickness (µm)	115	N/A	53
Buffer Density (g/cm^3)	0.97	N/A	1.11
IPyC Thickness (µm)	35.6	N/A	33
IPyC Density (g/cm^3)	1.88	N/A	1.85
IPyC BAF	1.057	N/A	1.062
SiC Thickness (µm)	35.6	N/A	38.2
SiC Density (g/cm^3)	3.22	N/A	3.22
OPyC Thickness (µm)	47.8	22.8	43.8
OPyC Density (g/cm^3)	1.90	1.95	1.85
OPyC BAF	1.034	N/A	1.037
Total Particle Diameter (µm)	824	389	786
SiC Defects (burn-leach)	3.5×10^{-4}	N/A	1.6×10^{-5}
Heavy-Metal Contamination	5.4×10^{-6}	N/A	0.00

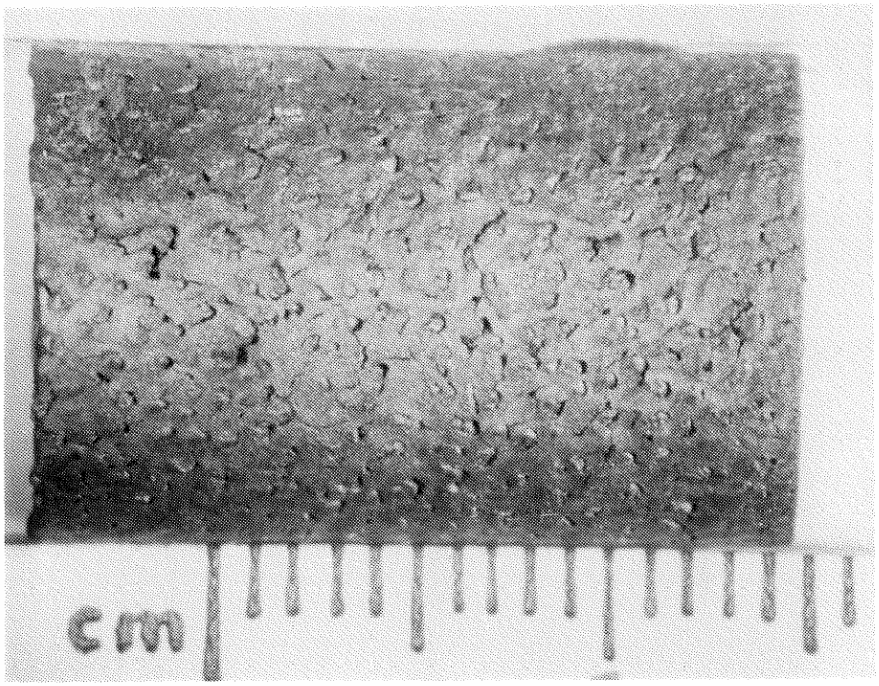

SR85003–2 (a)

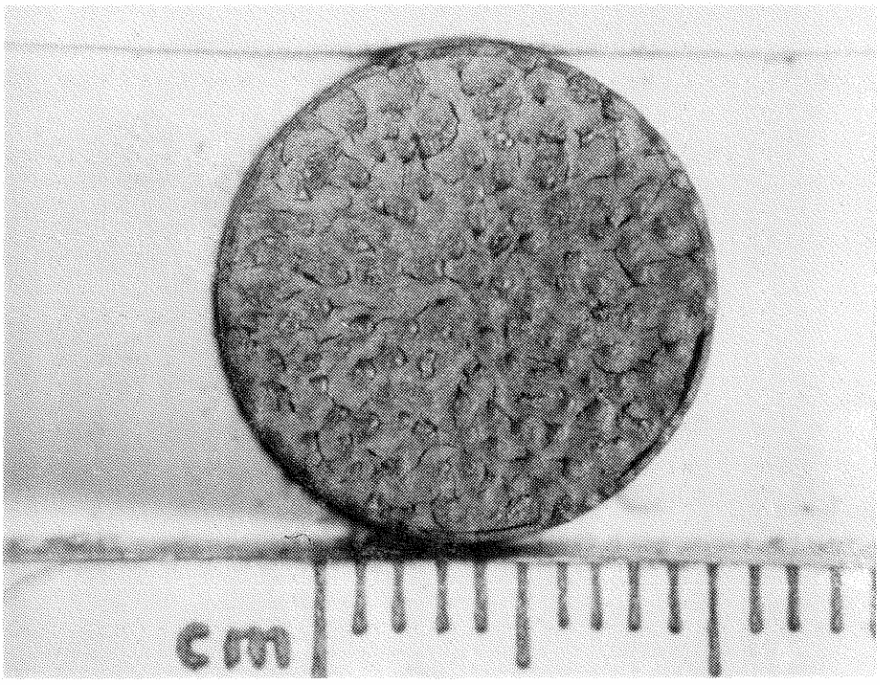

SR 85003–4 (b)

Fig. 4-7. Typical preirradiation appearance of HFR-B1 fuel compact

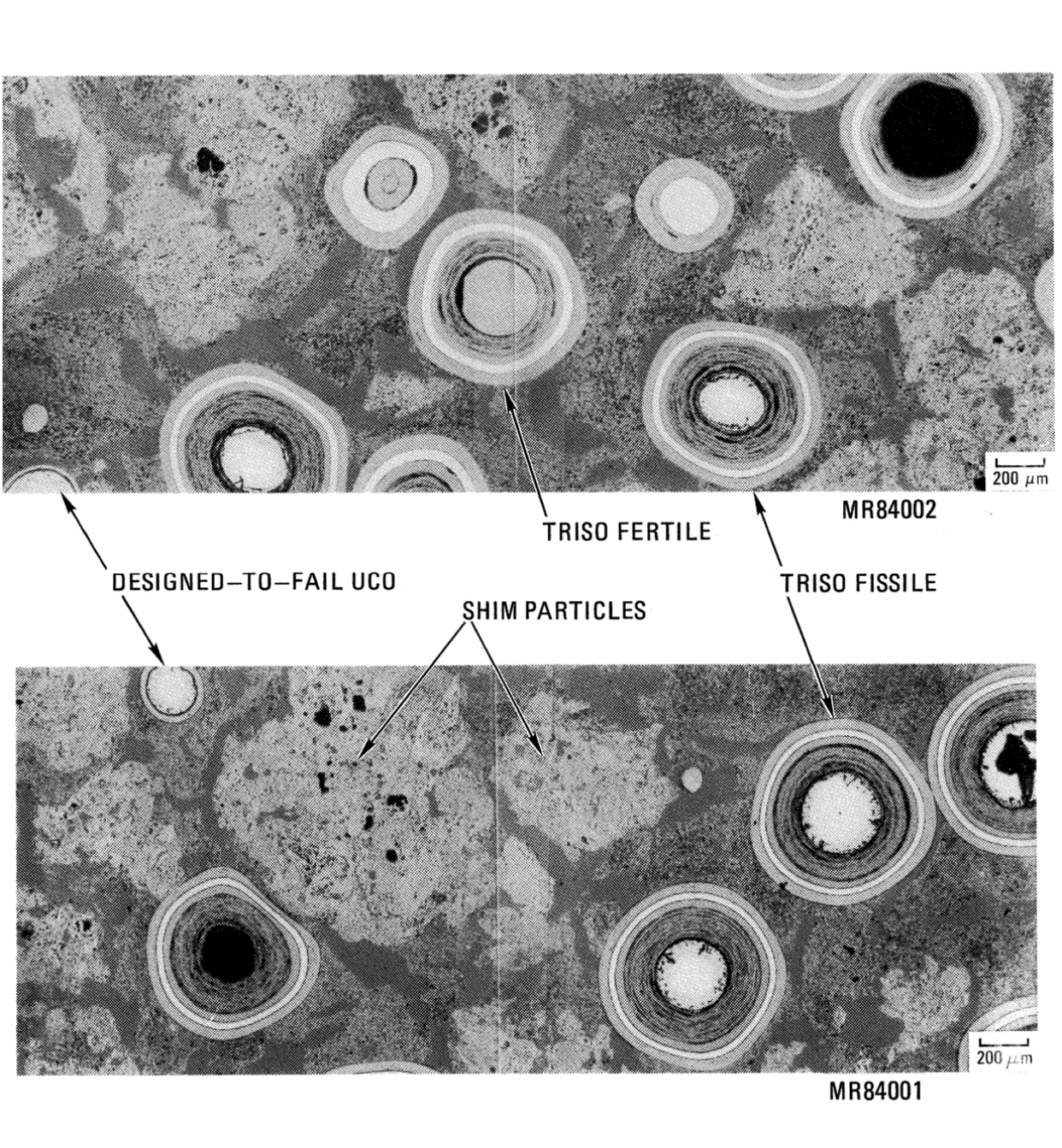

Fig. 4-8. Photomicrograph of HFR-B1 fuel compact

four-hole injection press. The green compacts were packed in alumina powder in graphite crucibles and carbonized at 900 °C for 30 minutes in nitrogen. After cooldown, the alumina was removed from the crucibles and brushed from the carbonized compacts. Final firing in an argon atmosphere at 1,700 °C for 15 minutes was accomplished with the compacts free-standing in the crucibles without alumina packing.

The compacts were characterized to evaluate their conformance to the design specifications given in the FMB-3 procedures (Miller 1992). The various tests and measurements were done to verify the even distribution of fuel particles, the total heavy-metal loading, and the amount of heavy metal outside of the particle coatings, and the properties and preirradiation condition of the compacts themselves. Properties measured on the actual capsule compacts were weight, dimensions, surface condition, overall fuel homogeneity by radiography, and fission gas release by TRIGA activation. All other properties and measurements were made on companion compacts. Because some of these tests are necessarily destructive ones, properties thus determined are assumed to be representative of all compacts in the fabrication lot, since they were all fabricated at essentially the same time under the same conditions.

Both the green compacts and final fired compacts were characterized using standard QC/QA techniques. An indirect method had to be employed with the HFR-B1 compacts to determine the fraction of defective particles, because of the presence of the dtf particles. The single PyC coatings of these particles would be removed during the burn phase of the standard burn/leach procedure, leaving exposed kernels that would easily leach and mask the comparatively smaller quantities of metal leached from fuel particles with defective SiC coatings. Thus, special characterization compacts were made during the fabrication run which did not contain any of the dtf UCO particles. One type contained only driver fissile particles, the other only fertile particles, with all other parameters, including the total volumetric particle loading, identical to the regular capsule-type compacts.

Fission gas release measurements were made on all compacts selected for use in HFR-B1. These results are especially important for this capsule because the circulating gas activity levels will be monitored closely during irradiation. The compacts were subjected to a 30-minute irradiation at 1,100 °C in the GA TRIGA Mark 1 reactor. The key preirradiation properties of the HFR-B1 fuel compacts are given in Table 4-2. Additional property measurements are provided in the preirradiation report.

TABLE 4-2
KEY ATTRIBUTES OF HFR-B1 FUEL COMPACTS

Attribute	Value
Particle Type:	Batch Number
TRISO Fissile	6157-11-010
Dtf Fissile	6450-00-010
TRISO Fertile	6252-12COMP
Shim	3804-141-1
Number of Particles/Compact:	
TRISO Fissile	896
Dtf Fissile	87
TRISO Fertile	530
Average Total Particle Packing Fraction	0.551
Matrix Data:	
Batch Number	MO-12 51
Filler Content (wt. %)	40.0
Fired Matrix Density (Mg/m^3)	1.16
Macroporosity (%)	28.7
Coke Content [g coke/(g coke+g filler]	0.27
Dimensions	
Diameter (mm)	12.44 to 12.48
Length (mm)	19.00 to 19.12
Loading Uniformity:	
Fissile, end-to-end	1.015
Fertile, end-to-end	1.048
Heavy Metal Contamination (HNO_3 leach):	
Fissile	1.55×10^{-5}
Fertile	4.73×10^{-5}
SiC Defects (burn/leach)	
Fissile	2.97×10^{-4}
Fertile	1.19×10^{-4}
R/B Kr-85m at 1100 °C	2.43×10^{-5}

4.2.3 Piggyback Samples

Piggyback samples occupy otherwise unused irradiation space and are used to accomplish goals of secondary importance to the main capsule objectives. Several piggyback types, both fueled and unfueled, were loaded into the three HFR-B1 fuel bodies, each type is described briefly in this section. Figure 4-9 gives the relative locations of all piggyback samples within the three capsules.

A considerable effort was expended in preparing these piggyback samples. The pre-irradiation report (Ketterer 1985a) provides a complete description and characterization of them, and the operating history report (Burnette 1994) provides power and temperature histories for the fueled piggyback samples. Unfortunately, there is no indication in the PIE status reports (e.g., Myers 1994) that any of these piggyback samples were ever examined during the destructive PIE at KFA, nor is there any indication of their ultimate fate. These piggyback samples, especially the encapsulated fuel particle piggyback, are an elegant example of test article miniaturization and graphite micromachining, and they are given attention here primarily for that reason.

4.2.3.1 Encapsulated Fuel Particles

These samples consisted of intact and laser-failed fuel particles sealed within small niobium encapsulations. The encapsulation permits a complete mass balance of all fission products to be attained after irradiation and allows various particle configurations to be studied without interference from other sources of fission products. Figure 4-10 shows the four types of these encapsulated particle sample holders included in HFR-B1. All sixteen of these encapsulations are shown in Fig. 4-11, alongside the graphite crucibles into which they were loaded. These graphite crucibles in turn were loaded into the central holes of the fuel bodies in the locations shown on Fig. 4-9.

4.2.3.2 Unbonded-Particle Trays

Unbonded driver fissile (batch 6157-1010) and fertile (batch 6252-12COMP) fuel particles in graphite trays were included in the test to provide: (1) a comparison with the same particle types bonded into the fuel compacts and (2) a source of irradiated, unbonded particles in the event they are needed for postirradiation heating studies. Figure 4-12 shows one of these trays containing its loading of fissile particles. Ten of these trays, five fissile and five fertile, were stacked into the central hole of fuel body 2, and an identical set was placed in body 3.

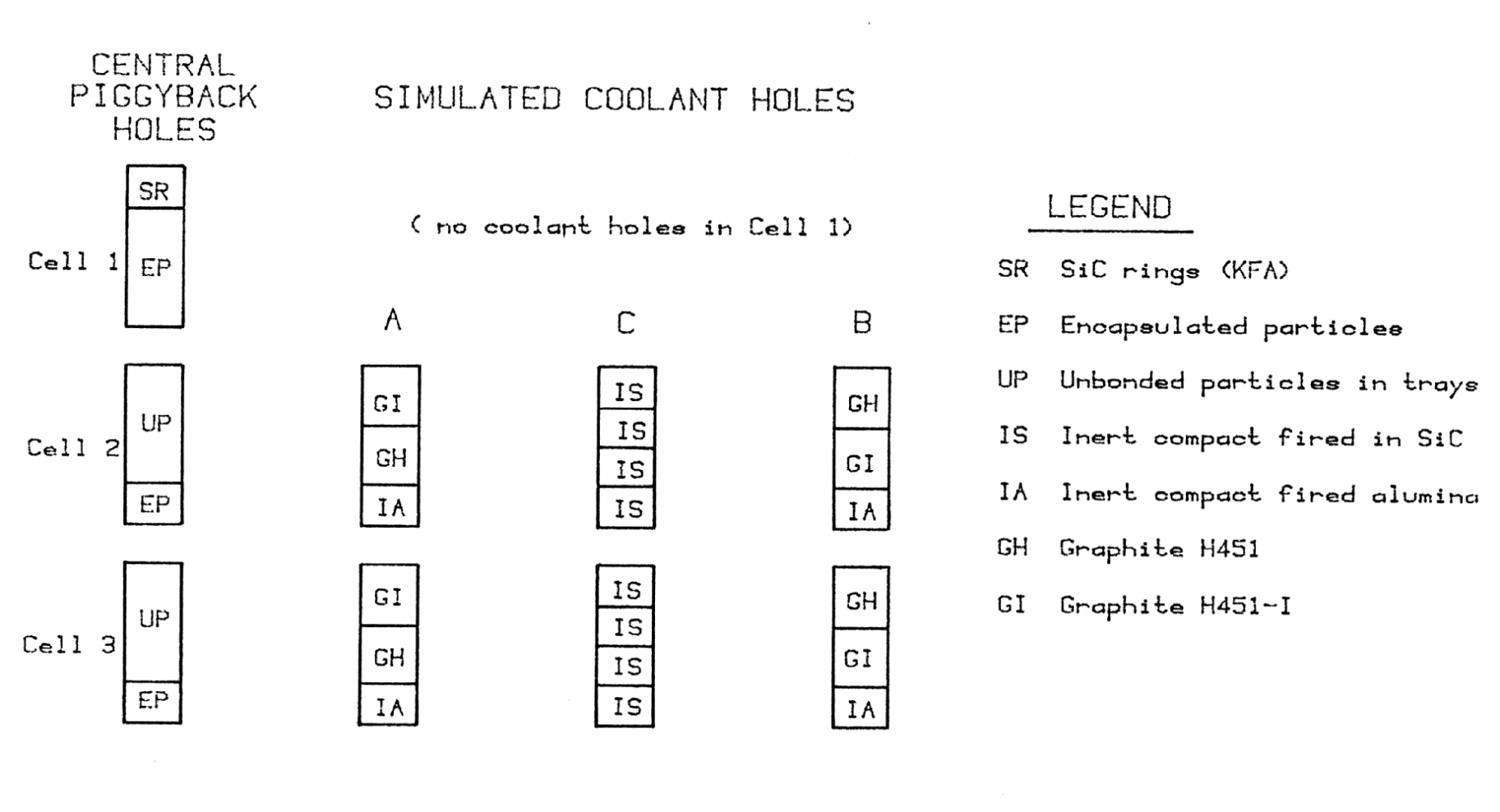

Fig. 4-9. Location of piggyback samples in HFR-B1

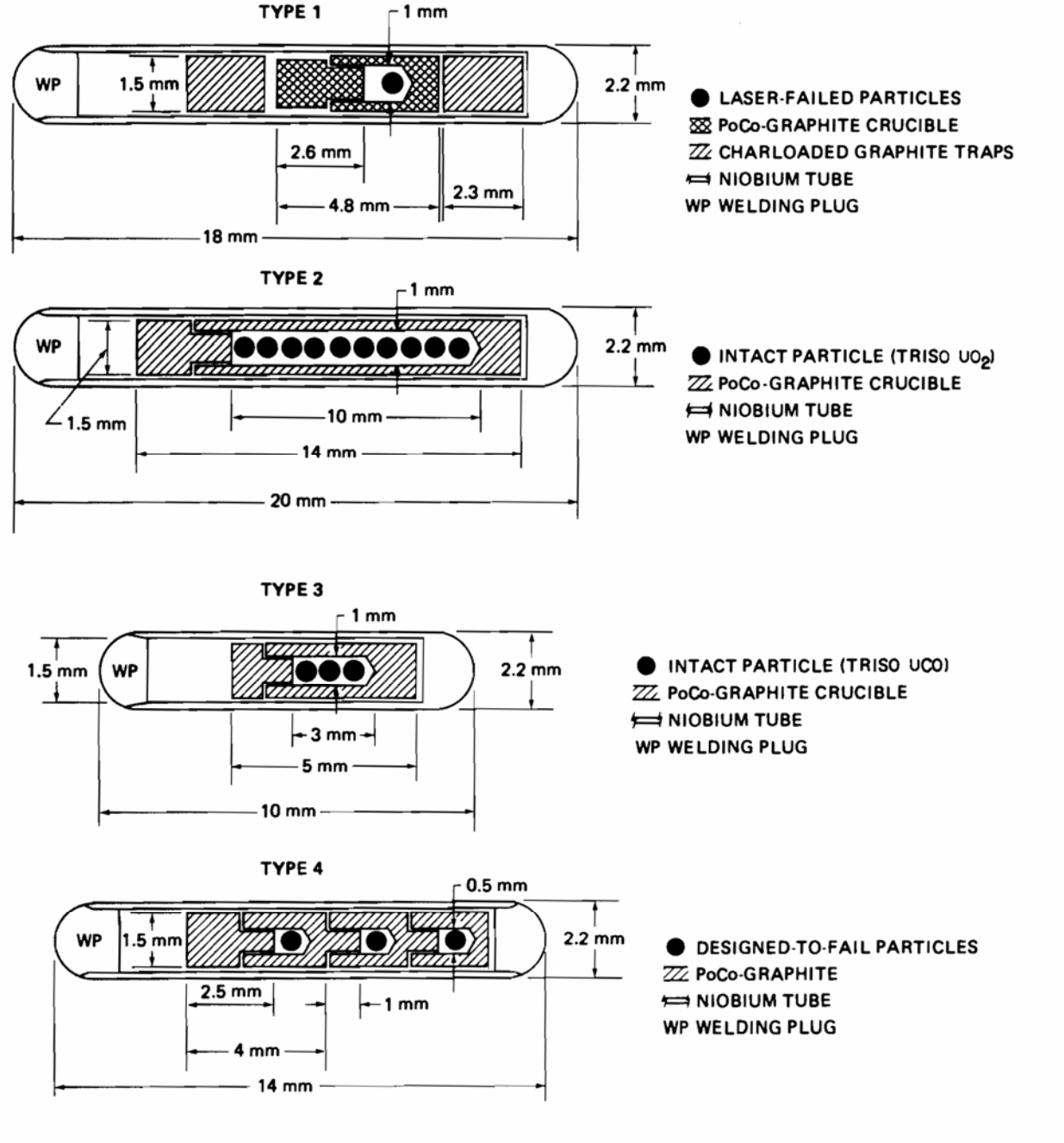

Fig. 4-10. Piggyback sample holders for encapsulated particle samples

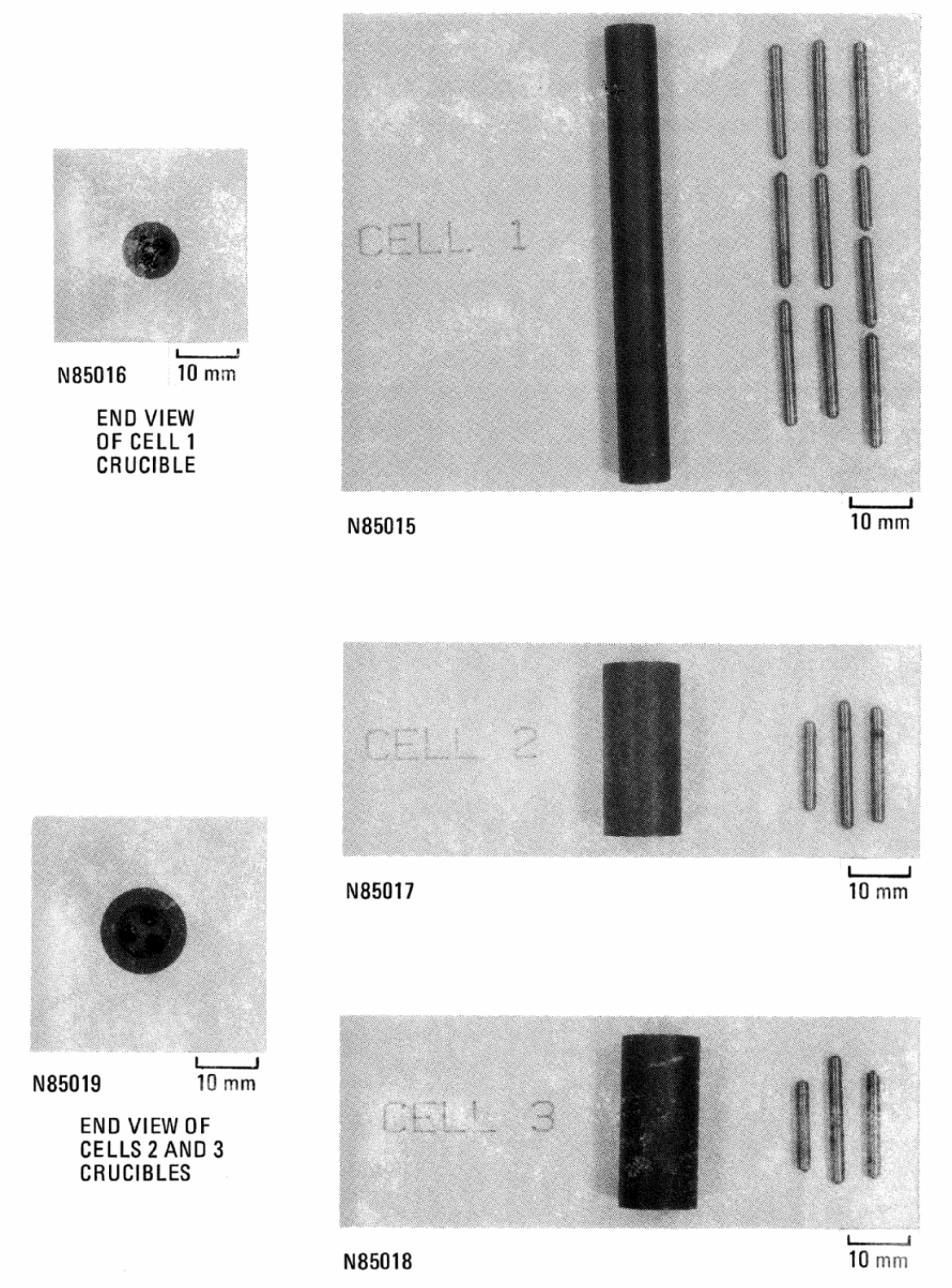

Fig. 4-11. Encapsulated piggyback samples and their graphite crucibles

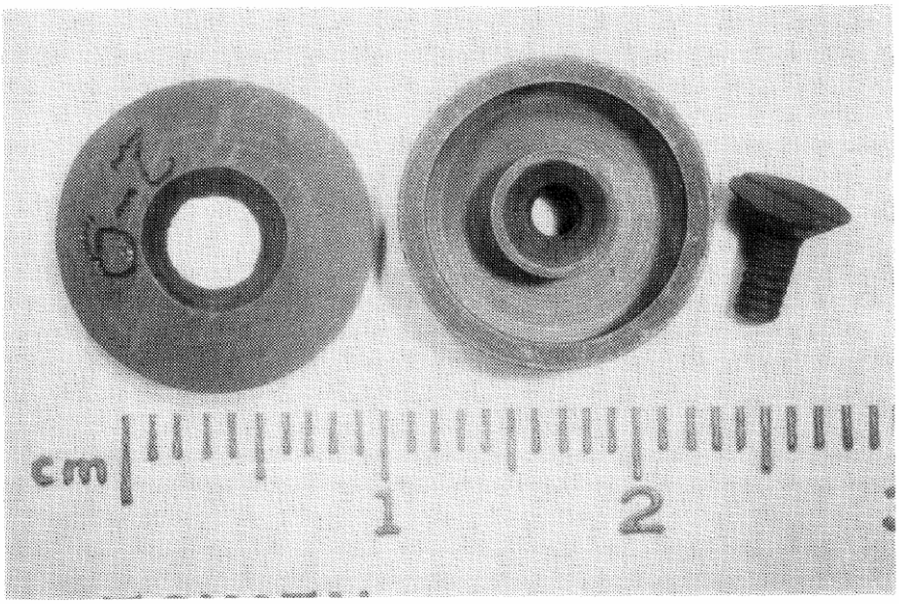

N85012–1 (a)

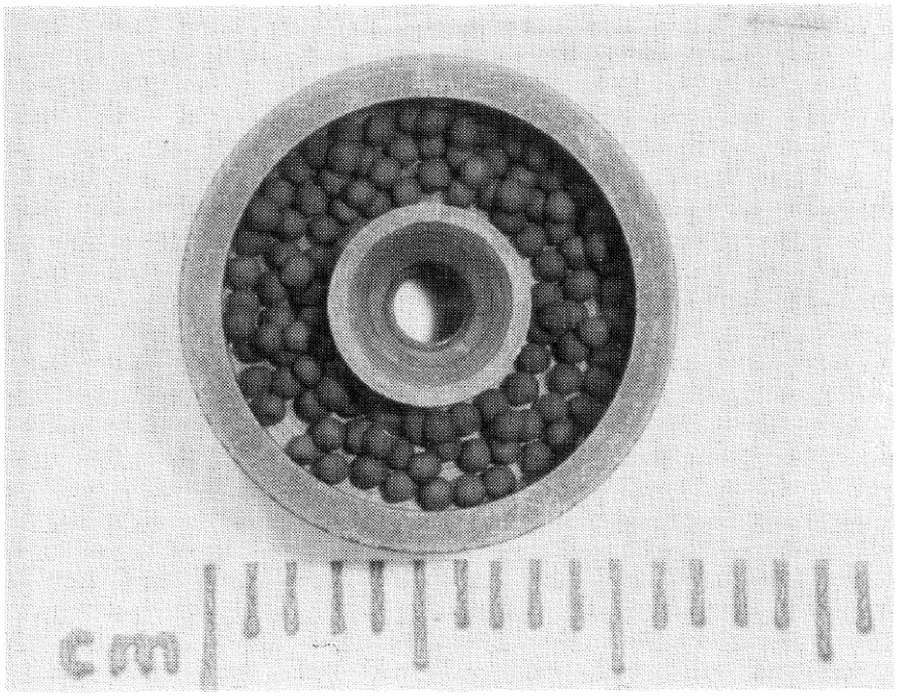

N85012–4 (b)

Fig. 4-12. Loose particle samples in trays

4.2.3.3 Non-Fueled Piggybacks

Inert particle compacts were irradiated in piggyback positions in HFR-B1 as part of an ongoing study at GA to investigate possible process improvements resulting from heat-treating the compacts in SiC granules instead of the present reference alumina powder. During the HFR-B1 compact fabrication run, 24 compacts were made with a volume of inert particles equivalent to the volume of fuel particles in the capsule compacts. Shim volumes, matrix, and pressing conditions were all identical to those for the regular production run. Fourteen of the 24 were then carbonized and fired in SiC powder in place of alumina. Eight of these inert particle compacts were fired in the conventional manner in alumina powder for comparison purposes.

KFA supplied SiC rings for piggyback irradiation in HFR-B1. These are circular sections of SiC coatings from TRISO particles that were to be used to determine the effects of irradiation on the strength of SiC. All the ring samples were contained in a single, small graphite crucible that was placed in the top section of the Cell 1 central piggyback cavity.

Samples of H-451 and H-451-I graphites ("I" for improved, a candidate replacement graphite for H-451 that is the reference fuel-element graphite) in the form of short cylinders (~15 mm diameter x ~14 mm length) were stacked in the simulated coolant holes of graphite bodies 2 and 3. The purpose of these samples in Cell 2 was to compare dimensional changes, coefficients of thermal expansion, and Young's modulus changes as a function of fast fluence between the two graphite types. Those in Cell 3 were used to measure the effect of water oxidation during irradiation on the tensile strength and Young's modulus.

4.2.4 Graphite Bodies

Each of the three cells in capsule HFR-B1 contains a graphite body housing all fuel and piggyback samples in a well-defined configuration and providing for all necessary in-cell instrumentation. The bodies were machined from a single log of H-451 graphite (to the dimensions and specifications on GA Drawings 027956, 027955, and 028251.

The Cell 1 fuel body differs considerably from bodies 2 and 3 in that it is actually an assembly of many parts. The assembly consists of six wedges surrounding a small, inner ring all held together within a larger, outer ring. Standoff pads on the wedges create 1-mm gaps between all parts to allow for coolant flow and quantifiable fission product transfer during irradiation. Three of the wedges contain fuel holes where the fuel compacts were stacked. The other three wedges were "sinks" for fission products released from the fuel during irradiation. The sink wedges were made many times more sorptive than regular graphite by impregnation with a furan resin. Also, in order to study the combined effects of oxidation and neutron irradiation on metallic fission product transport in graphite, one of the fuel wedges was oxidized to -1 wt. % burnoff. End disks secured to the sink wedges with graphite screws complete the assembly. All

piggyback samples in Cell 1 were contained within the central, inner ring that has threaded caps at each end. Figure 4-13 shows the completed Cell 1 fuel body.

Fuel bodies 2 and 3 (GA Drawing Nos. 027955 and 028251) were identical except for their outside diameters. They contained the same fuel hole pattern as body 1, but in a single cylindrical block. Between the fuel holes were simulated coolant holes so that these bodies closely resemble the configuration to be found in a prismatic HTGR fuel element. Piggyback samples in these bodies occupied the central holes (fueled samples only) and all the simulated coolant holes (unfueled samples only).

For all three bodies, stepped diameters on the outer circumferences aided in minimizing temperature differences within the fuel stacks, and standoff pads centered the bodies within the metal containment canisters. All fuel and simulated coolant holes and the central holes in bodies 2 and 3 had plugs at the bottom of each hole and threaded caps at the top. The plugs fit with a light press at the bottoms of the holes and provide a means to push the fuel or piggyback stacks out of the bodies after irradiation, should this be necessary during remote disassembly.

Identification marks on the bodies uniquely identified each fuel and piggyback hole. Fuel holes 1, 2, and 3 on each body are identified with one, two, or three small, shallow holes (0.040 in. diameter, 0.125 in. deep) adjacent to each fuel hole on the top ends of the bodies and on the plugs and caps for each fuel hole. Simulated coolant holes in bodies 2 and 3 were similarly identified with the letters A, B, and C on the plugs and caps of each hole. Bodies 2 and 3 themselves had Roman Numerals II and III, respectively, scribed on their sides as shown in Figs. 4-14 and 4-15. Sink wedges in Body 1 were uniquely identified with shallow holes (same as for the fuel holes) giving their location with respect to the fuel wedges as shown in Fig. 4-13. Fuel wedge #1 in Capsule 1 was the oxidized fuel wedge.

The release rate-to-birth rate ratios (R/Bs) of the 12 groups of three compacts selected for capsule use ranged from 1.36 to 4.43 x 10^{-5} with an average of 2.43 x 10^{-5} Kr-85m at 1000 ^{o}C. The compacts have been placed within HFR-B1 in such a way that the individual cell R/Bs at start of irradiation will be 1.66, 1.18, and 1.89 x 10^{-5} Kr-85m for Cells 1, 2, and 3, respectively, corrected for BOL temperatures.

Additional information about the three fuel bodies is contained in the preirradiation report (Ketterer 1985a).

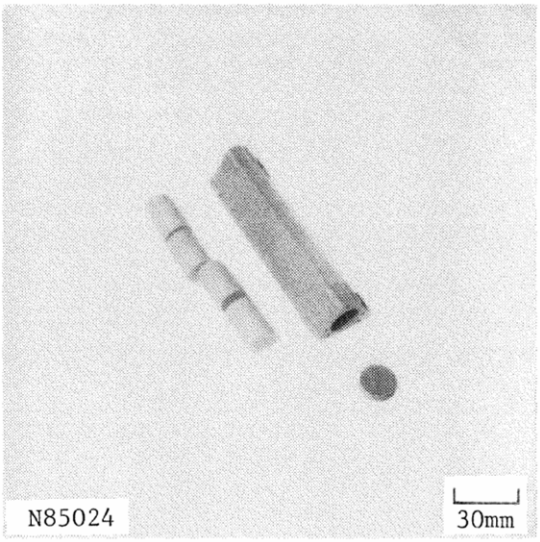

FUEL WEDGE WITH COMPACTS AND CAP

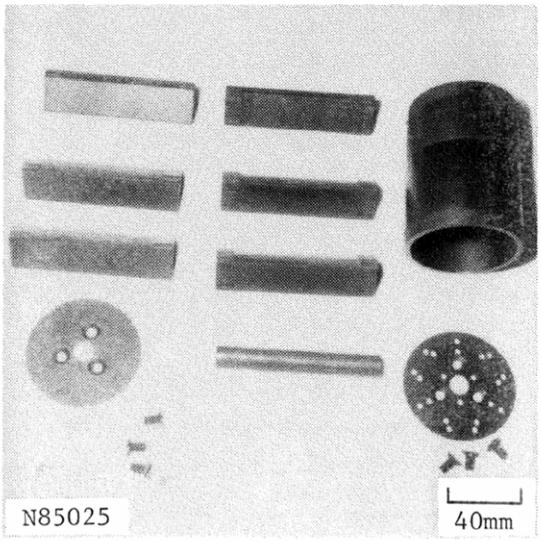

SEPARATE PARTS OF FUEL BODY 1

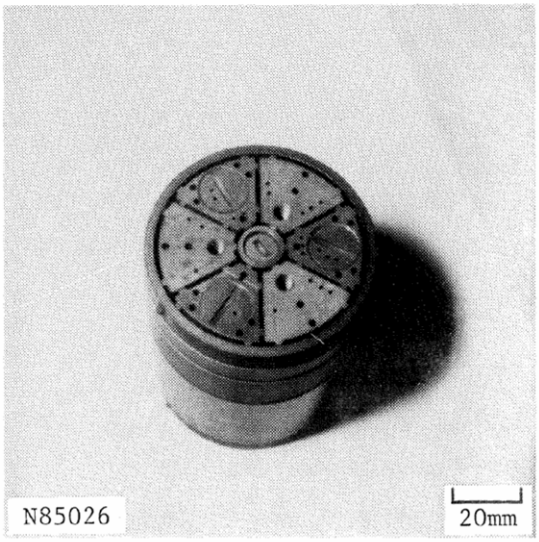

TOP END VIEW OF COMPLETED ASSEMBLY

Fig. 4-13. Capsule 1 fuel body

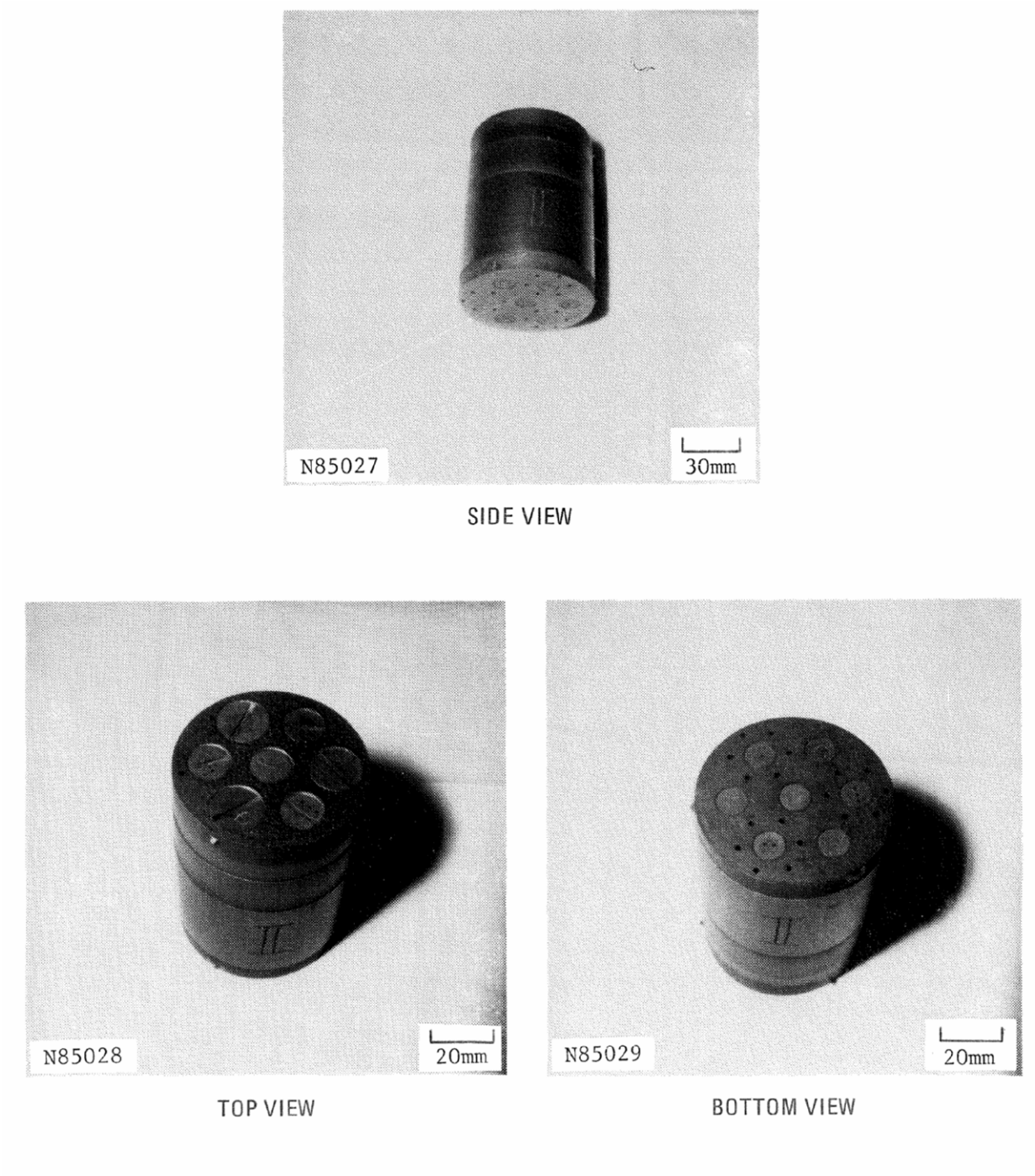

Fig. 4-14. Capsule 2 fuel body

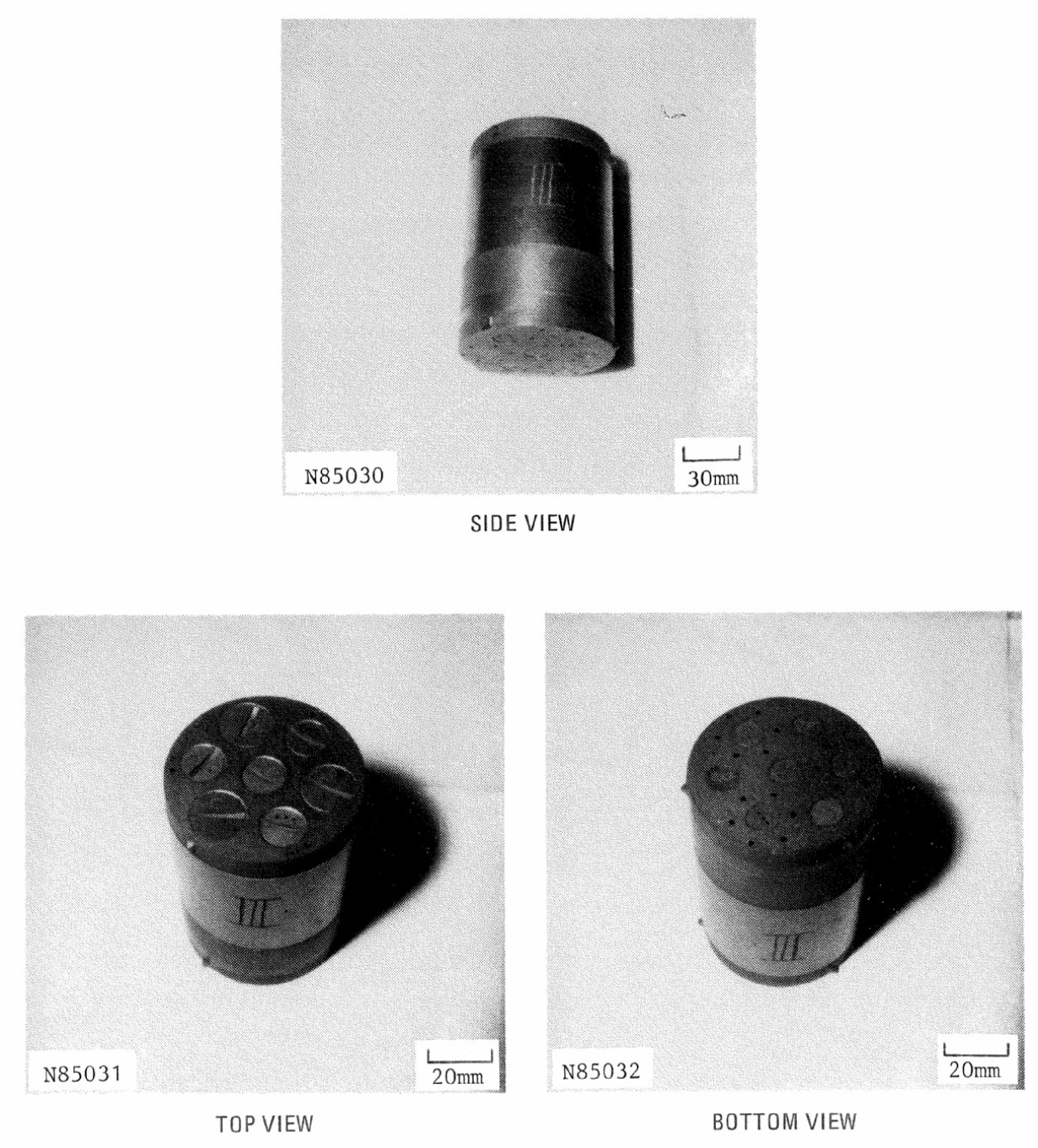

Fig. 4-15. Capsule 3 fuel body

5 IRRADIATION PHASE

The irradiation of the HFR-B1 experiment was carried out in 20 reactor cycles, starting on April 7, 1987 (HFR cycle 87.3), and ending on July 10, 1989 (HFR cycle 89.6). During the first year of operation, the rig was removed from the core for a total of five cycles. The length of each HFR irradiation cycle was between 20 and 26 days, and the total duration of the irradiation was 444 EFPD. There were normally 3 to 6 days between each cycle with the exception of the maintenance shutdowns that occurred in March and August for periods of 30 and 45 days, respectively.

The D214.01 (JRC Petten designation for HFR-B1) rig was irradiated in core position F8 or F2. The rig was turned 180^{o} after each cycle. The vertical displacement units were used only in the first four cycles; thus, the axial positions were constant for the remaining 16 cycles. Capsules 1 and 2 were in the axial midplane of the core and received similar neutron fluences, while Capsule 3 was below midplane.

Before the start of each cycle, instructions about the conduct of experiments during the cycle were given to technicians and reactor operators. Instructions for special tests, such as the addition of water vapor and hydrogen to Capsule 3, were included along with any requests to accelerate monitoring via the gas chromatograph (GC) and/or the multi-channel analysis (MCA). At least 24 hours before the start of each cycle, purge gas flows and pressures were reestablished in all capsules. The HFR was normally brought to power, 42 to 45 MW, within about 8 hours. Scheduled reactor stops were either at 24 or 16 hours of the last day of the cycle and were accomplished by rapid insertion of control rods. Consequently, temperatures in all experiments declined rather quickly.

The helium used in all capsules was the normal reactor "service He" and was purified by a "deox" and by molecular sieve beds for the removal of oxygen and water vapor, respectively. A final ultrapurification was accomplished with the use of a bed of activated carbon at liquid nitrogen temperature. The Ne used was purified by only the deox and molecular sieve methods.

MCA measurements were usually started on the second day of the cycle. Nine isotopes of Xe and Kr were measured in the effluent gas from each capsule once daily, except during special tests involving, for example, water vapor addition to Capsule 3 or temperature cycling in Capsule 2; in such cases, data were taken more frequently. Procedures for and conditions of the specific capsules are given below.

The planned HFR-B1 test program and the test articles fabricated by GA are described in the preirradiation report (Ketterer 1985a). The test rig assembly and the actual conduct of the test at JRC Petten are described in the operating history report (Burnette 1994). Those two key

documents are excerpted in this section. The summary information in the tables and figures is from the operating history report (Burnette 1994).

5.1 Description of Equipment

5.1.1 HFR Petten

The HFR at Petten, the Netherlands, is a materials test reactor that contains water as coolant and moderator (Burnette 1994). The normal reactor operating power is 45 MW. The core lattice is a 9 by 9 array (729 by 750.4 mm), containing 33 fuel assemblies, 6 control members, 19 experimental positions, and 23 beryllium reflector elements. The reactor is normally operated at full power for 11 cycles per year of 25.7 days each, with 2- to 6-day shutdown between cycles for refueling, maintenance, and for installation or removal of test rigs. There are two month-long shutdowns for extended maintenance and holidays per year, in March and in August. In-core test positions can provide a thermal flux up to 2.1 x 10^{18} $m^{-2}s^{-1}$ and a fast flux up to 5.1 x 10^{18} $m^{-2}s^{-1}$. The HFR staff provides all services associated with the reactor and also the 24-hour operation of all irradiation experiments.

5.1.2 Test Facility

5.1.2.1 In-Pile Rig

The irradiation rig was designed and fabricated at JRC Petten (Conrad 1985). The rig, designated D214.01, was a modification of the Brennelementsegment (BEST) rig type, shown in Fig. 5-1, which was successfully used in the irradiation of German high-temperature reactor (HTR) fuel. The D214.01 in-pile rig was connected to out-of-pile equipment, called the "Sweeploop," which has provision for controlling and monitoring up to six independent capsules. The rig consisted of three capsules, in-line, each of which was independently temperature-controlled and monitored, and had independent gas purge lines for the introduction of various gas mixtures, including He, Ne, H_2, and H_2O. Temperatures were adjusted by the introduction of He-Ne mixtures in the sweep gas. The capsules were contained by a stainless steel tube of 74 mm diameter that ended at approximately 975 mm above the core centerline. This tube served as a protection tube and bounded the cooling water channel on the interior. Capsules 1 and 2 were connected to each other and could be adjusted vertically by means of an electrically driven vertical displacement unit (VDU) for the purpose of changing temperature or flux. Capsule 3 could be moved by an independent VDU.

Of primary importance in this test was the monitoring of individual gas lines for the measurement of fission gas release and the gaseous products of fuel hydrolysis and graphite oxidation. Figure 5-2 is a schematic of the gas lines within the rig and rig head, showing the

separate lines in and out for each capsule. Two gas lines enter each capsule, the inlet at the

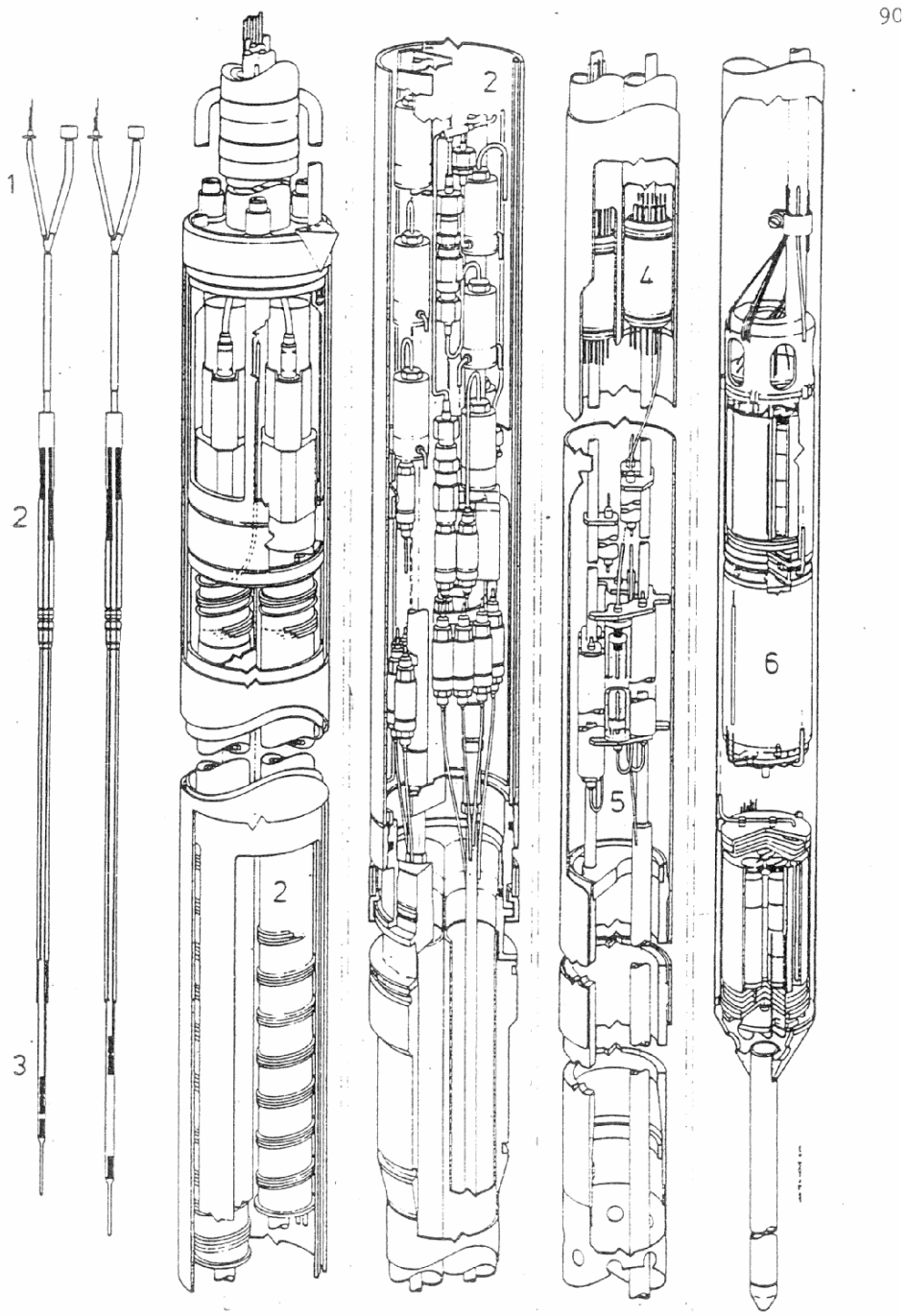

Fig. 5-1. BEST irradiation rig used for HFR-B1 test

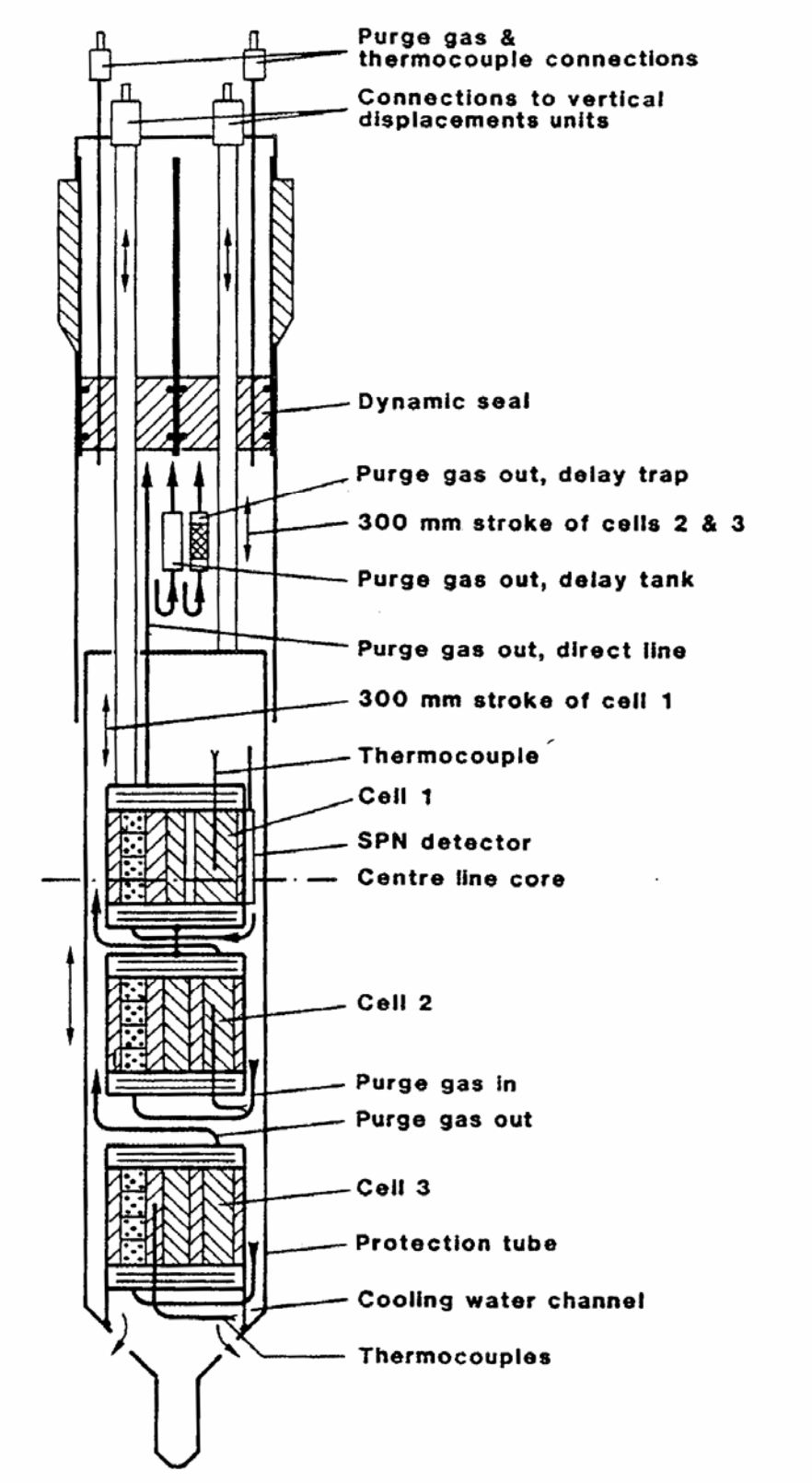

Fig. 5-2. Schematic of the HFR B1 test rig

bottom and the exit at the top. The exit gas could flow directly to the sampling stations, or before entering the sampling station in the case of elevated radioactivity levels, through an empty 360-cm^3 delay tank or through a 360-cm^3 charcoal delay bed. These flow paths could be chosen by means of remotely operated solenoid valves within the rig head.

5.1.2.2 Out-of-Pile Facility

The out-of-pile system, the “Sweeploop,” was designed and constructed specifically for irradiation of HTR fuel and graphite specimens. Before the HFR-B1 test, the Sweeploop had been used in a number of irradiations of German pebble bed fuel. The major component of the Sweeploop system is a "once-through system that provides purified gases at controlled pressures and flows and permits the sampling and monitoring of fission and gaseous products of hydrolysis and oxidation in as many as six separate capsules.

5.1.3 Assembly and Commissioning

The irradiation rig was designed by JRC Petten and manufactured and assembled by subcontractors (i.e., the in-pile part by ECN Petten and the instrumentation rig head by NTG Gelnhausen). The fuel compacts and graphite bodies were assembled by GA according to JRC plans, including dimensions and provisions for thermocouples (TCs) and gamma-scan wires. The bodies were shipped to Petten fully assembled except for the KFA SiC rings, which were inserted by JRC into the central hole of the fuel body in Capsule 1. The final commissioning of the rig was accomplished by JRC QA.

All required checkout activities were accomplished by ECN Petten during and after assembly. The required checks are described and certified in the assembly report (unpublished). The final checkout of the rig was accomplished by JRC QA. They repeated all of the required tests before and after installation and connection to the Sweeploop system. A final check of the safety and functionality of the test rig was performed by the HFR review committee prior to test authorization.

5.2 Irradiation History

5.2.1 Capsule 1

Capsule 1 was intended to operate at steady-state conditions of temperature, neutron flux, and gas environment. Neon was never added, and temperatures tended to fluctuate from cycle to cycle due to changes in reactor power, declining capsule power, changes in gas gaps and thermal conductivity in the fuel body, and occasional changes in neutron moderation or absorption in adjacent tests in the reactor.

The mean temperature of the graphite body was 790 ± 30 °C; the estimated fuel temperatures were between 880 and 990 °C. The gas environment was pure helium with less than 1 ppm of impurities, such as CO, CO_2 , O_2, or H_2. During operation at temperature, the outlet gas usually showed trace impurities of about 2 ppmv H_2, and about 0.1 ppmv CO and CO^2. The gas flow rate was constant at 300 ± 10 cm^3/min at standard conditions of 0.1 MPa and 298 K. The inlet pressure was nominally 0.4 ± 0.02 MPa, while the outlet pressure was 0. 36 ± 0.02 MPa.

5.2.2 Capsule 2

Capsule 2 was intended to operate over the accessible range of temperatures with the maximum being near the highest temperature expected in the core of an HTGR. The measured mean temperature of the graphite body was 870 ± 35 °C, and the estimated fuel temperatures were between 880 and 1,230 °C. The latter range in temperature was achieved by adding neon to the sweep gas in half of the reactor cycles to a maximum fractional concentration of unity. For each 1% of neon added, the temperature increased about 3.5%; the maximum increase was 350 °C. The effect of temperature on fission gas release at constant nuclear conditions was determined by varying the temperature in some cycles as frequently as two to five times. The flow rates, pressures, and gas impurity concentrations were similar to those of Capsule 1. Whenever neon was added, however, impurity measurements could not be made with the gas chromatograph due to the overlap of the huge neon elution peak with that of the trace impurities. During these periods, the outlet impurities were inferred from the Capsule 1 data and from the inlet gas measurements.

5.2.3 Capsule 3

The purpose of Capsule 3 was to measure the effect of water vapor on fission gas release from exposed UCO fuel over a temperature range for which the graphite surrounding the exposed fuel would not react with the water vapor at the lowest temperatures but would react at the higher temperatures. The mean temperature of the graphite body was 742 ± 30 °C, and the estimated fuel temperatures were between 820 and 1050 °C.

There were 16 water vapor injections that, except for two, had a duration of 4 to 10 days. The partial pressures ranged from 18 to 1,060 Pa. The final water vapor injection was started 16 hours before the end of the irradiation for the special purpose of determining whether volatile iodine (such as methyl iodide) would be formed.

Water vapor was added to the Capsule 3 inlet gas in the following way. First, the normal He inlet was replaced with a special source which was part of the “water vapor generator” system. This system comprised a bypass flow that bubbled through a water column at ambient temperature, after which it was mixed with dry helium. Knowing the temperature of the water column and therefore the partial pressure of water vapor, the flow rate through the water, the

total mixed flow rate, and the absolute pressures above the water column and at the inlet to the capsule, the concentration of water vapor in the mixed gas inlet could be calculated.

In several of the tests, an absolute frost point-type moisture monitor (General Eastern Model MI-1) was used to calibrate the water vapor generator system and to check on the accuracy of the methods of calculation. The calibrations corroborated the moisture generation system performance and calculations. The water vapor concentrations were known in the last 11 tests to be better than ±10%. In the first five injection tests, the flow rate through the bubbler was not known; rather, reliance was placed on readings of Panametrics capacitance-type cells. These cells were found later to yield low values. The true water vapor concentrations in these tests were inferred from an analysis based on the rate of graphite oxidation as determined by the GC measurements.

In two of the cycles, 100 Pa of hydrogen was added to the inlet gas, along with the water vapor, to determine the effect of H on the interaction of water vapor with the UO_2. This was accomplished by switching the normal He supply to a special tank containing 1,000 ppm hydrogen. The valving was arranged so that the H_2 could be turned on or off at any time during the test.

GC measurements were normally performed once a day for all capsules except Capsule 3 during the water vapor injection tests when measurements were made more frequently. Often, the GC was put on automatic cycle, so that any changes in oxidation rate would be readily detected.

5.3 Experimental Data

The irradiation of the HFR-B1 test rig in HFR Petten generated a huge volume of test data, most of which was logged electronically. The essential test data are documented in the operating history report (Burnette 1994). This section is intended to provide an overview of that report. The serious reader, especially anyone intending to perform an independent review of past test evaluations (see Section 7) or to perform a new evaluation of the test data, is encouraged to obtain and peruse the operating history report.

The key data for the HFR-B1 test can be categorized as follows: (1) nuclear data (power, burnup, and fast fluence), (2) temperatures, (3) fission gas R/Bs, and (4) coolant impurity data. The recommended values of these test parameters for each of the three capsules as a function of irradiation time are given in Section 6 of the operating history report (Burnette 1994). In Section 4 of that report, the data are described, and examples are given. Excerpts of the Section 4 descriptions and some examples of the primary test data are given below, following a brief description of the data archiving protocols.

5.3.1 General

The number of experimental data accumulated during irradiation of the HFR-B1 experiment was so large as to preclude presenting most of the raw data in the operating history report (Burnette 1994). According to that report, the HFR-B1 data documentation is organized in the following categories: (1) data files, (2) laboratory recorded data, (3) graphics and associated data, (4) GC data, and (5) postirradiation iodine decay data. All of these data have been given by JRC Petten to the ORNL Nuclear Fuel Section of the Metals and Ceramics Division. These data categories are described briefly below.

5.3.1.1 Data Files

A magnetic tape was generated in the HFR Vax-4300 System at Petten. A copy of this tape is available at ORNL. This tape contains 1,457 files and 270,464 blocks of data in three directories for the HFR-B1 experiment. The files include those with (1) the steady-state fission gas release values (R/B) for all capsules and cycles for both the total fissile loading and for the loading in the dtf particles only; (2) the plots of these R/B data as a function of time along with a reference temperature profile; (3) the vertical displacement history; (4) the activity history for the three capsules; (5) all TC temperature histories; (6) power and control rod histories; (7) shape factors (related to the axial distribution of neutron fluxes); (8) process data including flow, hygrometer, and pressure data; and (9) Sweeploop data including gas composition, pressure, hygrometer, and reference temperature data.

5.3.1.2 Laboratory Recorded Data

The principal data relate to the counting of the gaseous isotopes ^{85m}Kr, ^{87}Kr, ^{88}Kr, ^{89}Kr, ^{90}Kr, ^{133}Xe, ^{135}Xe, ^{135m}Xe, ^{137}Xe, and ^{l38}Xe. Associated with each counting are the specific capsule, date, spectrum number, sample collection time, start of counting time, reference temperature, flow rate and pressure, and the net number of counts for each isotope that is used in computing the steady-state fractional fission gas release, R/B. These data obtained during the irradiation, as well as associated data for all 20 cycles, were recorded in 11 ring-binder notebooks.

5.3.1.3 Graphics and Associated Data

The graphic displays and associated data obtained include: (1) power profiles in fuel compacts and piggyback samples; (2) burnup profiles with separate contributions from ^{235}U, ^{239}Pu, ^{241}Pu, and ^{233}U for fuel compacts and piggyback samples; (3) tabular power data and neutron fluxes; (4) tabular ORIGEN calculational data for each cycle for the profiles of (1) and (2) at nominal and maximum fluxes; (5) R/B profiles at 8.9 and 100% fissile power and corresponding reference temperature profiles for each cycle of each capsule; (6) profiles of the activity, pressure, hygrometer readings, and purge flow, and the self-powered neutron (SPN) detector outputs; (7) comparison profiles of the reference temperatures in Capsules 1, 2, and 3 for each

cycle; and (8) temperature profiles for each cycle associated with three fuel compacts and with each fueled graphite wedge in each capsule.

5.3.1.4 Gas Chromatographic Data

The GC data consist of the time histories of the products of hydrolysis of the carbonaceous components of the fuel elements in the three capsules, mainly CO, CO_2, H_2, and CH_4. In addition, the chart records of the multichannel recorder for pressures, selected temperatures, flow rates, and other process and Sweeploop quantities accompany the GC records.

5.3.1.5 Postirradiation Iodine Decay Data

The postirradiation measurements of the xenon isotopes resulting from the radioactive decay of iodine released from exposed kernels during irradiation and the corresponding spectral analyses leading to the net area counts for the xenon isotopes 133Xe, 135Xe, and 135mXe were obtained in the form of computer printouts. These data covered the measurements of the xenon isotopes after the termination of irradiation in cycles 88.10, 89.02, 89.04, 89.05, and 89.06.

5.3.2 Nuclear Data

The nuclear quantities and the fission power per capsule and fuel compact stack for each cycle and fuel element position are calculated, post-cycle, using the HIP-TEDDI computer code (Conrad 1980). This calculation yields volume-average data over a vertical distance (length) of 60 cm. The neutron flux and fluence values for a specific vertical location are obtained by using the curve of relative vertical neutron flux distribution for the fuel element positions used, F2 and FS3, and the shape factor that is the ratio of a specific flux to the average neutron flux. An example of the postcycle, HIP-TEDDI, volume-average nuclear data for cycle 89.06 (final cycle) is shown in Table 5-1. Such data are provided for all 20 irradiation cycles in Section 6 of the operating history report (Burnette 1994). The volume-average power generation rates and burnups for the fuel compacts are shown in Figs. 5-3 and 5-4, respectively. Similar tabular and graphical data for the fueled piggyback samples are also given in the operating history report.

5.3.3 Temperatures

For measuring the temperature, there were 18 TCs in each capsule located at three depths in the graphite bodies. The TC locations are shown in Figs. 4-1, 4-2, and 4-3. The TCs in Capsules 1 and 3 were type “K” with a sustained temperature limit of 1,000 °C. In Capsule 2, where temperatures were sometimes higher, 12 type “N” TCs (1,150 ^{o}C sustained limit) were used along with 6 type K thermocouples. The type K TCs were sheathed in stainless steel, and the type N had Inconel sheaths. All TCs were surrounded by niobium protection tubes.

TABLE 5-1
POST-CYCLE HIP-TEDDIE NUCLEAR DATA (CYCLE 89.6)

Cycle : 89.06
Position : F 8
Orientation : South

	Start-up fluence rate m^-2 s^-1*E 18	Neutron fluence m^-2*E 25	Cycle averaged fluence rate m^-2 s^-1*E 18
Neutron flux 1 E> 1.353 MeV	0.581	0.108	0.579
Neutron flux 2 1.353MeV>E>.0674MeV	1.044	0.194	1.04
Neutron flux 3 .06[illegible]MeV>E>.683 eV	1.388	0.259	1.388
Neutron flux 4 E<.683 eV	0.838	0.160	0.857
Fission flux	0.768	0.143	0.766
2200 m/s flux	0.774	0.147	0.788
Neutron flux E>1 MeV	0.732	0.136	0.729
Neutron flux E>.1 MeV	1.521	0.283	1.516
DAR Graphite (1)	2.227	-	-
Damage flux Graphite	1.808	0.336	1.800
EDN [illegible]lux (2)	0.994	0.185	0.991
Nuclear heating W/g	3.35	3.44	-
DPA Graphite (3)	-	0.244	-
Axial shape factors (4)			
- fast fluence	-	1.260	-
- thermal fluence	-	1.230	-
Full power days	-	21.60	-

(1): Damage to activation ratio for graphite
(2): Equivalent DIDO Nickel Fluence
(3): Displacement per Atom
(4): max/average

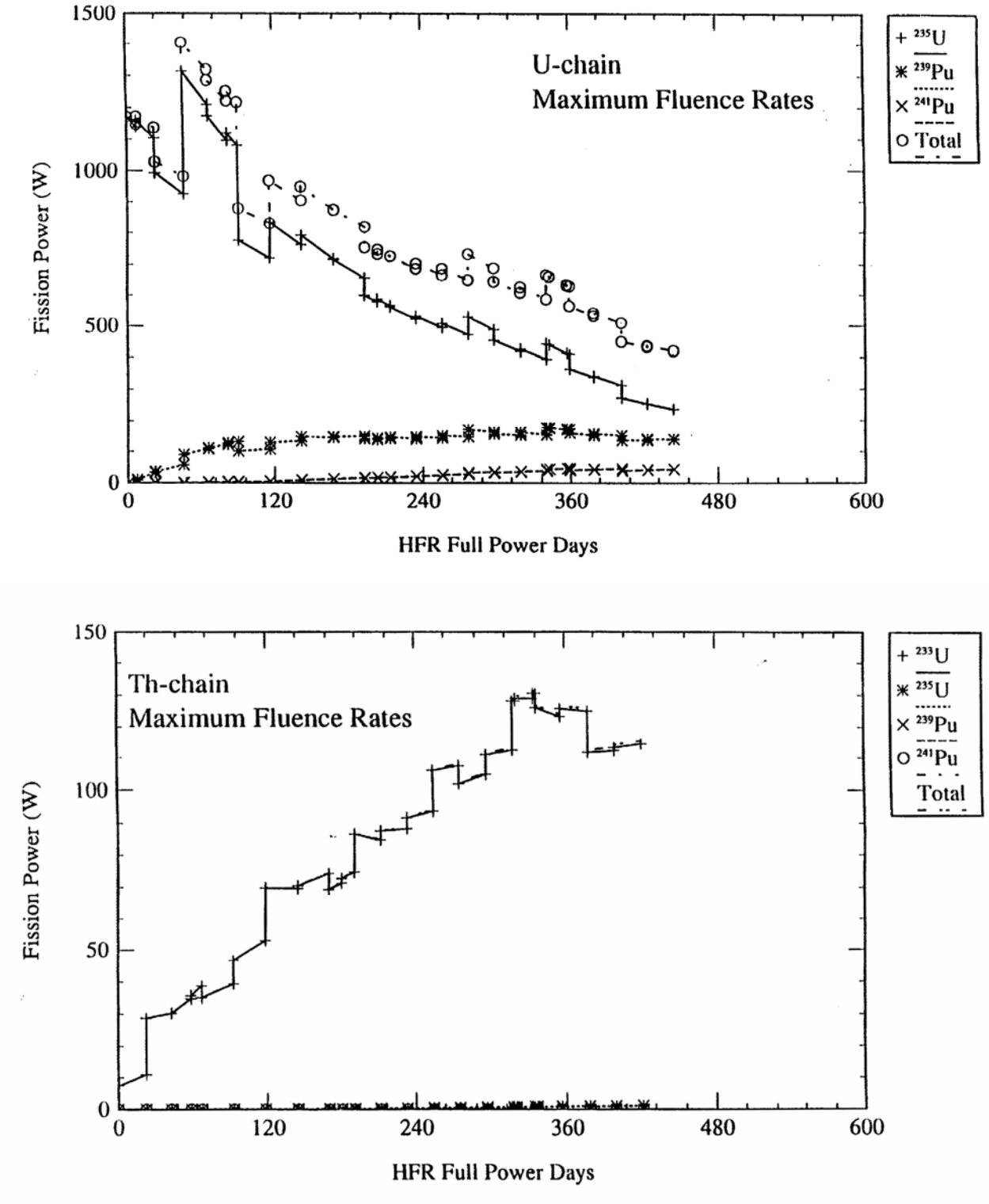

Fig. 5-3. Power production in HFR-B1 compacts

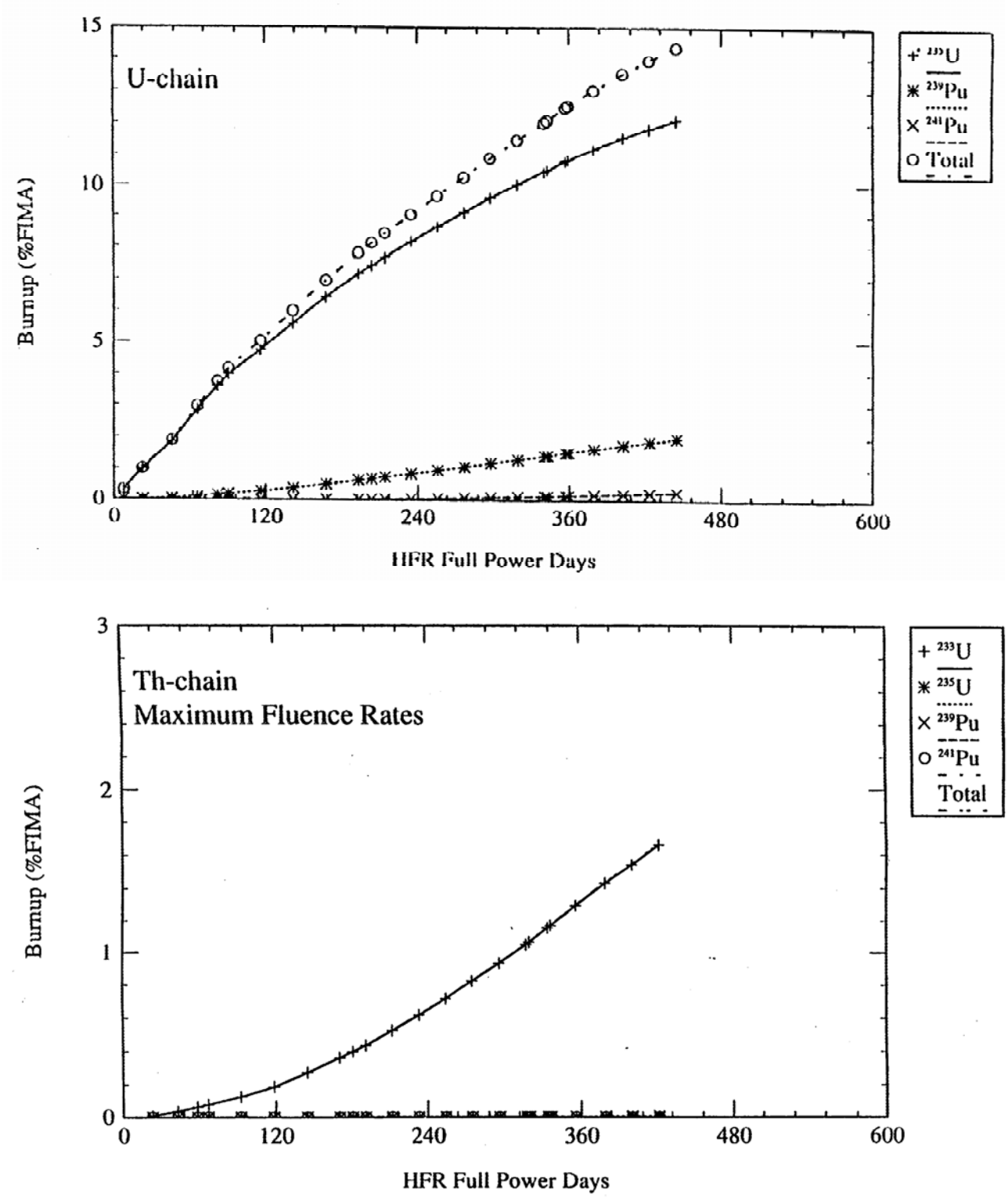

Fig. 5-4. Burnup in HFR-B1 fuel compacts

In Capsule 1, each stack of fuel compacts in alternate graphite wedges was surrounded by five TCs located at three radial distances, and in the sink graphite wedges, there was one TC (see Fig. 4-1). In Capsules 2 and 3, each of the stacks of fuel compacts per capsule was surrounded by six uniformly spaced TCs at a common radial distance from the centerline of the fuel compact stack (see Figs. 4-2 and 4-3). The TC temperature histories were recorded and stored on the magnetic tape by the HFR Vax-4300 System. Two examples of the temperature histories are presented in Fig. 5-5 for cycles 88.05 and 89.05, respectively. In both cases, TC profiles in Capsules A, B, and C (more generally referred to as Capsules 1, 2, and 3, respectively) for TCs numbered 12, 30, and 43, respectively, are shown.

Often, the temperature in a capsule during a single cycle was approximately constant as shown in Fig. 5-5 for TC #12 (Capsule A); however, in Capsule B (TC #30), the temperature was changed occasionally to investigate the temperature dependence of fission gas release at temperatures above 1,100°C. Note that in these figures, the temperature values are those of the graphite bodies. The fuel temperatures will be higher by approximately 100 to 150 °C.

5.3.4 Fission Gas Release

5.3.4.1 Fission Gas Measurement

The concentration of released noble gases was monitored using a Canberra multichannel analyzer along with a Canberra high-efficiency Ge(Li) gamma detector. The system was calibrated once or twice a year, during reactor shutdown periods. Four isotopes of krypton and five isotopes of xenon were routinely measured during irradiation. At the end of several cycles, measurements of Xe isotopes continued, for the purpose of determining the fractional releases of iodine isotopes with resolvable Xe daughters (i.e., ^{133}I and ^{135}I).

The Canberra MCA assays the entire gamma spectrum and with the use of the Spectran F (version 2.07) program integrates the number of counts above background in each photopeak, prints out the net counts associated with each gamma line, and identifies each line with possible isotopes. Subsequently, the counts per minute (cpm) data for each isotope were used to calculate R/B values, using a computer code called RUBICON.

5.3.4.2 Data Reduction

The R/B values calculated with the RUBICON code are rigorously correct only for the following three restrictive conditions characteristic of the beginning of the irradiation:

1. Fission gas is released from only those fuel particles with exposed kernels. Shortly after the beginning of irradiation, the number of particles with exposed kernels is equal to the number of dtf particles; the dtf particles fail shortly after the beginning of irradiation, leaving the kernels exposed.

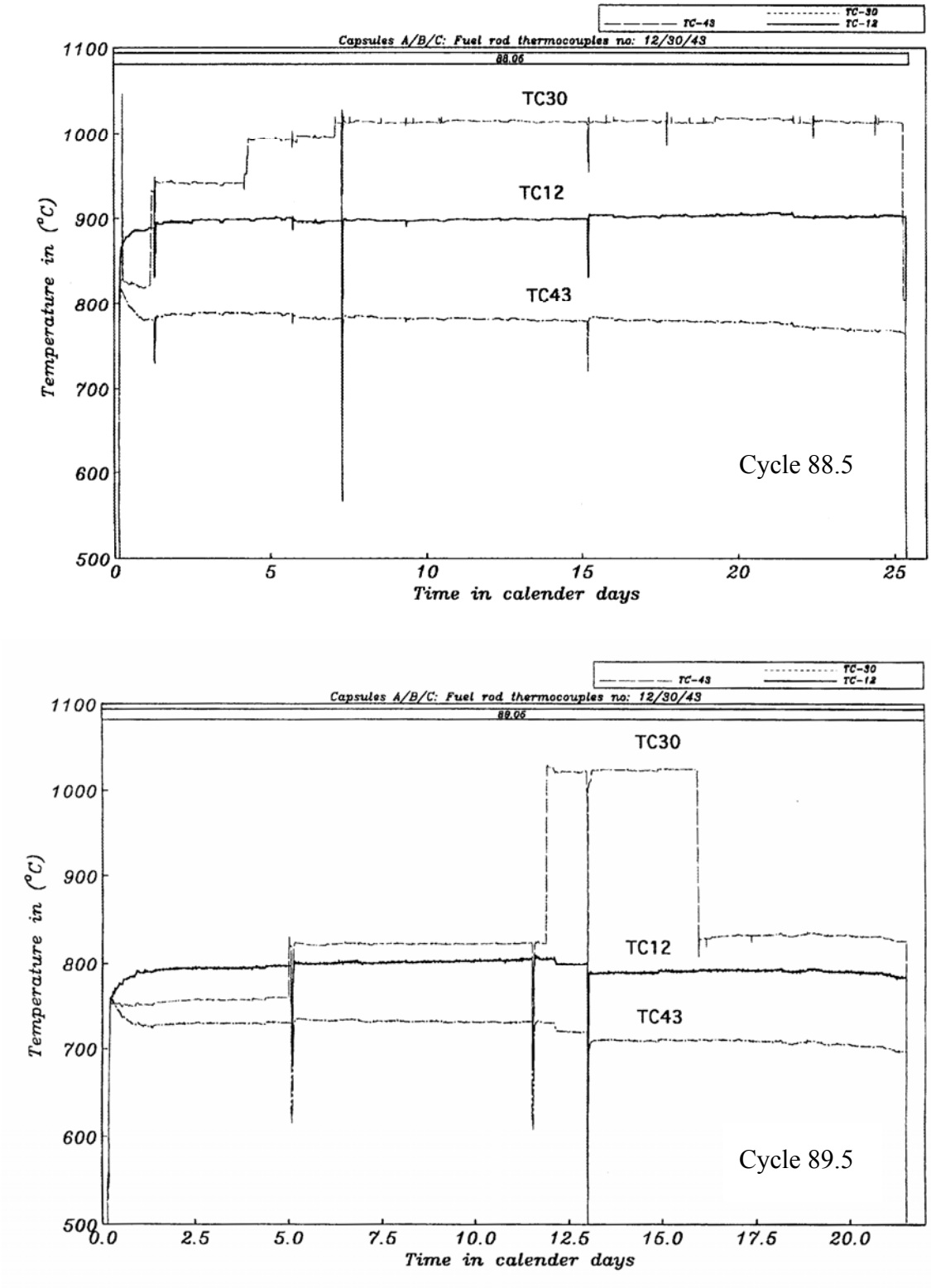

Fig. 5-5. Temperature histories for irradiation cycles 88.5 and 89.5

2. The power in the UCO particles with exposed kernels is that at the beginning of irradiation in the dtf particles.
3. The dtf particles contain UCO, and the fission gas generated is the result of the fissioning of ^{235}U only; hence, the yields of fission products are those corresponding to the fissioning of ^{235}U only.

To account for the changes in the number of exposed kernels, power, and yields as irradiation proceeds, the R/B values calculated under these restrictive conditions must be corrected. At the beginning of irradiation, there were fertile fuel particles containing ^{232}Th and fissile fuel particles containing ^{235}U and ^{238}U; the initial weight ratio of $^{232}Th/^{235}U$ was 5.82. As the irradiation proceeded, the concentration of the fissionable isotopes ^{233}U in fertile fuel particles and ^{239}Pu and ^{241}Pu in fissile particles grew while the concentration of ^{235}U declined. Thus, the power has to be calculated as a function of time for the fertile and fissile particles.

Similarly, as the isotopic composition of the fuel particles changes with time, the yield of any fission product isotope has to be recalculated to account for the various contributions to the overall yield by the fissionable isotopes. Shortly after the beginning of irradiation, the dtf particles failed in a manner that exposed the UCO kernels. Previously, experience in experiment HRB-17/18 (Ketterer 1987) demonstrated that all dtf particles failed within 50 hours of beginning irradiation. The failure of each dtf particle was recorded as a distinct spike in the signal from an online ionization chamber. In the HFR-B1 experiment, the R/B profile reached a plateau after 500 hours, indicating the completion of the failure of the dtf particles. The longer time for complete failure in the HFR-B1, as compared with the HRB-17/18 experiment, is attributable to the difference in fission rate density that was an order of magnitude smaller in the HFR-B1 experiment. Thus, shortly after the beginning of irradiation, there were 87 exposed kernels per compact and 1,044 exposed kernels per capsule.

During the remainder of the irradiation, the possibility of failure of the normally configured particles has to be addressed. On the basis of an experiment in another reactor, the R2 reactor at Studsvik, Sweden (a reactor with similar neutron spectral characteristics), one would expect the failure of normally configured fertile or fissile particles during irradiation for about the same reactor time (444 EFPD) to be 0.5 ± 0.1%. The latter corresponds to about 7 particles per compact that would be expected to fail during the irradiation. This number of failures would correspond to 8% of the dtf particles; the uncertainty in the R/B is estimated to be about ±15% so any failure of the driver fuel particles during irradiation should not introduce a significant error.

5.3.4.3 Reported R/B Data for HFR-B1

The so-called "final" irradiation data for HFR-B1 are given in Section 6 of the operating history report (Burnette 1994). The reported R/B data correspond to following assumptions as elaborated in Section 5.3.4.2:

1. Fission gas is released only from dtf particles whose kernels are exposed shortly after the beginning of irradiation.
2. The fission gas is generated from the fissioning of ^{235}U only.
3. The yield of fission products are those corresponding to the fissioning of ^{235}U.
4. The power in the particles with exposed kernels is constant at the initial irradiation value.

Examples of R/B data are plotted in Figs. 5-6, 5-7, and 5-8. These figures give the calculated R/B values for Capsules 1, 2, and 3, respectively, during the first and last irradiation cycles. These R/B values are based upon 8.9% of the power in the fissile particles (the number of dtf particles is 8.9% of the total number of fissile particles.

5.3.5 Gas Composition

A gas chromatograph (GC) was used to monitor the compositions of the inlet and outlet gases of all capsules for trace impurities and, in Capsule 3, for the reaction products of the hydrolysis of the carbonaceous material in the fuel elements. The species CO, CO_2, H_2, N_2, and CH_4 were measured by GC. The gas chromatograph used at Petten was a model TBT, manufactured by L'aire Liquide/Orthodyne in France. It utilized an Ne ionization detector and delay columns of porapak Q at 50 ^oC, and molecular sieves at a temperature of 75 °C. In addition, there was a molecular sieve column that is cooled with liquid nitrogen. This column was used at -140 °C for the measurement of H_2 whenever there was Ne contamination.

The Sweeploop system utilized Panametrics hygrometers with aluminum oxide sensors for measuring H_20 in the capsule purge gases. Such hygrometers have very fast response times and provide measurements over a wide range, from a dewpoint of -110 to +20 °C. However, the sensors may decalibrate with time and therefore, for quantitative measurements must be recalibrated frequently. Several of the eight hygrometer sensors used in the test were found to have drifted considerably since their original purchase. Upon re-calibration after initial use, it was determined that one sensor was reading low by a factor of three. This circumstance meant that the water vapor concentrations in the first five water vapor injection tests were higher than originally planned. A correction factor of three has been applied to those data after being justified by a thorough analysis. An example of the gas composition data is given in Table 5-2, which summarizes the impurity data for Capsule 3 during Cycle 87.09.

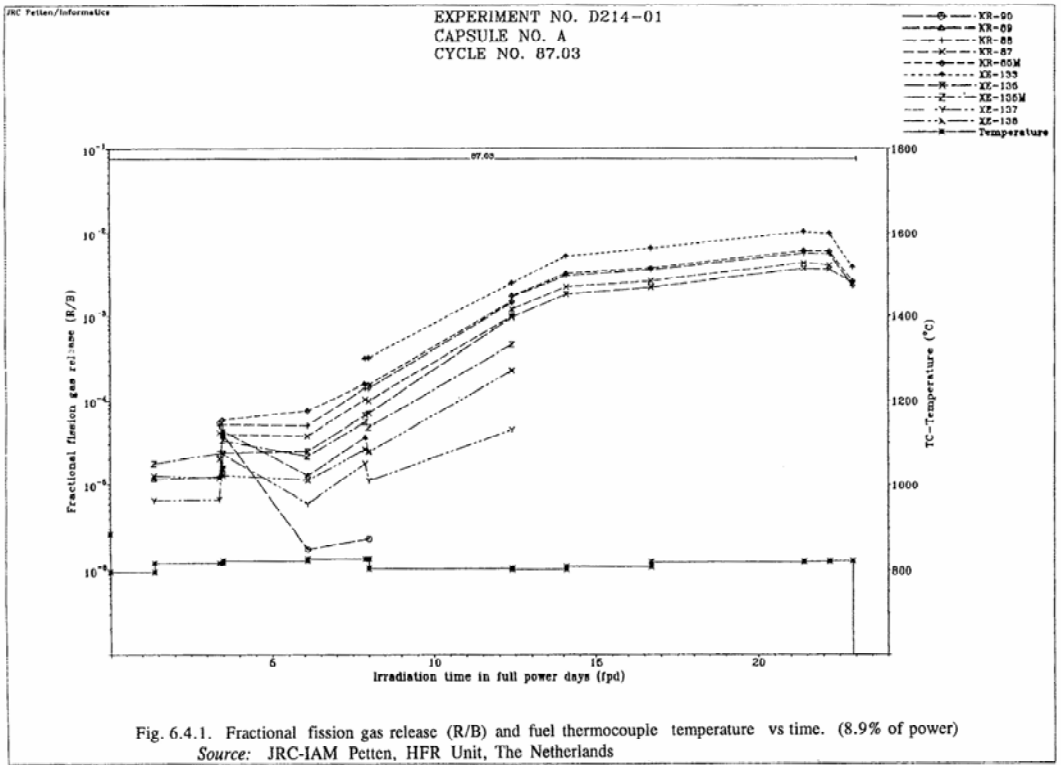

Fig. 6.4.1. Fractional fission gas release (R/B) and fuel thermocouple temperature vs time. (8.9% of power)
Source: JRC-IAM Petten, HFR Unit, The Netherlands

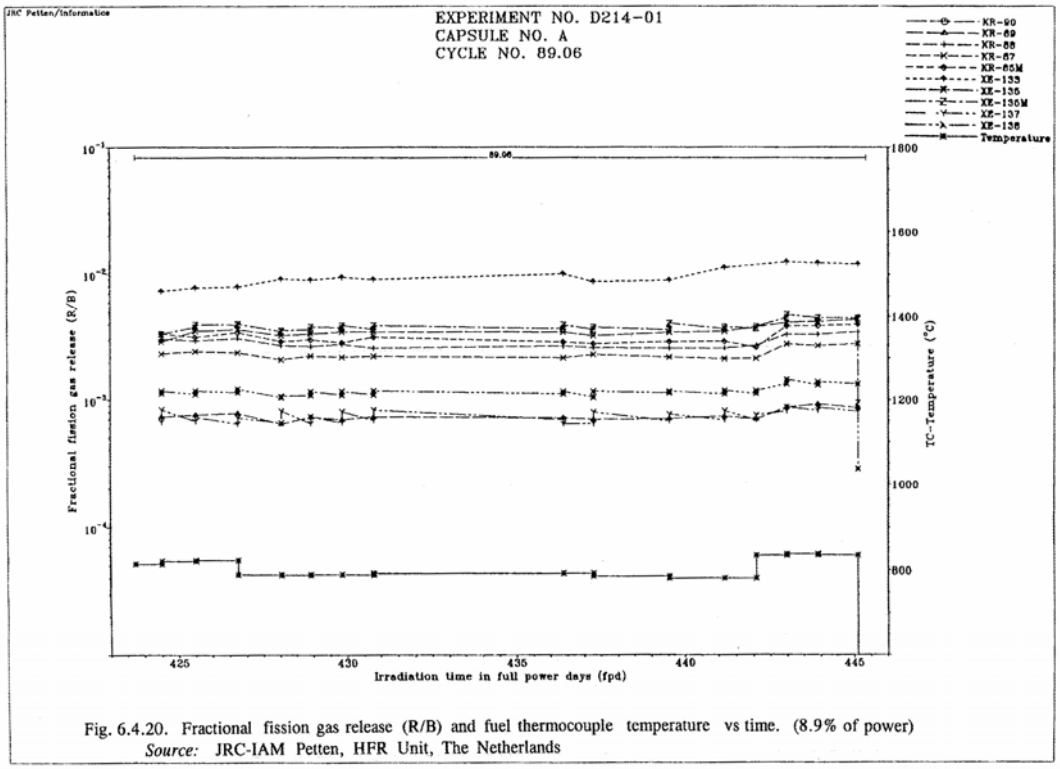

Fig. 6.4.20. Fractional fission gas release (R/B) and fuel thermocouple temperature vs time. (8.9% of power)
Source: JRC-IAM Petten, HFR Unit, The Netherlands

Fig. 5-6. Fission gas release for Capsule 1

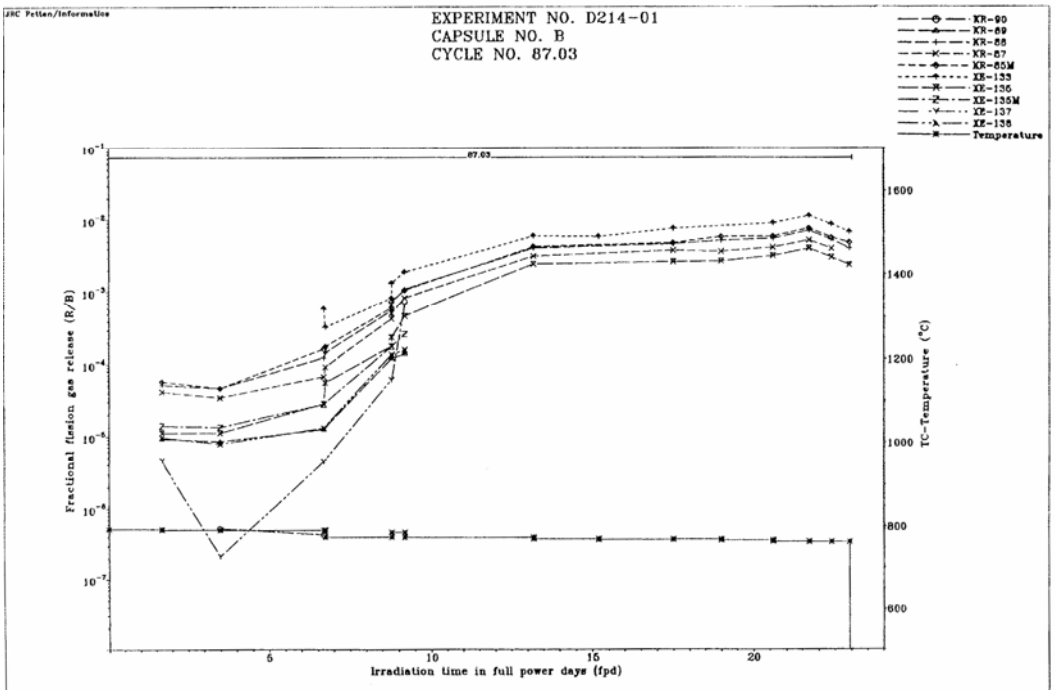

Fig. 6.4.21. Fractional fission gas release (R/B) and fuel thermocouple temperature vs time. (8.9% of power)
Source: JRC-IAM Petten, HFR Unit, The Netherlands

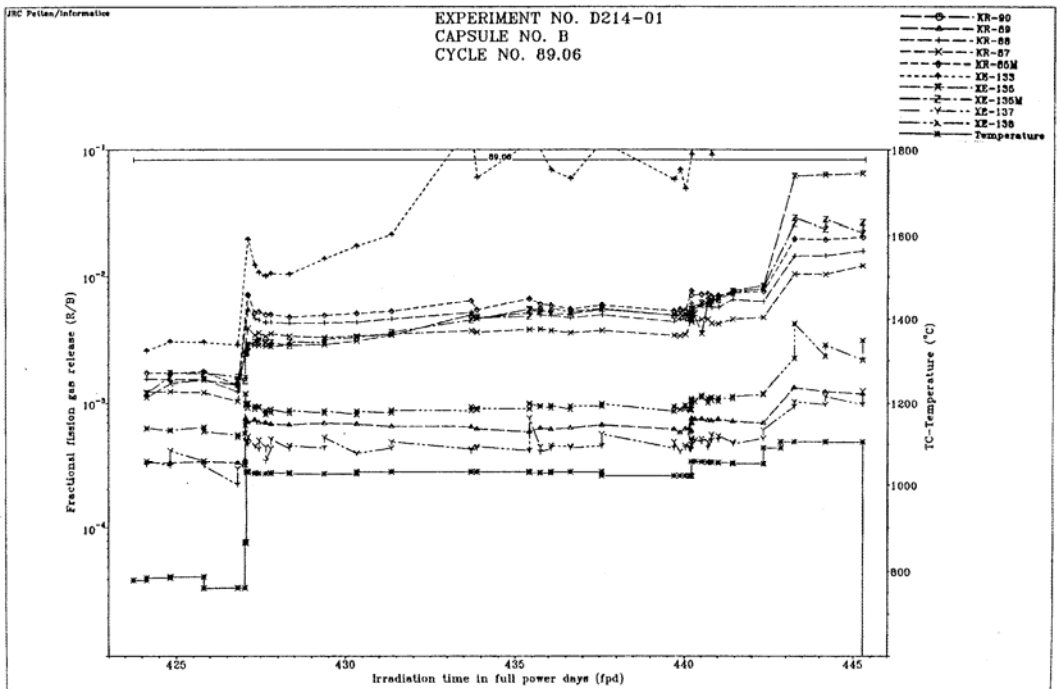

Fig. 6.4.40. Fractional fission gas release (R/B) and fuel thermocouple temperature vs time. (8.9% of power)
Source: JRC-IAM Petten, HFR Unit, The Netherlands

Fig. 5-7. Fission gas release for Capsule 2

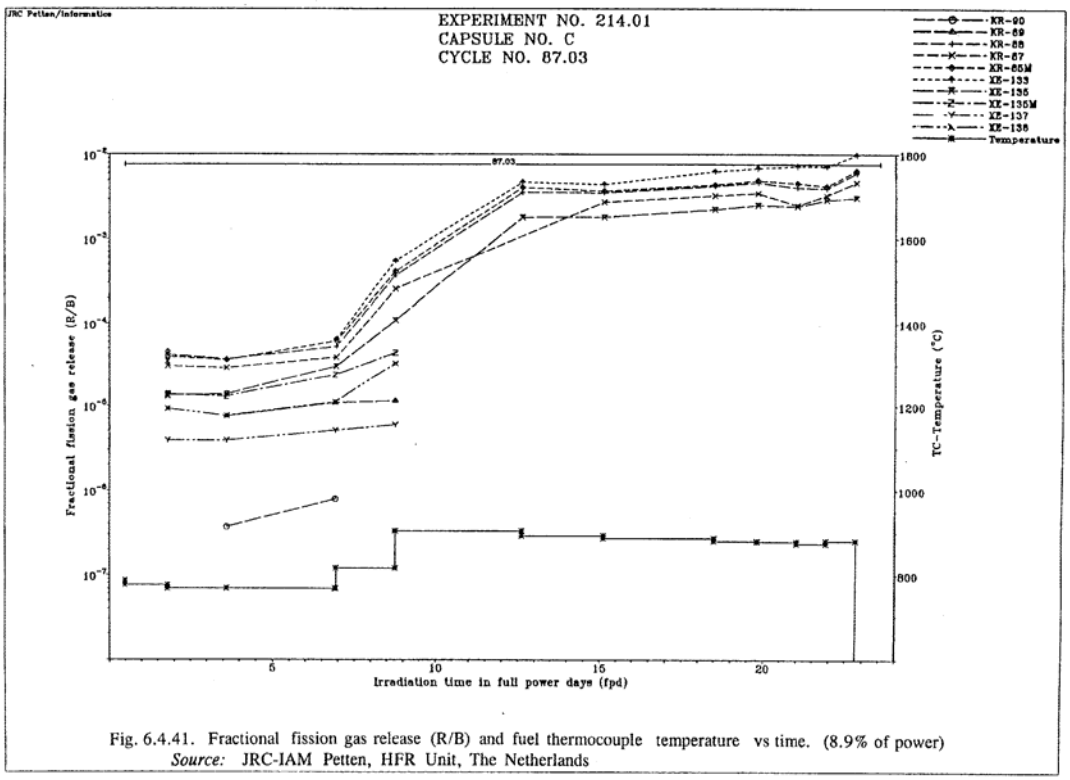

Fig. 6.4.41. Fractional fission gas release (R/B) and fuel thermocouple temperature vs time. (8.9% of power)
Source: JRC-IAM Petten, HFR Unit, The Netherlands

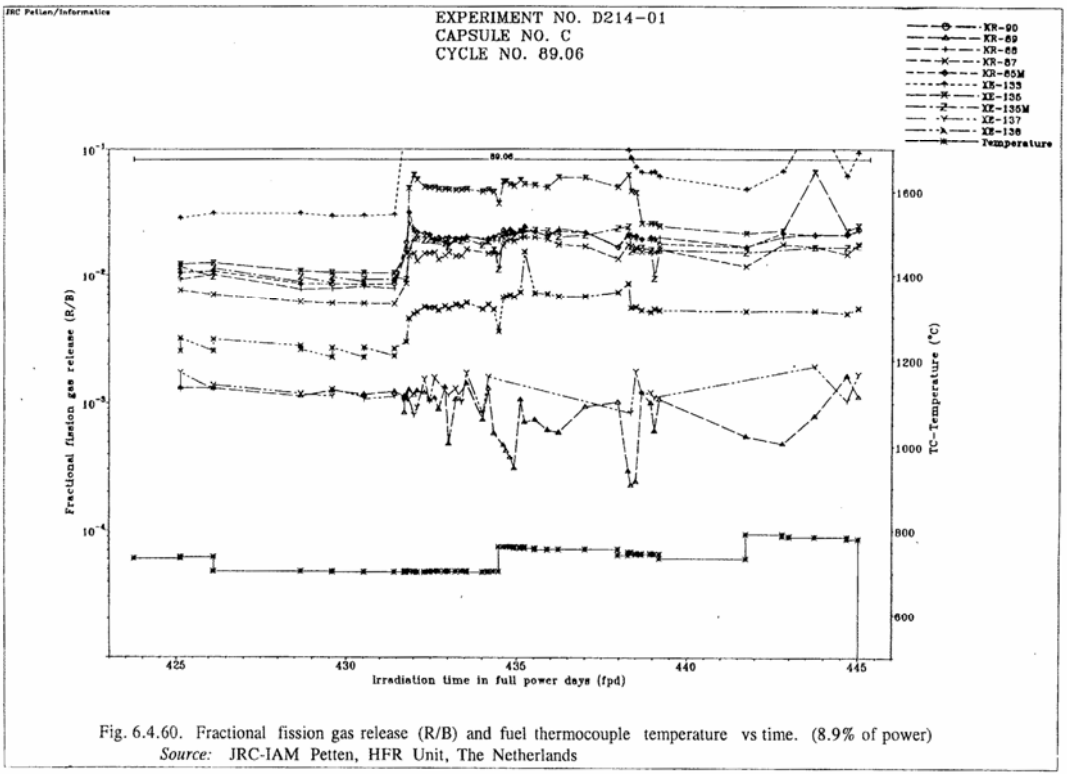

Fig. 6.4.60. Fractional fission gas release (R/B) and fuel thermocouple temperature vs time. (8.9% of power)
Source: JRC-IAM Petten, HFR Unit, The Netherlands

Fig. 5-8. Fission gas release for Capsule 3

TABLE 5-2
GAS COMPOSITION DATA FOR CAPSULE 3 DURING CYCLE 87.09

Table 6.5.7. Gas composition data
Source: JRC-IAM Petten, HFR Unit, The Netherlands

CAPSULE 3, CYCLE 87.09

Water-vapor injection No.3 ; Duration 192 h

			H_2O-vapor Injection Press.			Concentration of Effluent Gases (ppmv)				
cycle	date	time	(Pa)	start	stop	CO	CO_2	H_2	N_2	CH_4
87.09	28.10	1129				1.5	1.0	Ne (47)		
		14.15				2.9	0.5	Ne	6.5	
	3010	1148				0	0	1.5	2	
	02.11	0931				0	0	1	2.1	
	02.11	1000	45	xxxx						
		1115				0	0	1	1.6	0
		1323				6.7	26	45	4	0
		1425				8.9	27	54	4	0
		1714				11.0	30	68	4	0
		2153				13	30	80	3	-
	03.11	1013				19	33	102	3	0.5
		1152				17	32	103	3	0.5
		1433				22	33	104	6	0.5
		1515				22	33	104	2	1.0
		2246				24	34	105	2	0.5
	05.11	2220				26.8	43	110	4	1.0
		2247				26.8	44	110	2	1.0
	06.11	1509				25	36.5	110	3	1.5
	08.11	1250				28.9	36	120	2	1.0
	09.11	1754				33	41	125	3	1.5
	10.11	1000			xxxx					
		1027				28	38	20	18	0.8
		1055				29	36	100	9	
		1210				16.7	19	20		0.9
		1321				11	17	80		0.8
		1446				10	8	55		0.6
		1557				8.7	6	38		0.7
		2126				5.8	3	25		0.6
	11.11	1022				3.6	1	14		0.5
		1619				0	0	1.8	0	0.0

Note: A manual peak height analysis showed the automatic "Shimadzu" integrations were accurate, except for hydrogen, which was analyzed by a multi-point calibration method.

6 POSTIRRADIATION PHASE

The planned postirradiation examination of the HFR-B1 experiment was extremely important to meeting certain of the test objectives, especially for Capsule 1 for which essentially all of the critical data on fission metal transport in core materials were to be generated during the PIE. The original PIE plan (e.g., Scheffel 1989) was for JRC Petten to recover the three capsules from test rig after performing a gamma scan of the rig (see Section 6.1). All three of the capsules were to be shipped from JRC Petten to KFA Juelich. KFA would then ship Capsule 1 to ORNL for the destructive PIE, and KFA would perform the Capsules 2 and 3 PIEs in their hot cells.

After a year delay because of licensing issues, the three capsules were shipped to KFA Juelich, and much of the planned PIEs of Capsules 2 and 3 were completed. A decision was made to perform the Capsule 1 PIE at KFA as well. Consequently, a partial PIE of Capsule 1 was conducted at the KFA under a DOE subcontract administered through ORNL. A more complete description of these events and summary results is provided in Section 6.2.

6.1 Neutron Flux and Fluence Measurements

Before and after irradiation, spectroscopic measurements on nuclides activated during irradiation were made. The analysis of these led to axial and circumferential distributions of the neutron flux (fluence rate) and fluence and, in some cases, to estimates of the absolute values of the fluxes and fluences. Gamma spectroscopy was conducted at HFR Petten on the protection tube containing the three capsules (Dassel 1990). The nuclides measured in the tube are ^{58}C0, ^{54}Mn, ^{51}Cr, and ^{60}Co; the former two are products of and characteristic for fast neutron reactions, and the latter two, for thermal neutron reactions.

Measurements of the neutron flux and fluence were made using activation monitors (Ketema 1991), gamma-scanning wires and SPN detectors. Each capsule contained three niobium-encased wires located about 3 mm from a stacked set of four fuel compacts and extending more than the length of the stack. The gamma-scan wires from Capsules 2 and 3 were analyzed at KFA (Schroeder 1991). The results are summarized in the operating history report (Burnette 1994).

6.2 PIE of Capsule 1

As stated above, the original plan was to conduct the Capsule 1 PIE at ORNL, but a decision was subsequently made to perform the PIE at KFA Juelich. The reason for that change of plans is not clearly stated in the official test documents, but one can speculate with some confidence that the change of venue for the PIE related to the difficulties of obtaining licenses for the international shipment of irradiated nuclear fuel, even with the small quantities of fissile

materials associated with Capsule 1 at end-of-life. As evidence of this difficulty, the planned shipment of the three HFR-B1 capsules from JRC Petten in the Netherlands to KFA Juelich in neighboring West Germany was delayed a year by licensing difficulties.

6.2.1 Programmatic/Planning

The original test specification for HFR-B1 test, which was issued in 1986, made little mention of the PIE requirements other than to affirm that an extensive PIE would be necessary to meet the test objectives, especially for Capsule 1 (Ketterer 1986). A comprehensive PIE plan was issued by GA in March 1989 (Scheffel 1989) prior to the completion of the irradiation in July 1989. No PIE test specification was prepared; the 1989 test plan simply cites the original 1986 test specification. The operating history report (Burnette 1994) does not cite the 1989 test plan, which does include some PIE scope (e.g., test rig gamma scanning) that was performed at HFR Petten.

As stated previously, the shipment of the three capsules from JRC Petten to KFA Juelich was delayed by licensing approval difficulties from November 1989, to December 1990. The postirradiation examination of Capsules 2 and 3 began in the first quarter 1991 (Myers 1994); at this point the plan was to ship Capsule 1 to ORNL for PIE. In November 1991, ORNL issued a new PIE plan (Myers 1991) for all three capsules, and the plan to ship Capsule 1 to ORNL remained. The 1991 ORNL test plan (Myers 1991) only commented that its "…test procedures…differ significantly…" from those in the 1989 GA test plan without providing any specific examples.

At some unspecified point in time, a decision was made to perform the Capsule 1 PIE at KFA Juelich under a DOE subcontract administered by ORNL, and in November 1993, a new PIE plan for Capsule 1 was issued by ORNL (Myers 1993). Contrary to programmatic protocols, a test specification for the Capsule 1 PIE was issued by GA (cognizant design organization at the time) in February 1994 (Richards 1994) after the ORNL had already been issued. The GA PIE specification was updated in May 1994 (Medwid 1994). Despite the fact that the test specification and the test plan/test procedures were prepared out of the normal sequence, the test plan/test procedures (Myers 1993) are responsive to the test specification (Medwid 1994).

The Capsule 1 PIE in the FZJ hot cells began some time in late 1993, and a series of progress reports were prepared over the next two years (Hanson 2003). In the summer of 1995, a programmatic decision was made to close out the U.S. DOE HTGR program in FY96, and all technical work, including the Capsule 1 PIE at FZJ, stopped. As discussed below, no closeout report (or even letter) documenting the final status of the Capsule 1 PIE appears to have been prepared by FZJ, ORNL, or GA.

An attempt was made in 2004 to determine how much of the Capsule 1 PIE data could be recovered (Hanson 2004b); the purpose of that investigation was to assess whether sufficient data for Capsule 1 could be obtained for use in meeting a portion of the DDNs identified by the AGR program regarding fission metal transport in HTGR core materials. The results of that 2004 assessment are summarized in the following subsections.

6.2.2 Recovery of the HFR-B1 Capsule 1 Database

As described in earlier sections, the fabrication and irradiation phases of the Capsule 1 experiment are well documented (Ketterer 1985a and Burnette 1994, respectively). However, the recovery of documents related to the Capsule 1 PIE has been problematic as discussed below. The available Capsule 1 PIE results are summarized in Section 6.2.3 (Hanson 2004b).

Section 6.2 of the PIE plan (Myers 1993) called for the following documentation to be prepared:

> Observations, photographs, and other data will be recorded in laboratory notebooks or in other permanent forms that will thereafter be available for inspection or use by qualified representatives of the U.S. Department of Energy (DOE) or their subcontractors. Progress in the PIEs will be described in ORNL management reports, which will include information on the progress of the PIE at KFA. The latter laboratory will issue brief periodic reports according to preceding accomplishments; these reports will be included in the ORNL monthly reports and will be distributed to DOE. During the PIE, copies of the PIE plan and the test procedures document will be used as working documents, and changes in the plan or the procedures will be recorded, dated, and initialed as they occur. Three months prior to the milestone for the draft of the final, comprehensive PIE report, the complete PIE report of KFA shall be received by ORNL; the comprehensive PIE report will be written at ORNL after the completion of all PIE work.

Presumably, these documentation requirements were reflected in the ORNL contract with FZJ, although a copy of the actual contract has not been recovered.

With the above expectations, the HTGR archives and databases at ORNL, FZJ (KFA), and GA were examined with the following results (Hanson 2004b).

6.2.2.1 ORNL Resources

R. Morris has searched the ORNL archives and found little information with the notable exception of Progress Report No. 5 (see below). The personal files of the late Ben Myers,[7] who was the principal U.S. architect and overseer of the HFR-B1 experiment, have been reviewed, and they contain no PIE results for Capsule 1 even though they contain numerous documents about other aspects of the HFR-B1 experiment.

6.2.2.2 HFR Petten Resources

The HFR-B1 activities at JRC Petten in the Netherlands are well documented in a series of progress reports and a comprehensive final report (Burnette 1994).

6.2.2.3 FZJ Resources

With the assistance of H. Nabielek and K. Verfondern of FZJ, seven FRG reports about the Capsule 1 PIE were recovered and have been reviewed; the results are summarized in Section 3. In summary, it appears that much, but not all, of the planned destructive PIE was completed. These seven FZJ progress reports are data compilation reports that contain essentially no data evaluation or conclusions. The titles of these progress reports ("Progress Report No. X") imply that there were at least two additional progress reports (i.e., numbers 1 and 5) that have not been recovered; Number 5 was subsequently found at ORNL. A final data evaluation report was planned, but none has been discovered in the files at FZJ, ORNL, or GA.

6.2.2.4 GA Resources

No HFR-B1/Capsule 1 PIE report or even progress reports have been found in the GA HTGR program archives (or in the writer's personal files). The aforementioned planning documents and the KZJ progress reports are cited in the GT-MHR closeout report (Silady 1996).

6.2.3 Evaluation of the HFR-B1 Capsule 1 PIE Database

Copies of seven progress reports on the Capsule 1 PIE were recovered from the personal files of W. Kuehnlein of the FZJ (KFA) hot cells. These copies were scanned by K. Verfondern, and electronic copies were transmitted by email to the writer (Schroeder 1993, Schroeder 1994a, Bueker 1994, Schroeder 1994b, Schroeder 1995a, Schroeder 1995b, Bueker 1995). At least two progress reports (i.e., numbers 1 and 5) were missing from the set provided by FZJ; a copy of number 5 was subsequently found at ORNL (Derz 1994). Progress Report No. 1 has not

[7] Dr. B. F. Myers was a GA employee when the HFR-B1 test was first conceived. He was an ORNL employee during operational phase of the test, and he continued to actively support the test program during his retirement, almost up to the time of his death in August 2001. His files are now in the custody of F. Homan, a former employee of and now a consultant to ORNL.

been recovered at this writing. The contents of each of these reports are described below and summarized in Table 6-1.

When reviewing these Capsule 1 PIE data, it is important to recognize that the HFR-B1 irradiation in HFR Petten was completed in July 1989, but that the PIE did not begin in the FZJ hot cells until sometime in 1993. An in-depth programmatic explanation for this protracted delay is beyond the scope of this review. It may be sufficient to recall that the German HTR program was cancelled in 1989, and that its demise ended the expectation that the Germans would perform the Capsule 1 PIE at no expense to the U.S. HTGR program.

In any case, the technical consequences of this protracted delay are significant: *viz*., those radionuclides with short and intermediate half-lives had decayed to below detection limits before the PIE was initiated. Included in the latter category is 250-day Ag-110m, a mobile radionuclide that is a dominant dose contributor to occupational exposures in HTGRs operating with LEU fuel.

Several common themes in these FZJ progress reports are noteworthy. These reports are data compilation reports that contain essentially no data evaluation or conclusions; moreover, they are quite cryptic. They make no references to test procedures; in fact, they contain no references to any external documents. Significantly, most of the spectrographic results are relative count rates that have not been reduced to absolute inventories or concentrations. This circumstance greatly limits the utility of these data for deriving quantitative conclusions and effectively precludes their use for code validation purposes.

Progress Report 2 – 15.12.1993 (Schroeder 1993)

This report contains the gamma scans of the three graphite wedges containing the fuel compacts. Relative count rates are reported for the following radionuclides: Ce-144, Cs-134, Cs-137, Ru-106, Eu-154, Nb-94, and Co-60. The latter two radionuclides are presumably from the neutron activation of the gamma scan wires and thermocouple sheathes. The relative count rates were not reduced to absolute inventories.

Progress Report 3 – 31.05.94 (Schroeder 1994a)

This report contains the tomography results for the cross sections of the graphite wedges at three different axial locations along the length of the wedges. Color-coded, relative count rates are reported for the following radionuclides: Ce-144, Cs-134, Cs-137, Ru-106, Eu-154, Nb-94, and Co-60. The relative count rates were not reduced to absolute inventories. Typical results for Cs-137 are given in Figs. 6-1 and 6-2.

A much debated topic during the planning for the Capsule 1 PIE was the experimental method to be used for determining the radionuclide distributions within the graphite wedges (i.e., concentration profiles). Two approaches were considered: coring/slicing/gamma counting and

tomography. The first approach is traditional, tedious, and very expensive but yields accurate absolute concentrations. The second approach is developmental; the fundamental issue is whether proper calibrations can be performed to obtain reliable quantitative results. The decision was made by the KFA to employ the tomographic method in conjunction with the coring method: tomography to determine relative concentrations with possibly finer resolution and certainly less effort than in the coring method, and coring/slicing/gamma counting to establish absolute concentrations. This report contains only the relative tomography results. It is not known if an attempt was made to cross correlate the tomography and the coring results.

TABLE 6-1
FZJ PROGRESS REPORTS ON HFR-B1/CAPSULE 1 PIE

Ref.	Report No	Title (Abbreviated)	Date	Contents	Comments
Schroeder 1993	IWE 1-TN-21/93	Progress Report 2 – 15.12.1993	12/93	γ scans of three graphite wedges containing fuel compacts	Relative counts only; no reduction to absolute inventories.
Schroeder 1994a	IWE 1/HZ-TN-22/94	Progress Report 3 – 31.05.94	5/94	Tomographic results for the graphite body at three elevations	Relative counts only; no reduction to absolute inventories.
Bueker 1994	1/HZ-TN-35/94	Progress Report 4	8/94	Capsule disassembly, visual inspection, dimensions, weights	Routine disassembly. Fuel compacts and graphite wedges in good condition.
Derz 1994	1/HZ-TN-37/94	Progress Report 5	10/94	Ceramographic Examination of Coated-Particles in Fuel Rods	UCO fissile and THO_2 fertile particles in good condition; no evidence of in-service failure. The dtf particles were essentially bare kernels with high porosity and irregular shape.
Schroeder 1994b	IWE 1/HZ-TN-44/94	Progress Report 6	11/94	Fuel compact RN inventories and burnups from Cs-137	Routine PIE methodology
Schroeder 1995a	IWE 1/HZ-TN-10/95	Progress Report 7	3/95	Inventories of γ-emitting RNs for metal canister, heat shields, and graphite components	Absolute inventories
Schroeder 1995b	IWE 1/HZ-TN-8/95	Progress Report 8	7/95	Inventories of γ-emitting RNs in the fuel-compact matrix	Specific activities in Bq/g
Bueker 1995	IWE 1/HZ-TN-12/95	Bohrprobennahme aus Grafitteilen der Kapsel 1	10/95	Coring samples from graphite wedges; sample weights	No gamma counting of samples

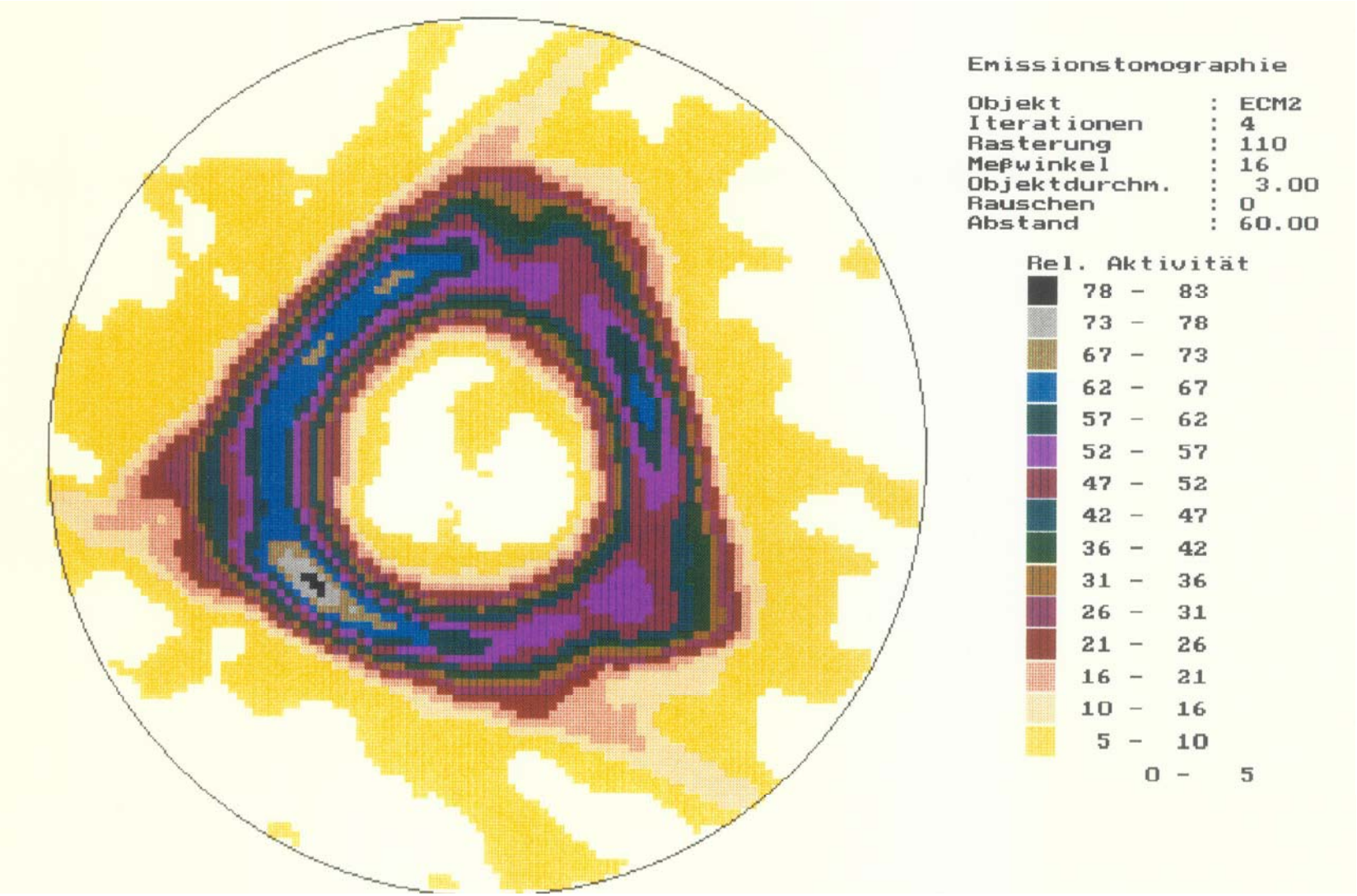

Fig. 6-1. Cs-137 distribution in fuel wedge 1 at midplane of Capsule 1

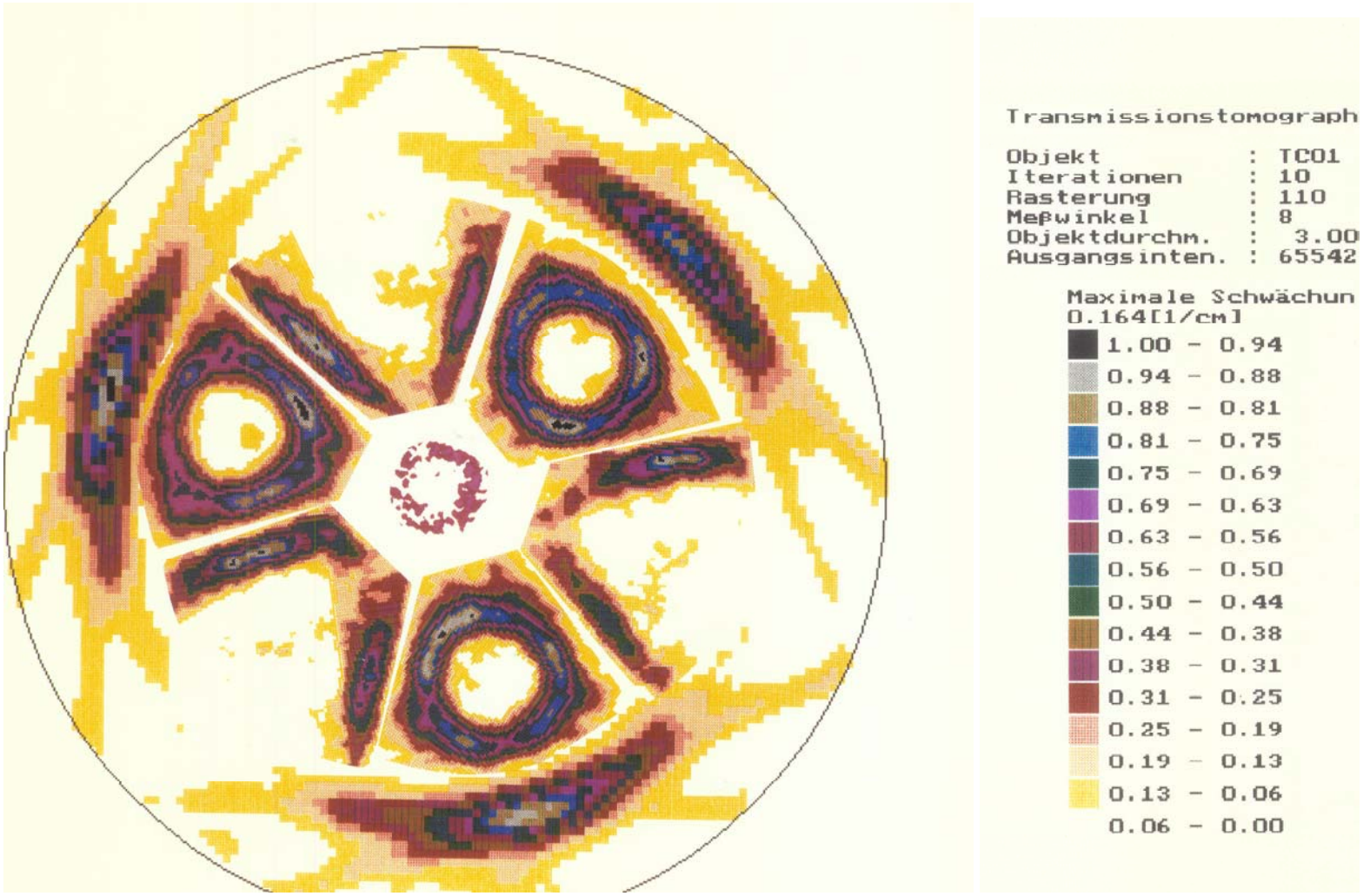

Fig. 6-2. Composite of all Cs-137 tomographies at top of Capsule 1

Progress Report 4 (Bueker 1994)

This report contains the following: (1) a description of the disassembly of Capsule 1, (2) visual inspection and photography, and (3) metrology and weighing of the capsule components. The upper graphite end plate was broken into multiple pieces. The three screw heads of the lower graphite end plate were also detached and were found at the bottom of the transport container. However, the fuel compacts and graphite wedges all appeared to be in good condition. A few fuel particles were dislodged from several fuel compacts during removal from the graphite wedges, which is a routine occurrence during capsule disassembly.

Progress Report 5 (Derz 1994)

This report contains the results of ceramographic examination of coated particles in three fuel compacts,[8] one from each of the three fuel columns. All of the UCO fissile and ThO_2 fertile particles examined were in good condition with typical features for these particle types at these burnups and temperatures. There was no evidence of in-service failure of the fissile or fertile driver fuel particles. The dtf particles were essentially bare kernels with high porosity. Some remained nearly spherical, but others had assumed highly irregular shapes. Representative photomicrographs of UCO fissile particles, ThO_2 fertile particles, and dtf UCO particles are shown in Figs. 6-3, 6-4, and 6-5, respectively.

Progress Report 6 (Schroeder 1994b)

This report contains the results of gamma scanning the fuel compacts and calculation of the fuel burnups from the Cs-137 inventories. The equipment and methodology used are well established for coated-particle fuel PIEs. The following radionuclides were detected and quantified: Ce-144, Cs-134, Cs-137, Ru-106, Eu-154, and Sb-125. The average calculated burnup for Capsule 1 was 21.5% FIMA.

Progress Report 7 (Schroeder 1995a)

This report gives the absolute inventories of gamma-emitting radionuclides for the metal canister, heat shields, graphite wedges (fuel compacts removed), and graphite parts. The only radionuclides detected on the metal components were Cs-134, Cs-137, and Co-60 (the latter from *in-situ* neutron activation); this observation implies that only the Cs isotopes were able to migrate through the graphite components at an irradiation temperature of 931 °C (not unexpected). With the graphite, components Nb-94 and Eu-154 were also detected. The presence of Co-60 on the graphite components strongly suggests cross contamination in the hot cell, a common problem during fuel PIEs.

[8] The terms “fuel compact” and “fuel rod” are used interchangeably here. “Fuel compact” has become the favored terminology for U.S. HTGR programs; the report uses the terminology “fuel rod,” which is an older construction.

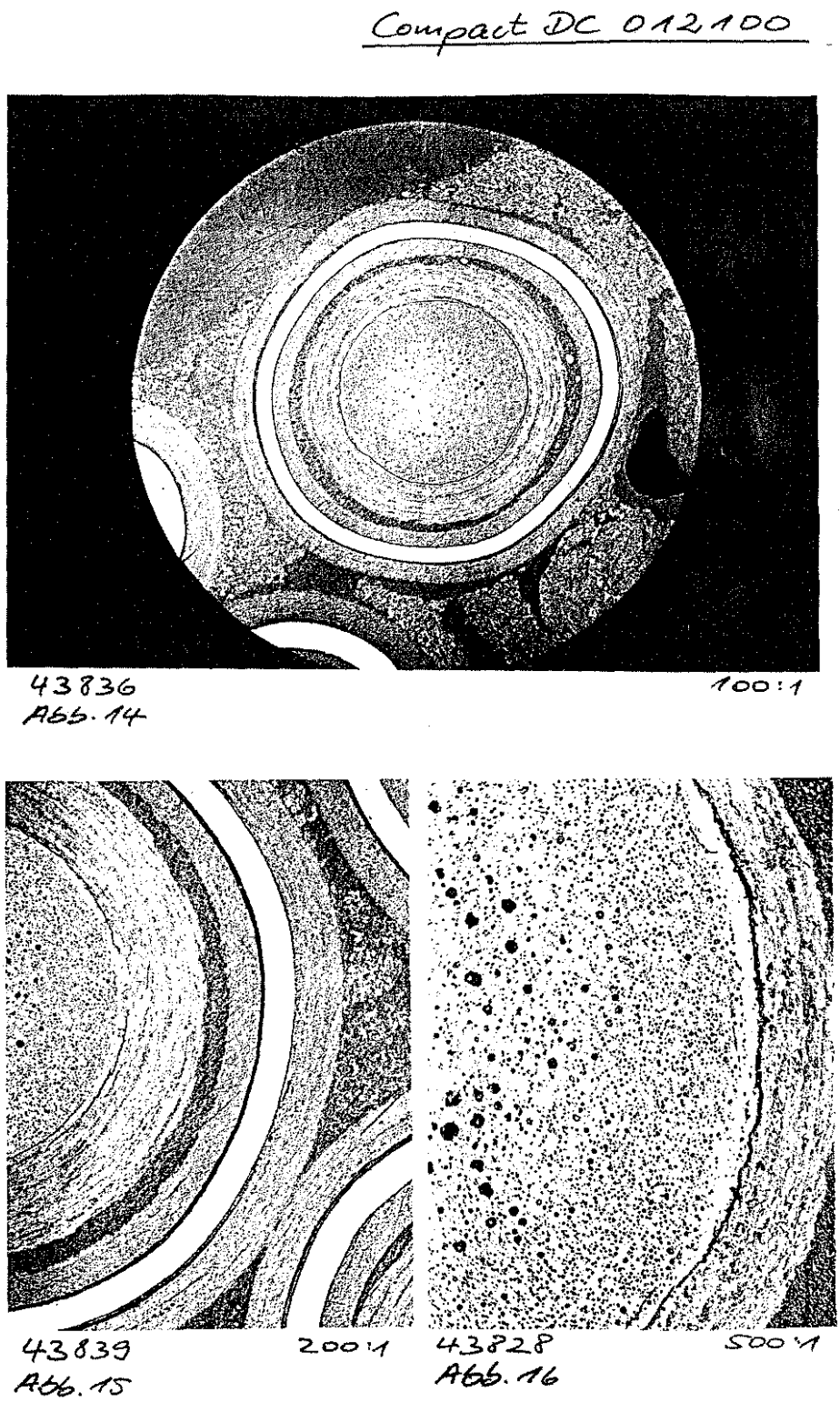

Fig. 6-3. Photomicrograph of UCO particle from Capsule 1 fuel compact

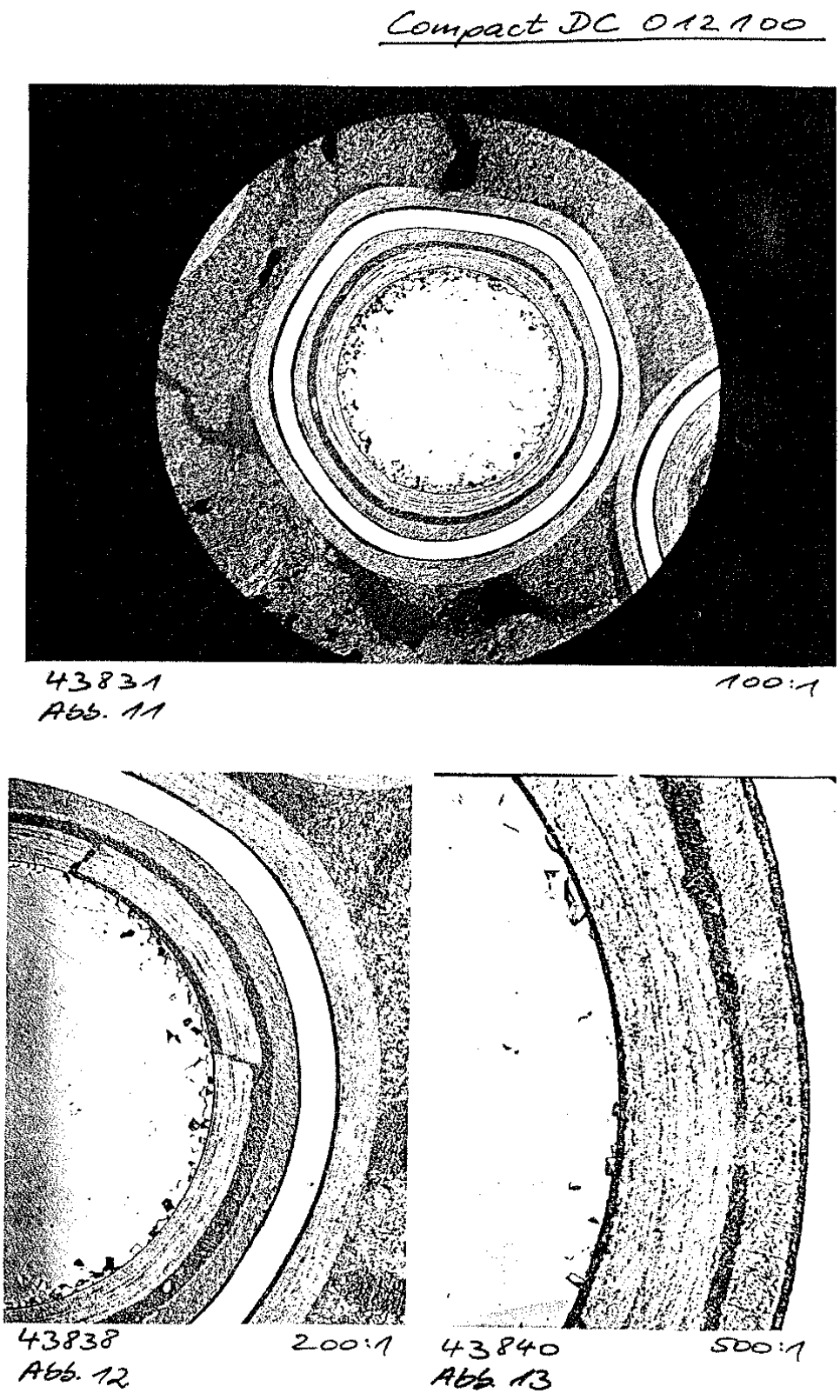

Fig. 6-4. Photomicrograph of THO_2 particle from Capsule 1 fuel compact

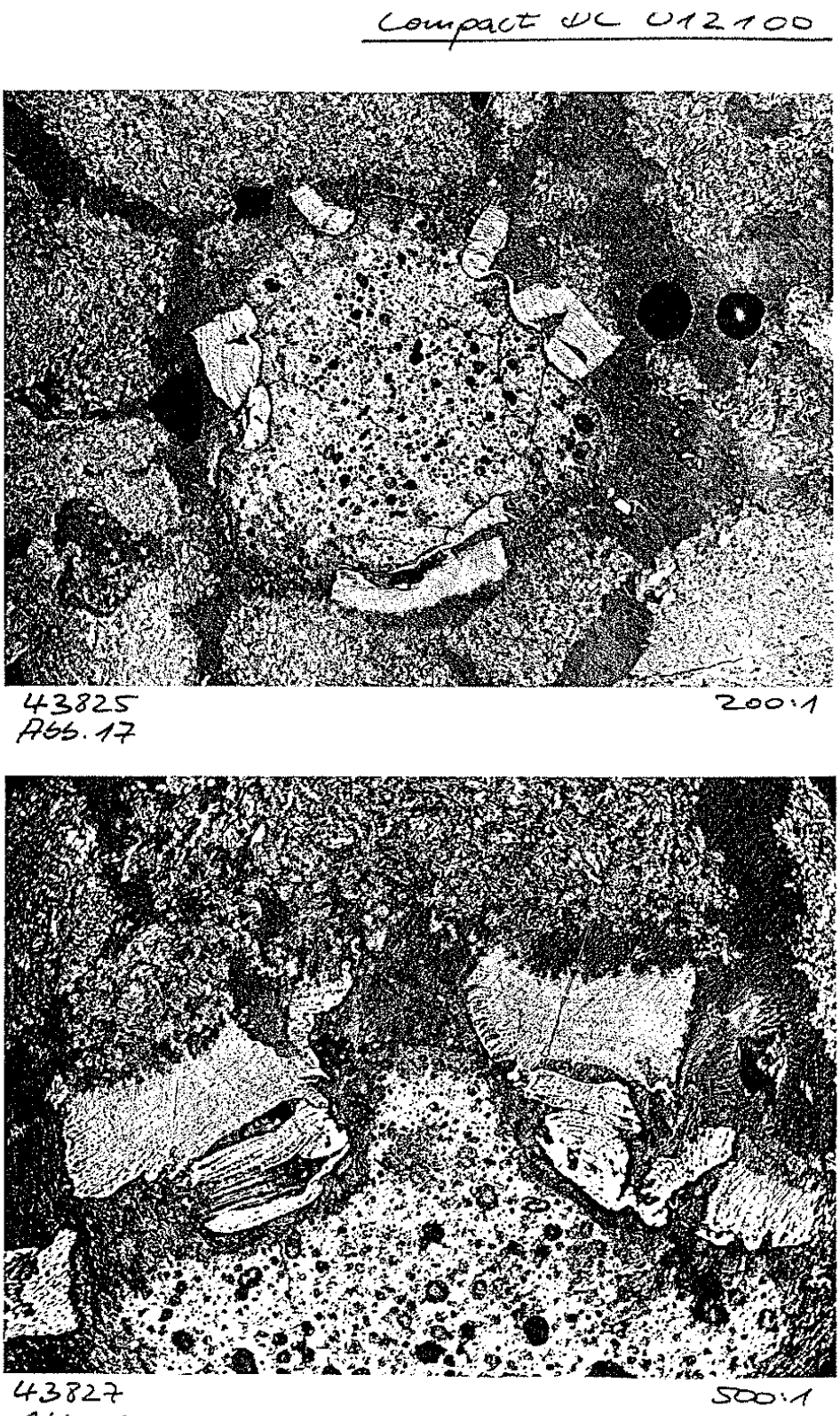

Fig. 6-5. Photomicrograph of dtf UCO particle from Capsule 1 fuel compact

Progress Report 8 (Schroeder 1995b)

This report gives the specific activities (Bq/g) of gamma-emitting radionuclides in compact matrix samples removed from the surfaces of several fuel compacts. The concentrations in the matrix are important because they are used to estimate the partition coefficients at the fuel compact/graphite block interface. These partition coefficients are a major uncertainty in the calculation of metallic fission product release from prismatic cores. The experimental technique for recovering matrix material from irradiated fuel compacts is rather primitive. Matrix material is mechanically abraded from the surface of the compact, and any dislodged fuel particles are removed by sieving. Eighteen matrix samples were so obtained from nine selected fuel compacts and gamma counted. Samples were also obtained from a fuel compact from Capsule 2 and another from Capsule 3. The following radionuclides were detected and quantified: Ce-144, Cs-134, Cs-137, Ru-106, Eu-154, and Sb-125. The results varied dramatically from compact to compact, and the apparent fractional releases from the dtf particles into the matrix were quite high. The report suggested that some fuel material from the dtf particles may have contaminated certain matrix samples because of the high apparent fractional release of Ce-144, which is normally retained in oxidic fuel kernels; this conclusion seems credible because the apparent fractional release of Ce-144 was occasionally higher than the apparent fractional release of the Cs isotopes.

IWE 1/HZ-TN-12/95[9] (Bueker 1995)

This report gives the locations of 37 coring samples taken from the six graphite wedges and the inner and outer restraining annuli. The locations are as specified in the PIE plan. The weights of the core samples are also given. No gamma counting results are included.

The next steps would have been to section the cylindrical core samples into multiple slices and gamma count the individual slices to determine the concentration profiles. There is no indication this work was actually completed.

6.3 PIE of Capsules 2 and 3

The postirradiation examination of Capsules 2 and 3 in the FZJ hot cells began early in the first quarter of 1991. After disassembly of the capsules, the examination focused on capsule components including fuel compacts, inert compacts fired in different media, graphite cylinders of different grades, unbonded coated fuel particles and unfueled graphite; in addition, heating experiments with intermittent injections of water vapor were conducted using fuel compacts and

[9] Not referred to as a progress report, but the content and style are consistent with the earlier progress reports; considering that it was issued three months after Progress Report 8, it probably could be considered Progress Report 9.

the kernels of uranium oxycarbide. Measurement involved gamma scanning and counting, photography, metallography, dimensional and weight changes, burnup determination, and fission product release. The planned PIE for Capsules 2 and 3 is shown as a flowchart in Fig. 6-6, and the abbreviations used in the figure are defined in Table 6-2 and the icons in Fig. 6-7.

A status report was prepared in September 1994 (Myers 1994) that is excerpted below. This report is clearly a status report and not a final data compilation report. It also provides little or no interpretation of the test data. With the termination of the U.S. HTGR program in the summer of 1995, evidently no further PIE work on Capsules 2 and 3 was completed at FZJ.

6.3.1 Planning

Much of the discussion with regard to the programmatic/planning aspects of the Capsule 1 PIE in Section 6.2.1 also applies to the Capsules 2 and 3 PIEs, particularly with regard to test control documentation. One important distinction is that the PIEs of Capsules 2 and 3 were always planned to be conducted at FZJ so that the work began shortly after receipt of the capsules at the FZJ hot cells in December 1990.

6.3.2 Disassembly of Capsules

The three capsules of HFR-B1 were received by the KFA. Capsules 1 and 2 were joined by a cross bar. The cross bar was severed, and Capsule 1 was placed in storage in anticipation of shipping it ORNL. The stainless-steel capsules showed light, spotted red-brown discoloration on the outer surfaces. By circumferential grinding of the capsules at the level of the welding joints, the end plates were removed. The graphite bodies were visible after removing the heat shields; a photograph of the partially disassembled Capsule 2 is shown in Fig. 6-8.[10] Thereafter, the graphite body was removed from the remaining metal canister. The TCs exhibited no visible damage. The visible inspection of the graphite body brought no special feature to light; all markings were well recognized. The fluence detectors from Capsules 2 and 3 were sent to Petten for evaluation in December 1991.

As a part of the disassembly of the capsules, gamma scans have been made of the steel-encased graphite bodies, of the graphite bodies after removal from the steel containers, and of the three gamma scan wires in each capsule. The gamma scans of the stainless steel capsule, having the graphite bodies within, were dominated by the nuclides ^{137}Cs, ^{134}Cs, ^{60}Co, and ^{54}Mn.

[10] This figure and the subsequent reproductions of photos from the PIE of Capsules 2 and 3 were scanned from an original copy of the ORNL status report (Myers 1994). The quality of the figures here reflect the quality of the figures in the ORNL report. It appears that most of the photos taken inside of the FZJ hot cells were underexposed and/or the lighting was not optimal.

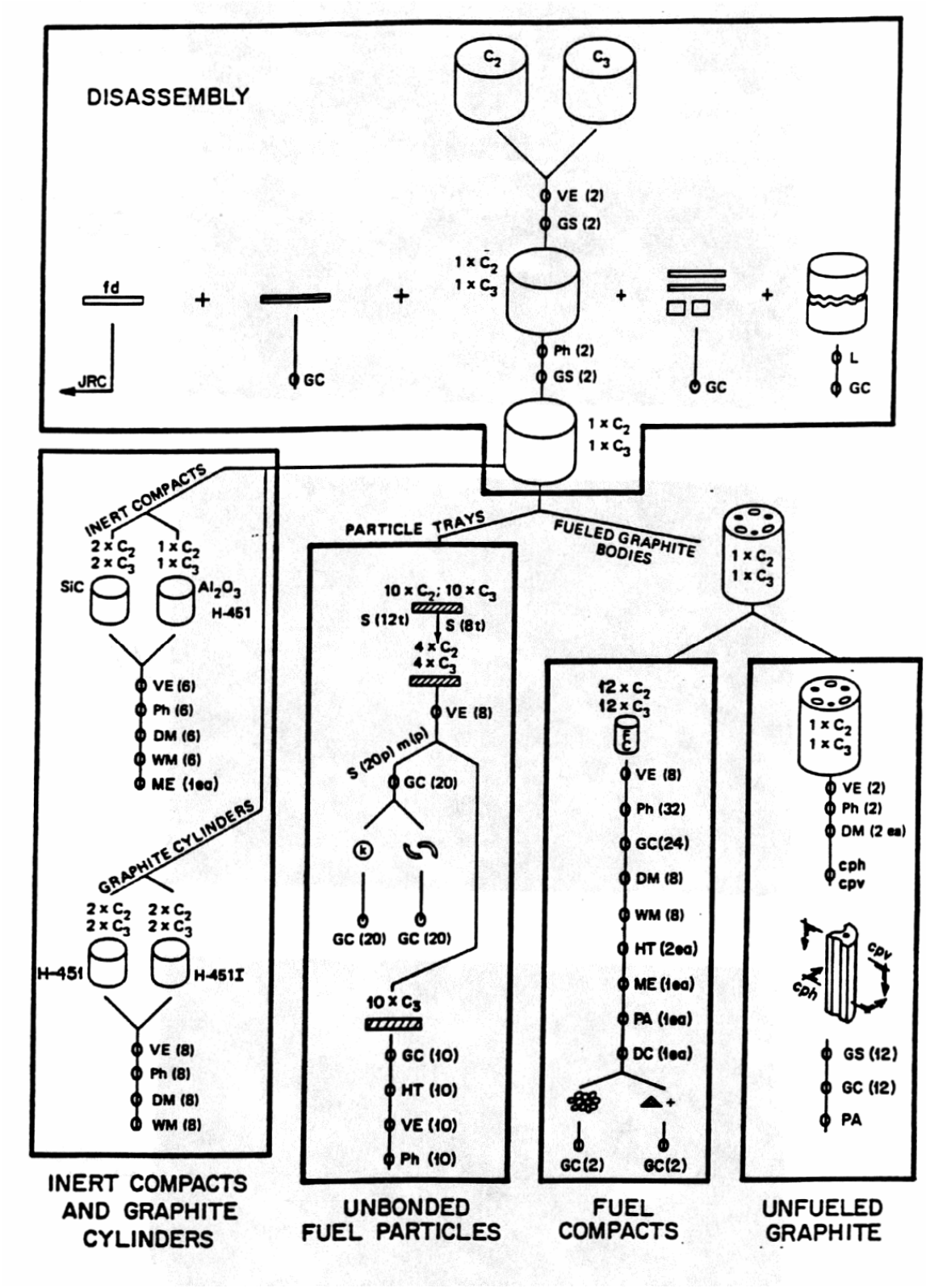

Fig. 6-6. Planned PIE for Capsules 2 and 3

TABLE 6-2
DEFINITION OF SYMBOLS IN PIE FLOWCHART

C_n	= capsule n or a component of capsule n
cph	= cutting plane, horizontal (h)
cpv	= cutting plane, vertical (v)
CTE	= coefficient of thermal expansion
DC	= deconsolidation including separation of parts
DM	= measurement of dimensions
FC	= fuel compacts
GC	= gamma counting to determine the quantity of fission products in the addressed component
GS	= gamma scan to determine the relative distribution of fission products along a selected direction of a component
HT	= heating tests
L	= leach
ME	= metallographic examination
m(x)	= maintain separation of components x [where x is identified in the definition of S(nx)] according to the definition in Table 5 of ref. 1
mxC^n	= number of components m from capsule n
PA	= partition measurements
Ph	= photograph
S(nx)	= selection of n components where x is given by c for compacts, g for graphite cylinders, p for particles, and t for tray
VE	= visual examination
WM	= weight measurement
YM	= measurement of Young's modulus
(1 ea)	= measurement to be made on one sample of each type from both C^2 and C^3
(x)	= number of measurements for the quantities defined above

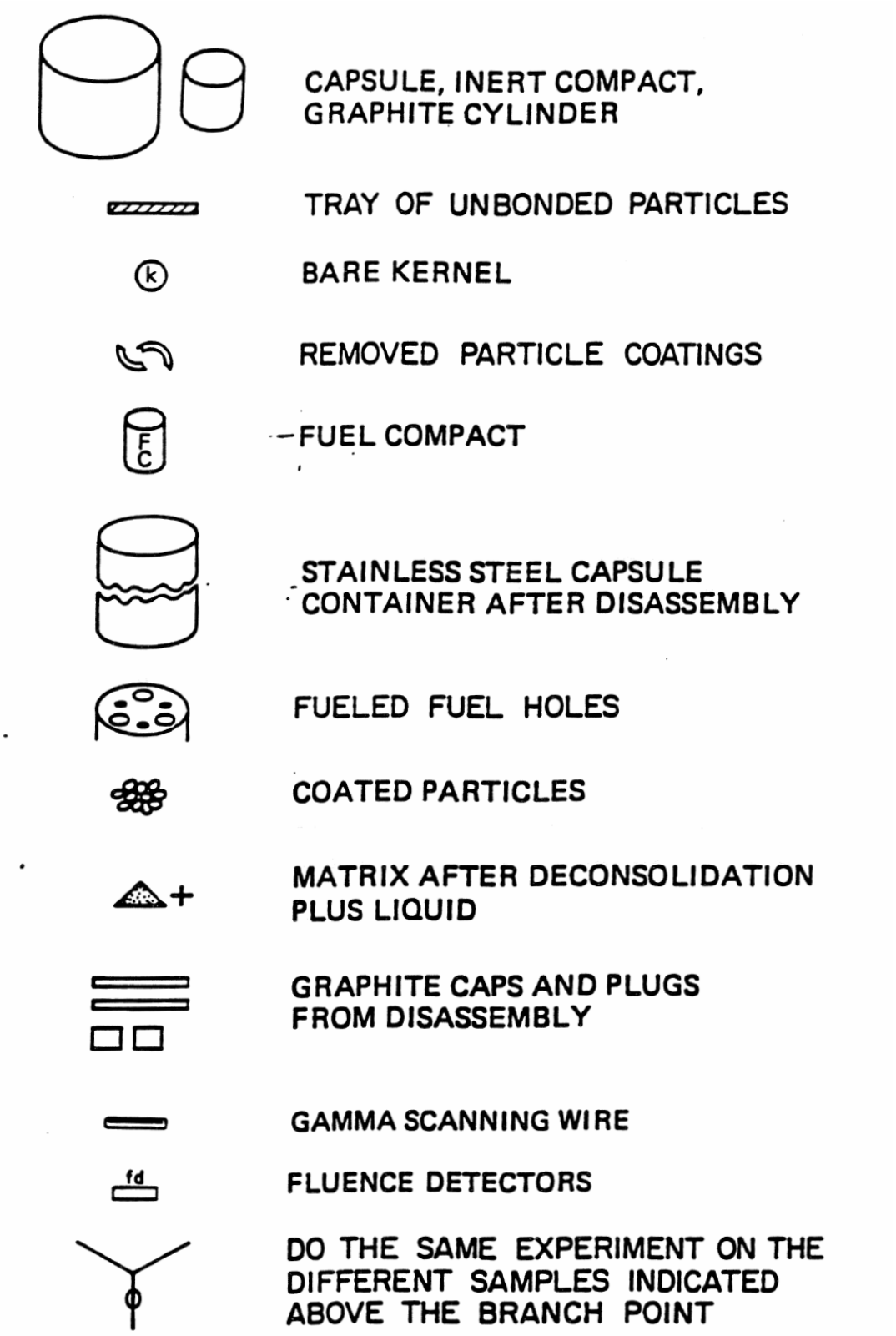

Fig. 6-7. Definition of icons in PIE flowchart

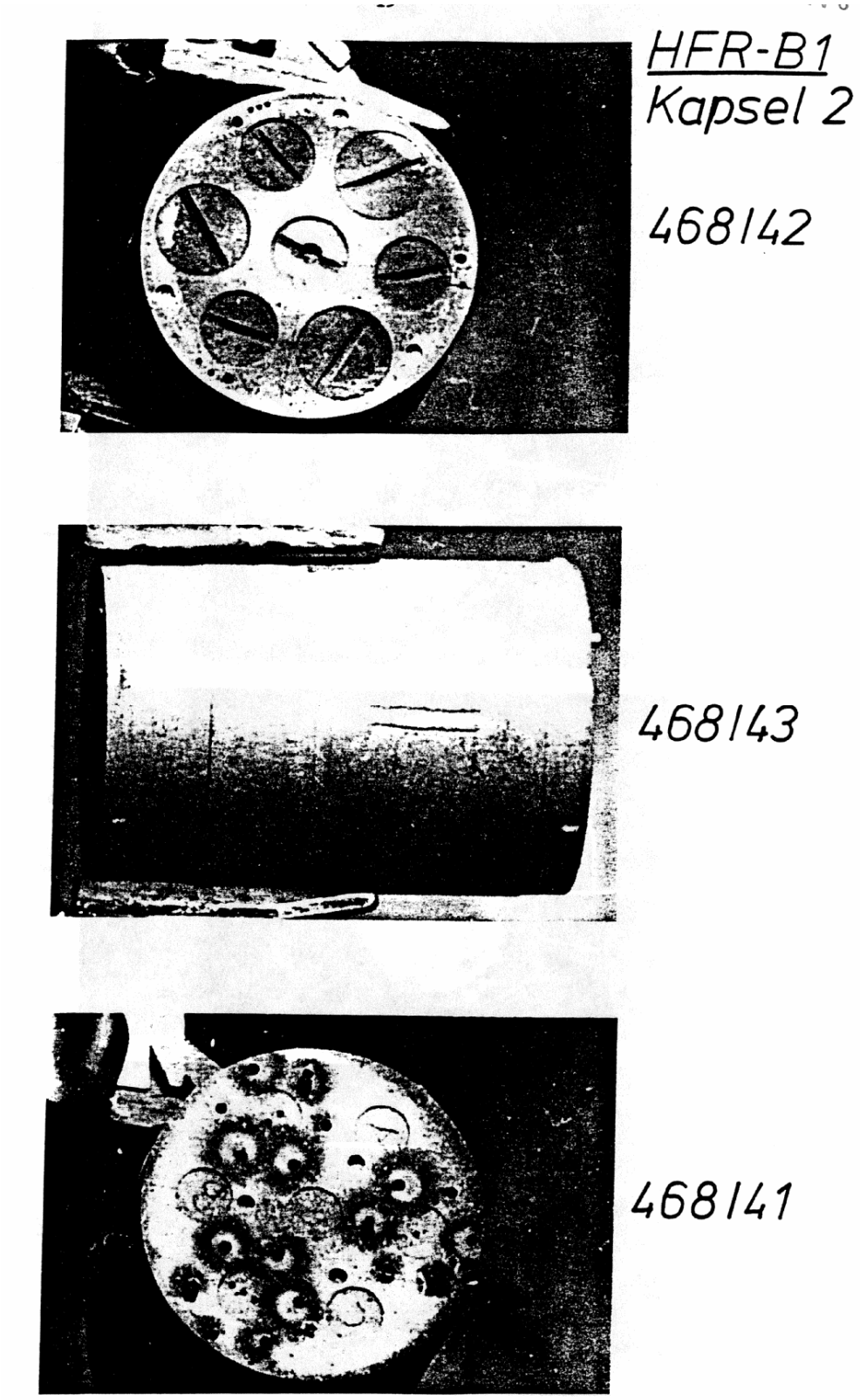

Fig. 6-8. Selected views of Capsule 2 components

The activity profiles for ^{60}Co, which had the least scatter, qualitatively matched the axial profile of burnup for the three capsules. The gamma scans of the fueled graphite bodies were dominated by the nuclides ^{144}Ce, ^{137}Cs, ^{134}Cs, ^{106}Ru, ^{95}Zr, and ^{60}Co. Only ^{60}Co and ^{54}Mn were resolvable in the gamma scans of the gamma scan wires.

6.3.3 Examination of Fuel Compacts

In each of Capsules 2 and 3 there were three fuel holes, and in each fuel hole there were four compacts. The examination of these fuel compacts involved visual inspection and photography, gamma counting, dimensional and weight measurements, metallography, fission product distribution between the fuel compacts and the contiguous graphite, and deconsolidation. In each capsule, fuel hole number 1 was opened for inspection and photography of the contents. In Capsule 2, visual inspection of fuel hole number 1 showed several small broken pieces of the top fuel compact. The four fuel compacts that now stood loose in the fuel hole were removed with a vacuum tool and photographed. The fuel compact from the bottom of the stack is shown in Fig. 6-9. In Capsule 3, visual inspection of fuel hole number 1 showed about 10 loose fuel particles that had debonded from the top fuel compact.

The fuel compacts were gamma scanned after removal of them from the graphite bodies. The resolvable radionuclides were ^{144}Ce, ^{137}Cs, ^{134}Cs, ^{106}Ru, ^{95}Zr, and ^{154}Eu. The inventory of selected fission products was determined from measurement of the gamma radiation on all 24 fuel compacts from graphite bodies 2 and 3. Because the compacts all had a very rough surface and the edges of the cylinders were very easily broken, the dimensional measurements were taken with a measuring microscope having a micrometer stage. The compacts were weighed with a Mettler balance.

No sectioning of the fuel compacts was reported, and no photomicrographs of fuel particles in the fuel compacts from Capsules 2 or 3 were provided in the status report. Representative photomicrographs of UCO fissile particles, ThO_2 fertile particles, and dtf UCO particles from Capsule 1 are shown in Figs. 6-3, 6-4, and 6-5, respectively.

6.3.4 Examination of Graphite Bodies

The unfueled graphite bodies were prepared by removing from the fueled graphite bodies of Capsules 2 and 3 the fuel compacts from the three fuel holes and the piggyback samples from the three simulated coolant holes and central hole. The unfueled graphite bodies were inspected but not photographed. The external appearance of the Capsule 2 graphite body is shown in Fig. 6-8.

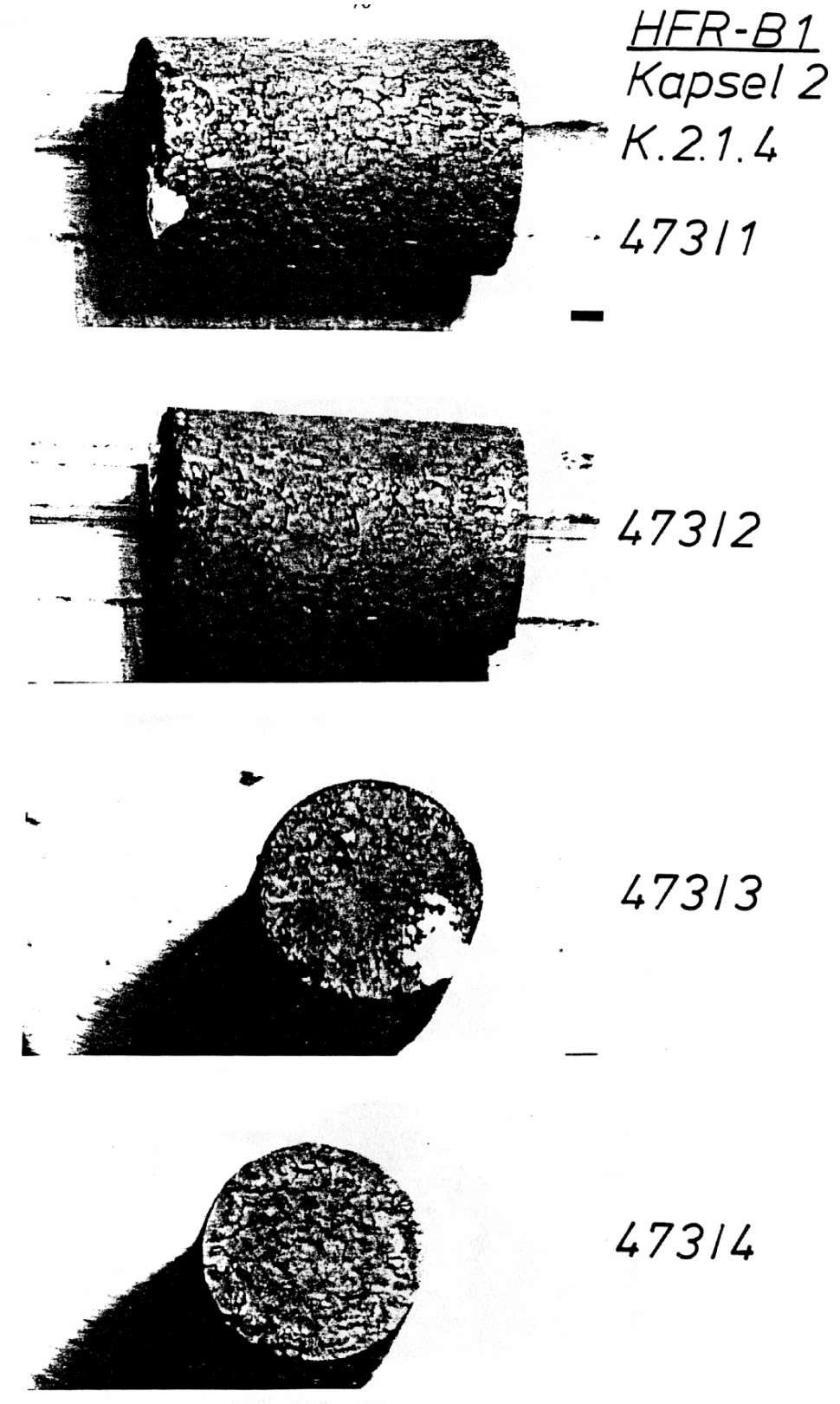

Fig. 6-9. Fuel compacts removed from Capsule 2

To prepare the unfueled graphite bodies for gamma scanning and counting, the two graphite bodies were each cut into 120° cylindrical sectors; the cuts were made vertically through the centers of the simulated coolant hole. Thereafter, cylindrical sectors were cut in half to provide six cylindrical sector halves per capsule.

Gamma scans of the graphite bodies with the fuel compacts removed were obtained for the nuclides ^{144}Ce, ^{137}Cs, ^{134}Cs, ^{60}Co, ^{94}Nb, and ^{182}Ta. These scans illustrated that the cesium activity in the graphite body of Capsule 2 was about three times larger than that in the graphite body of Capsule 3. By contrast, the inverse occurred with the concentrations of ^{60}Co, ^{94}Nb, and ^{182}Ta; their activities in the graphite body of Capsule 3 are about three times larger than those in the graphite body of Capsule 2. In the status report (Myers 1994), these differences were attributed to the effect of the frequent injections of water vapor into Capsule 3. Capsule 2 experienced no water vapor injection. The differences in burnup and temperature in Capsules 2 and 3 were small compared with the differences in the activities cited.

The status report provided the following rationale for this attribution. Water vapor oxidized the binder of the graphite body, thus reducing the retentivity of the graphite for fission products. For example, the diffusion coefficient of cesium increases with increasing graphite oxidation. Thus, ^{137}Cs and ^{133}Cs (the source of ^{134}Cs) spent less time moving through the oxidized graphite resulting in lower concentrations in the graphite. In transit, less time is available for the neutron activation of ^{133}Cs to ^{134}Cs. Consequently, the ratio of ^{134}Cs/^{137}Cs is expected to be less in the oxidized graphite of Capsule 3 than in the unoxidized graphite of Capsule 2. These deductions are consistent with the gamma scan results. The water vapor can also attack the metal components in such a way that the reaction products become mobile and then move into the graphite. This would happen to a greater extent in Capsule 3 than in Capsule 2. This is observed for reaction products involving ^{60}Co, ^{94}Nb, and ^{182}Ta.

The gamma scans also illustrated that the cesium activity in the graphite from Capsule 2 is far greater than the cerium activity. This reflects the known, greater retentivity of cerium than of cesium by the UCO kernels in particles with exposed kernels. The reduced cesium to cerium activity ratio in the graphite from Capsule 3 as compared with Capsule 2 was rationalized to result from a combination of factors involving the relative effects of water vapor in inducing the release of cerium and cesium from the fuel and the reduced retentivity or increased diffusivity of cerium and cesium on the graphite surfaces.[11] The release of cerium from the UCO kernels was much smaller than that of cesium in the absence of water vapor but comparable to that of cesium in the presence of water vapor.

[11] This rationale does not strike the author as compelling.

A comparison was also made of the total inventories of ^{137}Cs and ^{134}Cs in the graphite to that in the fuel compacts; the results are displayed in Fig. 6-10. The fraction of cesium in the graphite is small. For ^{134}Cs, the fractions for Capsules 2 and 3 are 0.045 and 0.019, respectively; for ^{137}Cs, the fractions for Capsules 2 and 3 are 0.039 and 0.016, respectively. The ratios of the fractional cesium content in the graphite to that in the graphite plus fuel compacts is about 2.4 for both Capsules 2 and 3. It is tempting to conclude that the fractional releases from the exposed UCO fuel kernels (the failed dtf particles) was about the same in both capsules, but such a conclusion is unjustified since there is not a complete Cs mass balance for the capsules because the metal canisters of the capsules were not leached to determine the release of Cs isotopes from the graphite bodies.

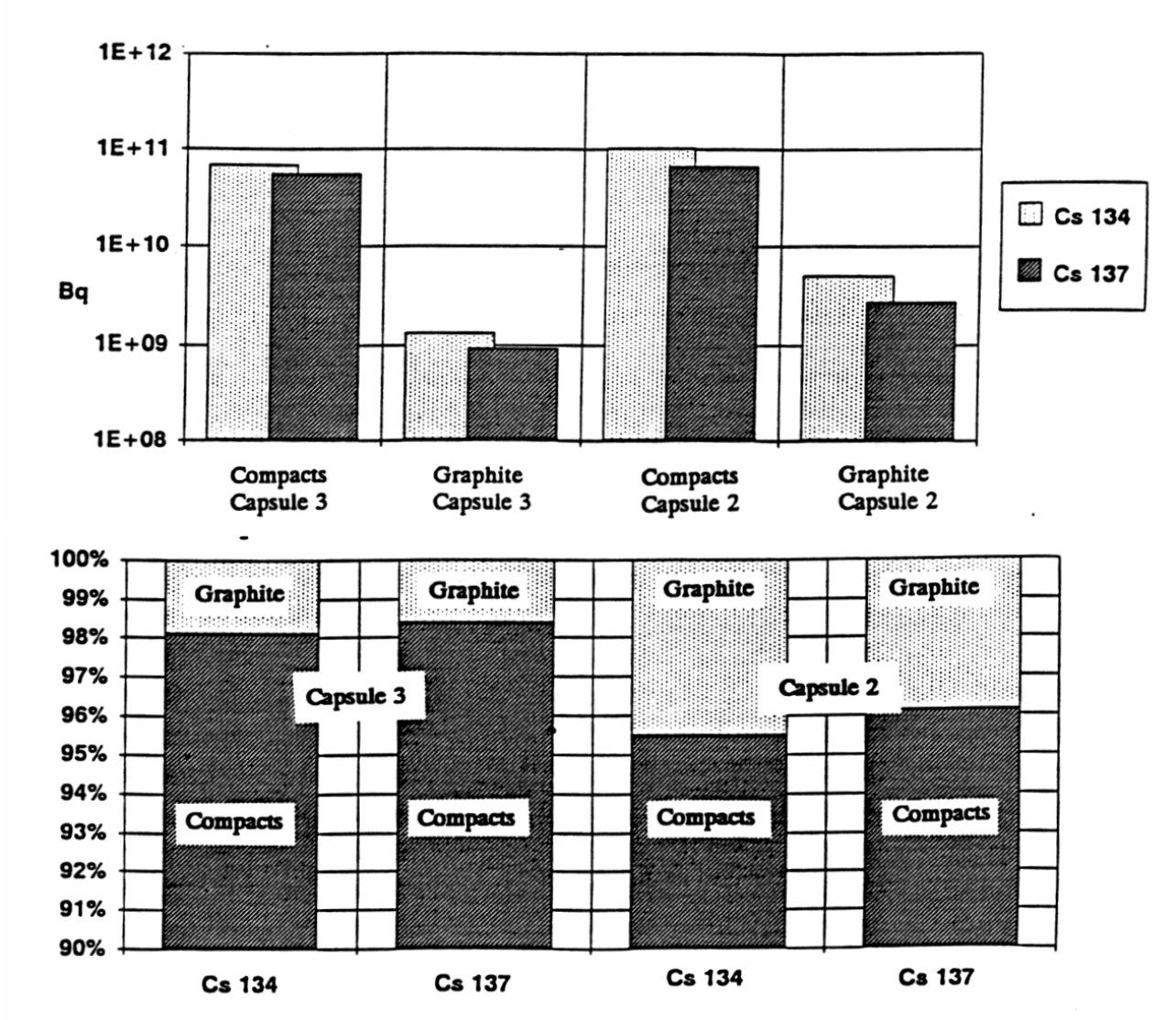

Fig. 6-10. Distribution of Cs-134/-137 between fuel compacts and graphite bodies

6.3.5 Examination of Piggyback Samples

All of the piggyback samples[12] irradiated in Capsules 2 and 3 were recovered from the graphite bodies. Some were examined as part of the PIE performed at FZJ, and the remainder were stored for shipment to other laboratories, including ORNL (Myers 1994).

6.3.5.1 Inert Compacts and Graphite Cylinders

The three normally coolant holes in the graphite body of each capsule contained a complement of six inert compacts, each within a graphite sleeve and eight graphite cylinders. The inert compacts were fired in either SiC or Al powder. The SiC powder was expected to lead to increased compact strength. The sleeves surrounding the compacts were intended to bridge the diameter of the hole. The graphite cylinders were either of grade H-451 or H-451I; the differences in dimensional change, coefficient of thermal expansion, and Young's modulus were to be assessed. Unfortunately, the KFA was unable to measure the coefficient of thermal expansion or Young's modulus in their hot cells.

6.3.5.2 Unbonded Coated Fuel Particles

Unbonded coated fuel particles in two configurations were placed in the central hole (hole 7), in both Capsules 2 and 3. One configuration involved ten covered graphite trays per capsule: half of which each contained 110 fissile, and the other half contained 50 fertile coated fuel particles. The other configuration involved niobium encapsulated particles contained in a graphite crucible. The latter particles were one of three types: dtf fissile particles, intact fissile particles, and particles with exposed kernels generated by laser drilling. The analysis of the particles from trays was conducted. For lack of proper equipment in the FZJ hot cells, analysis of the niobium encapsulated particles was not conducted.

The particle-tray piggyback samples were recovered, opened, and visually inspected. An opened tray from Capsule 2 is shown in Fig. 6-11 as an example.

Twenty particles were taken from the trays in each capsule; five from each of the trays 2-3, 2-4, 2-7, 2-8, and 3-3, 3-4, 3-7, 3-8. Trays 2-3, 2-7, 3-3, and 3-7 each contained 110 UCO fissile particles, and trays 2-4, 2-8, 3-4, and 3-8 each contained 50 $Th0_2$ fertile particles. Five particles were chosen from each tray. The resulting 40 particles from Capsules 2 and 3 were gamma counted individually, and after separating the kernels and coatings of each particle, these constituents were individually counted. From these measurements, the kernel release of fission products in intact particles was determined. The separation of the kernels and coatings was

[12] Here “piggyback samples” includes all test articles except the fuel compacts and graphite bodies

made by cracking the particles in an apparatus with which the force upon cracking could be measured. The following radionuclides were detected: ^{154}Eu, ^{144}Ce, ^{137}Cs, ^{134}Cs, ^{125}Sb, ^{106}Ru, and ^{60}Co.

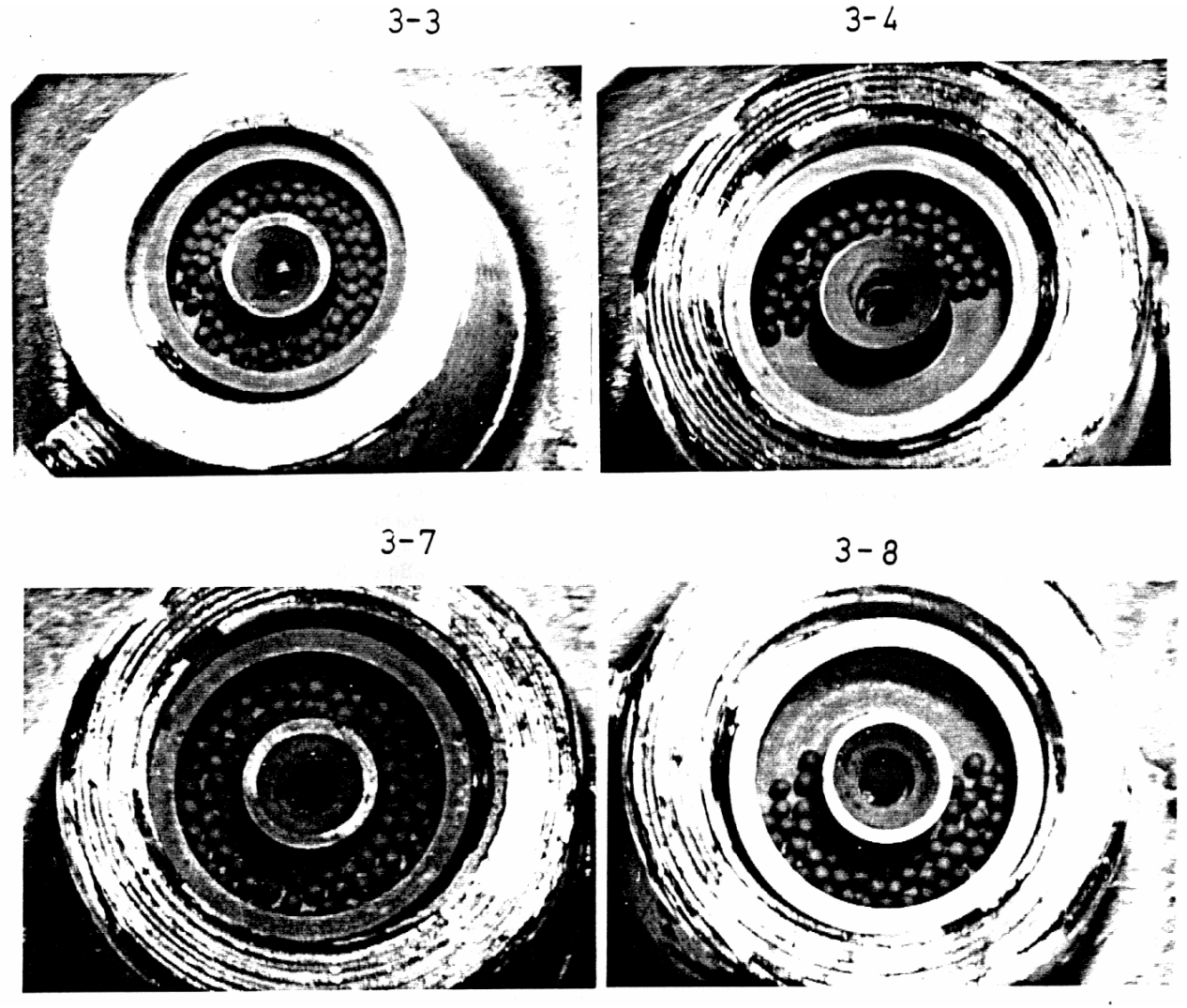

Fig. 6-11. Opened loose particle trays from Capsule 3

The retention of the fission products ^{154}Eu, ^{144}Ce, ^{106}Ru, ^{125}Sb, and ^{124}Sb (an activation product) was essentially complete. For ^{137}Cs and ^{134}Cs, the release from the kernel was between 1.5 and 3%. The releases for cesium seem to be quite small for an irradiation lasting 446 EFPD. The release of fission products from the kernel in an intact particle is known to be small in comparison with the release from an exposed kernel; for example, in the experiment R2-K13 (Myers 1985), the measured Cs kernel release in intact particles was 13 ± 7% of that for the exposed kernel. However, the averaged absolute release from the kernels in intact particles was about 15% for ^{137}Cs over the temperature range 900 to 1,200 °C during an irradiation of 517 EFPD.[13]

6.3.6 Postirradiation Heating of Fuel Compacts and Loose Particles

Heating tests with intermittent injections of water vapor were conducted with fuel compacts and unbonded fuel particles recovered from Capsules 2 and 3. These tests were conducted in the KORA facility (Schenk 1993) at KFA under postirradiation conditions.

The KORA facility consists of a flow apparatus in which the sweep gas, He, can be mixed with water vapor and sent through a furnace containing the fuel specimen (i.e., particles, compacts, or fuel spheres). The water vapor interacts or reacts with the exposed kernels and the carbonaceous material in the specimen. The former results in an enhanced release of fission products. The sweep gas mixture containing the released fission products passes through and is acted upon by ion chambers and the various filters in the gas train. At the end, the activity of the fission gases is measured. In the tested specimens, the activity of the moderate- and short-lived fission gas isotopes is negligible because of the protracted delay between the end of irradiation and the start of the KORA test. In KORA, only the long-lived gaseous isotope ^{85}Kr has been measured.

The specimens used in the four heating tests conducted with intermittent injections of water vapor were the fuel compacts 2.2.1 plus 2.2.2; 3.2.1 plus 3.2.2; and two sets of five kernels taken from ten particles that had been irradiated in tray 3-7. Tray 3-7 contained normally configured fissile UCO TRISO particles.

6.3.6.1 Water Vapor Injection Tests with Fuel Compacts

The fuel compacts 2.2.1 and 2.2.2 were irradiated in Capsule 2 and were not exposed to water vapor during irradiation. The release of ^{85}Kr during the heating test and water vapor injections at 800 ºC with the set of fuel compacts 2.2.1 and 2.2.2 is shown in Fig. 6-12 as a function of time in terms of the fractional release and the release rate.

[13] The R2 K13 test fuel was known to have a high, but poorly quantified, as-manufactured SiC defect fraction; therefore, this assertion should be viewed with a degree of skepticism.

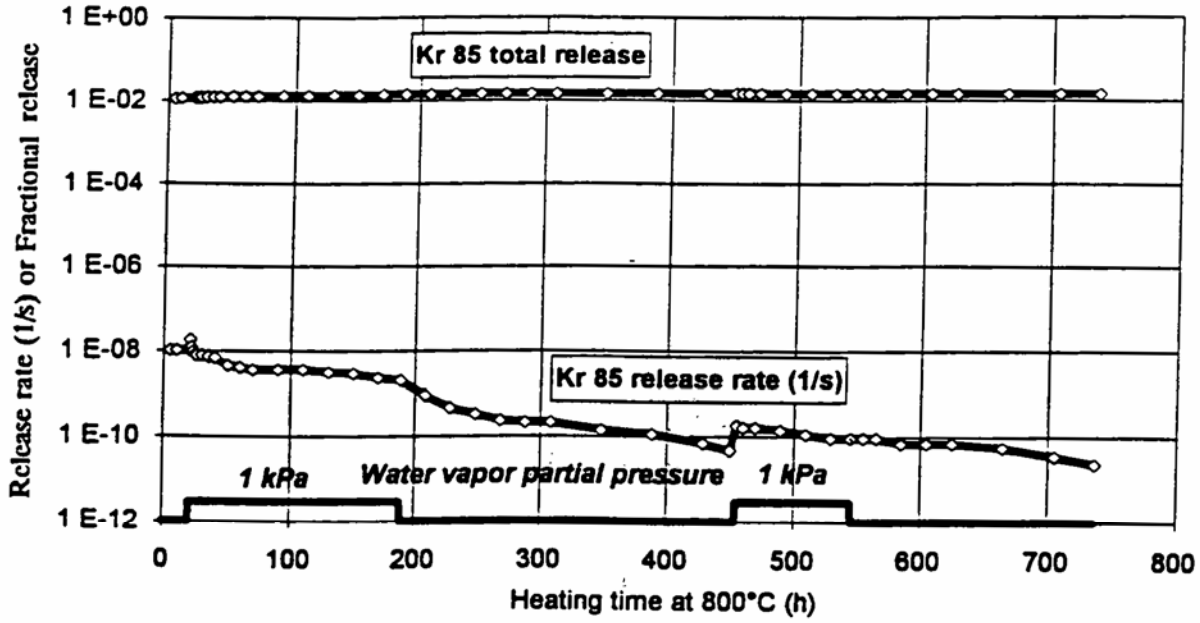

Fig. 4.121 The fractional release and release rate of ^{85}Kr at 800° C from fuel compacts 2.2.1 and 2.2.2 as a function of time and the partial pressure of water vapor Source: Forschungszentrum Jülich GmbH, Jülich, Germany

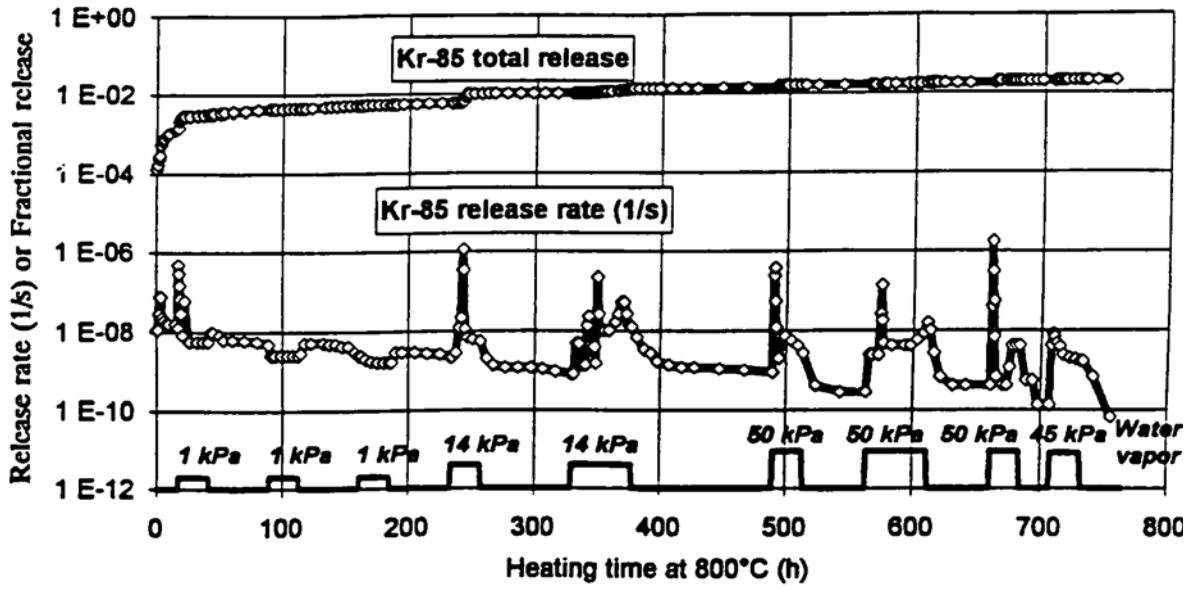

Fig. 4.122 The fractional release and release rate of ^{85}Kr at 800° C from fuel compacts 3.2.1 and 3.2.2 as a function of time and the partial pressure of water vapor Source: Forschungszentrum Jülich GmbH, Jülich, Germany

Fig. 6-12. Postirradiation heating of fuel compacts from HFR-B1

The data show a general decline in the release rate of ^{85}Kr, a trend consistent with a decline in the inventory of this isotope. At the beginning of the two water vapor injections, at a partial pressure of 1 kPa, there is a detectable rapid increase in the release rate. Thus, the ^{85}Kr release is enhanced and therefore the release is a function of the water vapor pressure. The increases are, however, small in accord with a small inventory of ^{85}Kr. The small inventory may be a consequence of the higher temperatures and frequent changes in temperature experienced during the irradiation undergone by the compacts in Capsule 2.

It appears that during the first water vapor injection that the release of ^{85}Kr following the initial rapid increase is higher than in the absence of the water vapor as indicated by the noticeable decline in release rate upon termination of the injection. However this persistent, enhanced release is not evident during the second water vapor injection and is somewhat obscured generally by the steady decline in release rate.

The fuel compacts 3.2.1 and 3.2.2 were irradiated in Capsule 3 and were exposed to water vapor during irradiation. Unfortunately, after the water-vapor injections, but with one exception, insufficient time was allowed for sintering and annealing; the same can be said of the tests under discussion. These relatively high frequencies of injection complicate the analysis.

The release of ^{85}Kr during the second heating test and associated water vapor injections at 800 ^{o}C with the set of fuel compacts, 3.2.1 and 3.2.2, is also shown in Fig. 6-12 as a function of time in terms of the fractional release and the release rate. The partial pressure of water vapor ranged from 1 to 50 kPa, and altogether there were nine injections. In seven of the injections, there were distinct and rapid initial releases of ^{85}Kr in qualitative agreement with previous experiments. Of the first three water vapor injections, all at 1 kPa of water vapor, the response of the fuel compacts to the second and third resulted in a distinct decrease to a steady value of the release rate, which at the termination of water vapor injection, returned to the pre-injection level.

Over the range of water-vapor partial pressures, a more or less typical release rate pattern is observed. There is an initial rapid release that declines to a level showing a much less rapid decline and then again, after the termination of the injection of water vapor, to a level with a still more gentle decline, a decline that over the period of 755 hours of the test apparently represents a roughly steady depletion rate for the inventory of ^{85}Kr.

6.3.6.2 Water Vapor Injection Tests with UCO Kernels

The kernels of $UC_{0.5}O_{1.5}$ from unbonded particles irradiated in tray 7 in the central hole of Capsule 3 were heated at 800 ^{o}C in the KORA facility with intermittent injections of water vapor. Two KORA experiments were conducted using five kernels in each test; the kernels had been

removed from the particles after cracking the particles. The release profiles of ^{85}Kr during the heating tests are shown in Fig. 6-13 for the two separate tests with the assumed identical sets of five kernels. The test data indicate that a strong variation occurs between the two release rate profiles. In one case, a large release occurs upon bringing the sample to the test temperature, and a smaller release occurs upon injecting water vapor at a partial pressure of 1 kPa. In the other case, the inverse occurs; i.e., the release is smaller upon bringing the kernels to the test temperature and larger upon injecting water vapor at a partial pressure of 1 kPa. Thus, a consistent response to the experimental conditions is absent. Such fuel behavior was not observed with essentially bare kernels embedded in fuel compacts heated under irradiation conditions with intermittent water vapor injections.

6.3.7 Status of Capsules 2 and 3 PIE

An overview of the state of completion of the planned PIE of Capsules 2 and 3 is given in Fig. 6-14, which is a markup of the PIE flowchart (Fig. 6-1) at the time the 1994 PIE status was prepared. No subsequent documentation has been recovered that indicates any significant additional PIE work was completed for these two HFR-B1 capsules.

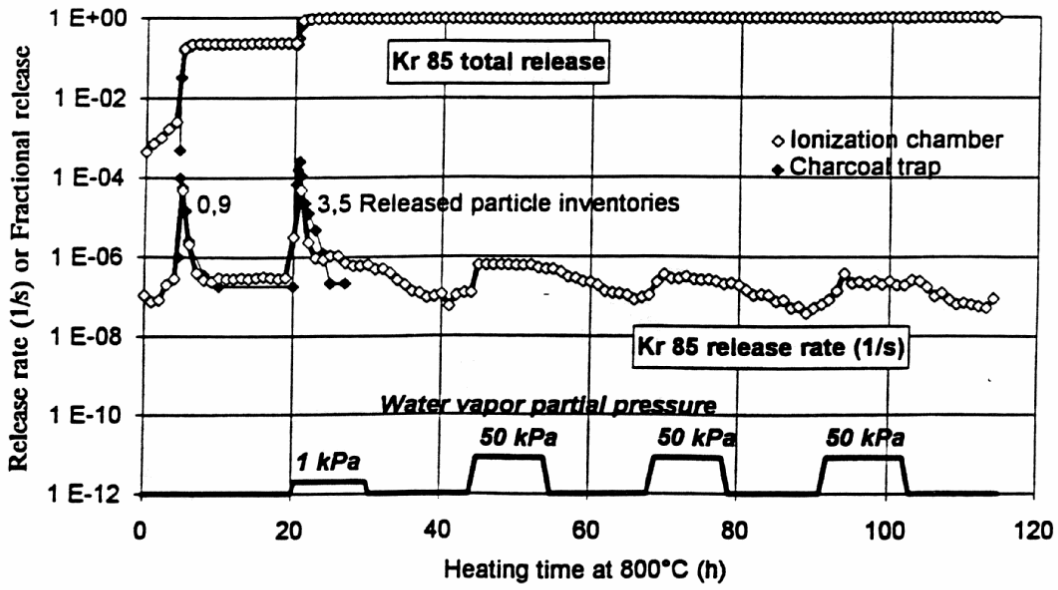

Fig. 4.124 The fractional release and release rate of ^{85}Kr at 800° C from 5 UCO kernels taken from particles in tray 3-7 as a function of time and the partial pressure of water vapor Source: Forschungszentrum Jülich GmbH, Jülich, Germany

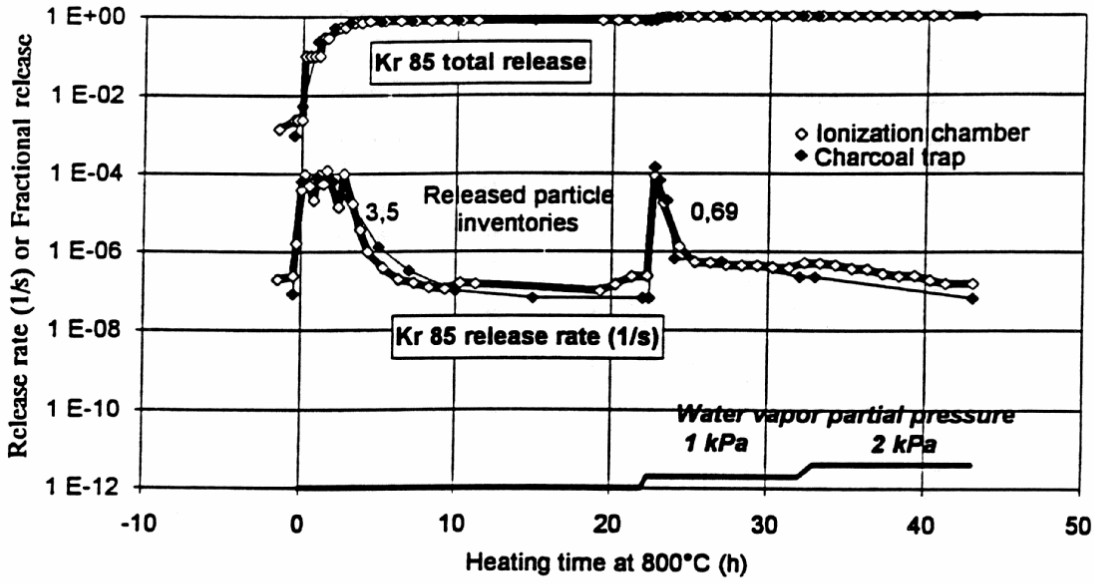

Fig. 4.125 The fractional release and release rate of ^{85}Kr at 800° C from 5 UCO kernels taken from particles in tray 3-7 as a function of time and the partial pressure of water vapor Source: Forschungszentrum Jülich GmbH, Jülich, Germany

Fig. 6-13. Release of Kr-85 from UCO kernels heated at 800 °C

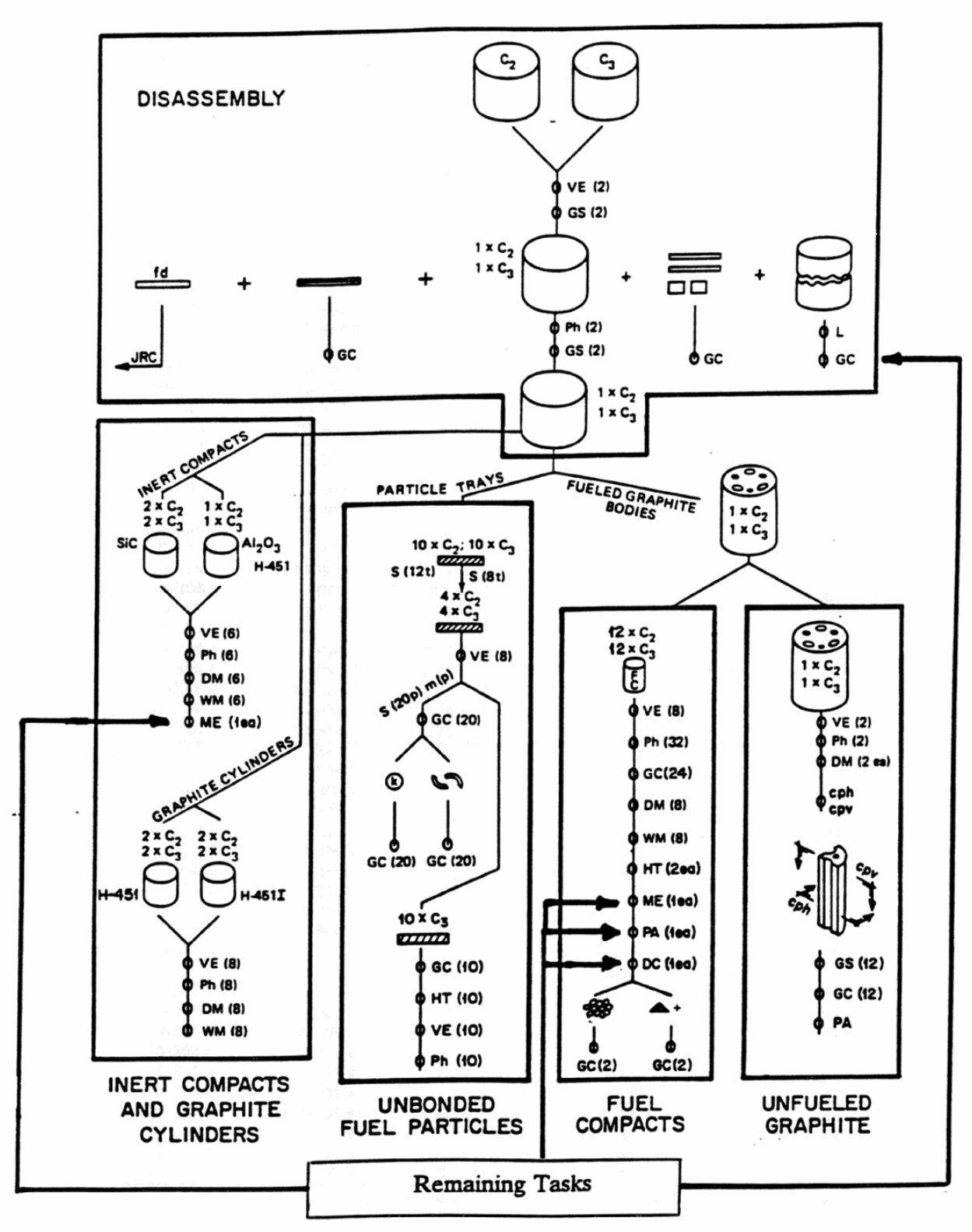

Fig. 6-14. Remaining PIE tasks for Capsules 2 and 3

7 EVALUATION OF THE HFR-B1 DATABASE

As described in Section 2, the motivation for the AGR program to fund the preparation of this summary report for the HFR-B1 test was twofold: (1) to assess the further utility of this database for meeting certain FP transport DDNs and (2) to determine what lessons might be learned to guide in the design of several planned AGR irradiation experiments (AGR-3, AGR-4, and AGR-8) that have test objectives closely related to those for HFR-B1.

With this motivation in mind, this section summarizes the previous evaluations of the HFR-B1 database that have been performed at ORNL and GA. This report was not intended to provide—and does not provide—a new independent evaluation of the experimental database; rather, it seeks to make an informed recommendation to program management regarding the programmatic value of funding such a new independent evaluation of any or all of the existing HFR-B1 data. Conclusions and recommendations are summarized in Section 8.

As previously described (Section 3.2), each of the three capsules had a specific purpose, and previous test evaluations have tended to focus on a single capsule. In fact, most of the past evaluations have focused on Capsule 3 and the effects of water ingress on fission gas release from exposed UCO fuel kernels (i.e., failed particles). This past emphasis on Capsule 3 is not surprising since large water ingress was a dominant risk event for steam-cycle HTGRs that were the reference designs in the United States and Germany when the HFR-B1 test program was conceived in the mid-1980s. Now that the global emphasis has shifted to direct-cycle, gas-turbine MHRs and hydrogen-production VHTRs, the risk of large water-ingress accidents is much reduced (e.g., Hanson 2004a). In addition, because of the higher core outlet temperatures (850 to 950 ^{o}C) for these advanced HTGR designs and because of the potential impact of fission metal plateout on turbine maintenance in direct-cycle plants, the release of fission metals from the core (Capsule 1) and the effects of high temperature on fission gas release (Capsule 2) have become higher priority design issues.

7.1.1 Capsule 1

The primary objective of the Capsule 1 experiment in HFR-B1 was to characterize the transport of fission metals in core materials, specifically in LEU UCO fuel kernels, TRISO particle coatings, fuel-compact matrix (petroleum pitch), and H-451 graphite. To that end, a complicated capsule design was conceived and implemented that included a well-defined fission product source (i.e., dtf particles) and fission product sinks (char impregnated graphite wedges) to obtain an overall FP mass balance. It also included various piggyback samples for characterizing fission metal transport in particle coatings (Section 4.2).

Because the purpose was to characterize fission metal transport in core materials, essentially all of the critical test data were to be generated during the Capsule 1 PIE. As described in

Section 6.2, an attempt was made in 2004 to determine how much of the Capsule 1 PIE data could be recovered (Hanson 2004b). The purpose of that investigation was to assess whether sufficient data for Capsule 1 could be obtained for use in meeting a portion of the DDNs regarding fission metal transport in HTGR core materials.

It appears that much, but not all, of the planned destructive Capsule 1 PIE was completed. The eight FZJ progress reports (Table 6-1) are cryptic data compilation reports that contain essentially no data evaluation or conclusions. It is surprising that no final documentation—no final data compilation report, not even an official letter closing out the ORNL contract with FZJ, etc.—has been discovered at ORNL or FZJ. Perhaps, it is less surprising when one recalls that cancellation of the U.S. HTGR program was announced in August 1995, and funding for the PIE was presumably terminated shortly thereafter.

The 2004 evaluation concluded that, unless additional information is subsequently discovered (considered unlikely), there is not sufficient quantitative data available to justify the use of the HFR-B1 Capsule 1 database for satisfying the aforementioned DDNs. The primary reasons for this conclusion were twofold: (1) a sufficiently long time lapsed between the completion of the irradiation phase of the experiment and the PIE such that 250-day Ag-110m decayed to below detection limits and (2) the reported gamma scan results for most of the Capsule 1 components (fuel compacts, graphite pieces, metal canister, etc.) are relative count rates that were not reduced to absolute radionuclide inventories.

While the above conclusion is disappointing with regard to satisfying FP transport DDNs, there are still valuable lessons to be learned from the Capsule 1 experience with regard to test article design for such experiments. The first lesson is that “dtf” particles work, that they provide a well-defined fission product source as intended. The photomicrographs of the irradiated dtf UCO particles in Capsule 1 (Fig. 6-5) indicate that the UCO kernels more or less retained their integrity. There is a suggestion that these exposed UCO kernels developed more porosity than the UCO kernels in intact TRISO particles (Fig. 6-3); however, the amount of porosity in these dtf UCO kernels does appear to qualitatively differ from the amount of porosity in failed UCO particles of comparable burnups that has been observed in fuel irradiation tests, such as HRB-21 (Acharya 1995). In any case, if exposed kernel in failed dtf particles develop additional porosity compared with failed standard particles, the result would serve to yield conservative data for fission product release. The fact that the online fission gas R/Bs for Capsule 1 remained virtually constant to a burnup of 21.5% FIMA suggests that this macroscopic porosity, which presumably increased with burnup, did not appreciably affect the fission gas release characteristics of the UCO kernel.

The next lesson learned from Capsule 1 should be obvious: the use of tomography to characterize fission metal concentration distribution in test articles is viable only if the tomography results are properly calibrated to give absolute concentrations. A much debated

topic during the planning for the Capsule 1 PIE was the experimental method to be used for determining the radionuclide distributions within the graphite wedges (i.e., concentration profiles). Two approaches were considered: coring/slicing/gamma counting and tomography. The first approach is traditional, tedious, and very expensive but yields accurate absolute concentrations. The second approach is developmental; the fundamental issue is whether proper calibrations can be performed to obtain reliable quantitative results. The decision was made by the KFA to employ the tomographic method in conjunction with limited coring: tomography to determine relative concentrations with possibly finer resolution and certainly less effort than with the coring method, and coring/slicing/gamma counting to establish absolute concentrations. If an attempt was made to cross correlate the tomography and the coring results, the results have apparently not been published. Without proper calibration, tomography only produces "interesting pictures" (see Figs. 6-6 and 6-7[14]) that are of very limited value for transport model development or methods validation.

That being said, the qualitative tomography results dramatically demonstrate the greatest lesson to be learned from Capsule 1 for guiding the design of future test articles. Although clever and imaginative, the design of Capsule 1 was hopelessly complex. Figures 6-6 and 6-7 show typical results from the tomography scans of the Cs-137 distributions in the graphite parts after the fuel compacts had been removed (Schroeder 1994). Suffice it to say that the Cs distribution is exceedingly complex. Even if the tomography results had been quantified by proper calibration techniques, it is difficult to imagine how effective diffusion coefficients could have reliably been derived from such data. As a point of departure, the data would by necessity have been analyzed as a permeation experiment because the apparent concentration profiles are exceedingly complex.

Even though Capsule 1 was specifically designed to characterize fission metal transport in graphite, the design still proved to be problematic. The physical configuration was simply far too complicated and too asymmetrical, which produced exceedingly complex Cs distributions. Because of these results, a simple, one-dimensional, test article geometry has been recommended for the AGR fission product transport capsules (Hanson 2005).

7.1.2 Capsule 2

The primary objective of the Capsule 2 experiment was to characterize the temperature dependence of fission gas release from failed UCO particles, including the effect of so-called "enhanced" fission gas release. This enhanced fission gas release, which has been attributed to release of stored fission gases as a result of kernel restructuring, was expected to occur between 1,000 and 1,500 °C only in the presence of a neutron flux. Capsule 2 was also

[14] The citation (Schroeder 1994) includes dozens of such tomography scans, all equally complex, for Cs-137 and Cs-134.

intended to supply irradiated fuel compacts and loose particles for postirradiation heating experiments.

An extensive amount of online, fission gas release data (R/Bs) was logged for Capsule 2 during the 444 EFPD irradiation (Section 5.2.2). Inspection of the raw R/B data in the operating history report (Burnette 1994) does indicate some apparent transient "enhanced" gas release when the operating temperatures were rapidly increased. However, caution is advised before drawing any firm conclusions because the R/B is essentially a steady-state construct. When applied to transient conditions, the rapid release of stored fission gases as a result of rapid increases in fuel temperatures produces an artificially high R/B value, which is not observed in the transient fractional release of the total fission gas inventory (the stored gas inventory plus the instantaneous production rate). This same effect is important when evaluating the Capsule 3 data and is discussed in greater detail in Section 7.1.3.

The above complication notwithstanding, there is no documented evaluation of the online fission gas release data from Capsule 2. As described in Section 6.3.6, two irradiated fuel compacts from Capsule 2 were used in postirradiation heating tests that involved periodic water vapor injection at 800 °C. An evaluation of those heating test data by Myers is provided in the PIE status report for Capsules 2 and 3 (Myers 1994) and again in IAEA TECDOC-978. The essential conclusions were summarized in Section 6.3.6.

The fission gas release data from Capsule 2 (and from Capsule 1) have not been analyzed in the available HFR-B1 documentation. These data were evaluated in preparing this report and judged to have substantial value for development of improved fission gas release models. Consequently, further quantitative analysis of these data is conditionally recommended; this analysis would include a comparison of the predicted gas release made with the FDDM/F models for the as-run test conditions to the measured R/B data. These results, in combination with the other existing UCO gas release data, should be used to upgrade the reference gas release models for LEU UCO particles as appropriate. However, enthusiasm for such an analysis is tempered by the reported inability to locate the electronic data files for the HFR-B1 test that were provided by JRC Petten to ORNL (Morris 2006). Consequently, any future analysis would have to be based upon the raw data available in the operating history report (Burnette 1994). In that regard, one should recall that the R/B values recorded in that report are approximate values based upon several simplifying assumptions described in Section 5.3.4.2. If the electronic data records were available, removing those undesirable assumptions would be relatively straightforward. Without the electronic data files, their removal would be more tedious.

7.1.3 Capsule 3

The objective of the Capsule 3 experiment was to characterize the effect of water on fission product transport, especially the effect of hydrolysis on the fission gas release rates from failed

UCO particles. Myers produced a large number of reports analyzing the considerable amount of test data generated from Capsule 3. The first report was issued in 1987 (Myers 1987) and one in 1995; Myers also wrote Section 5 of 1997 TECDOC-978, which summarizes all of the available data on the effects of water and air ingress on fission gas release from exposed fuel kernels.

It is important to note that the HFR-B1 Capsule 3 hydrolysis data were typically not analyzed in isolation. In fact, two other irradiation experiments to investigate the effects of water ingress on fission gas release during irradiation were conducted in roughly the same time period. The HRB-17/-18 irradiation was completed in the ORNL HFIR reactor in January 1986, prior to the beginning of the HFR-B1 irradiation in April 1987. The HRB-17/-18 test was actually a simultaneous irradiation of two identical capsules: HRB-17 had periodic water injections during the irradiation, and HRB-18 was irradiated dry but was subjected a large water ingress after final shutdown (Ketterer 1987). In simple terms, the HRB-17/-18 tests contained a single stack of six short fuel compacts surrounded by a graphite body. The fuel compacts were seeded with dtf LEU UCO particles from the same batch of dtf particles used in the HFR-B1 test; ~3% of the fissile particles were dtf particles. The greatest difference between the HFIR and HFR Petten irradiations was that the fission rate density was approximately ten times higher in HFIR.

The other water injection experiment was the HFR-K6 experiment, which was completed after the HFR-B1 test. The HFR-K6 test, which was irradiated in HFR Petten, contained four German fuel spheres with TRISO-coated LEU $U0_2$ particles dispersed in A3-3 matrix graphite and contained in three capsules (Nabielek 1995). Two of the particles had as-manufactured defects resulting in exposed kernels.

In addition to these three experiments that had water injection during irradiation, several postirradiation heating experiments with periodic water injection were conducted at FZJ in the KORA test facility (Section 6.3.6, Schenk 1993). Besides the heating tests with fuel compacts and kernels from Capsules 2 and 3, other tests with water injection were conducted with irradiated AVR fuel spheres with LEU TRISO UO_2 particles and with LEU UO_2 kernels extracted from irradiated AVR pebbles.

The point of introducing these other water effects tests here is that the data evaluation of the HFR-B1 Capsule 3 results and the associated modeling development by Myers generally utilized data from multiple sources. Three data evaluation reports are particularly significant as is the discussion of hydrolysis effects in TECDOC-978, and these four documents are summarized below. The serious reader is encouraged to obtain the original documents.

7.1.3.1 DOE-HTGR-88486

Myers issued DOE-HTGR-88486 in September 1991 (ORNL-6610, Myers 1991). It is a massive 238-page document that presents a comprehensive interpretation of fuel hydrolysis phenomena and complicated semi-empirical models for correlating the test data from the HRB-17 and -18 experiments. This work was also summarized in a journal article (Myers 1992). These same concepts and models would be subsequently used for Myers's analyses of HFR-B1 Capsule 3.

As introduced above, these experiments were conducted in the HFIR at temperatures between 700 and 1,000 °C, a system pressure of 200 kPa, and partial pressures of water vapor between 20 and 1,850 Pa. In HRB-17, the general sequential response of the exposed fuel kernels to water-vapor addition consisted of three stages: (1) a rapid release of stored fission gas with a concomitant increase in the steady-state release, (2) a period of constant steady-state release, and upon removal of the water-vapor source (3) a decline in the release to prehydrolysis values except where configuration changes occurred in the particles with exposed kernels. These effects are demonstrated in Fig. 7-1.

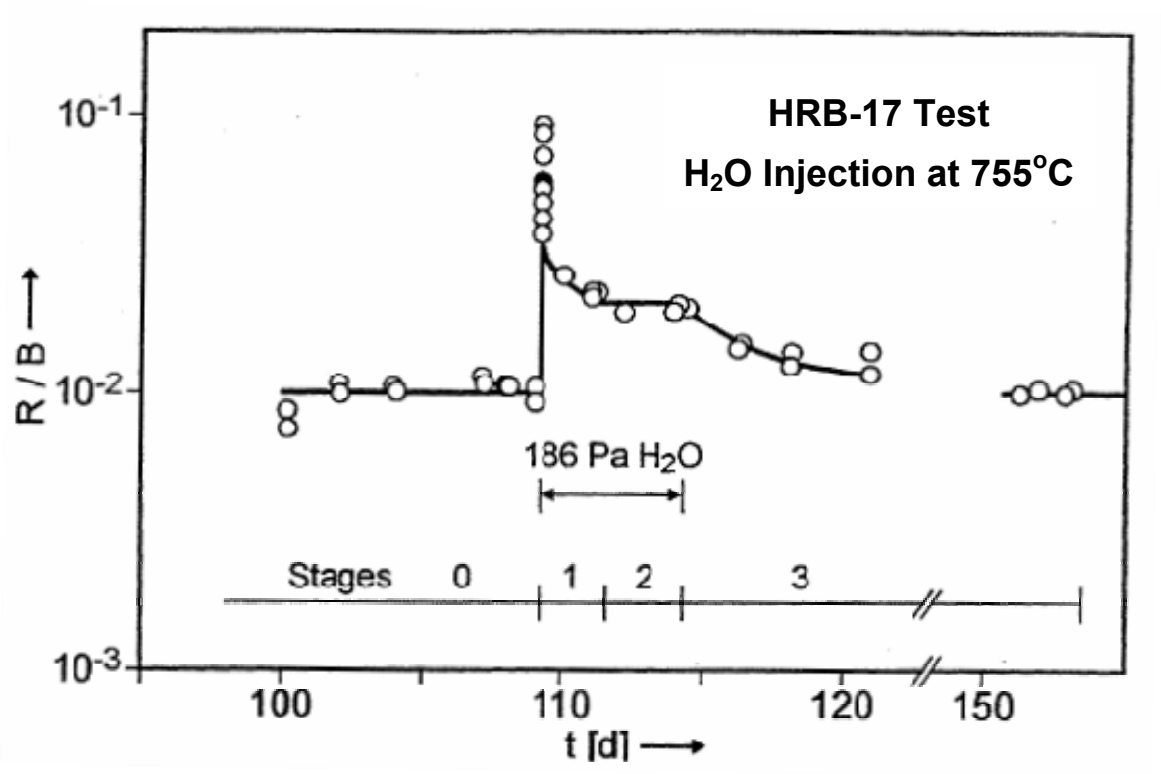

Fig. 7-1. Effect of water ingress on fission gas release

The release of stored fission gas was dependent on the square of the partial pressure of water vapor. The ratio of the steady-state fission gas release in the period of constant release to the prehydrolysis value was independent of the partial pressure of water vapor. The time constant

for the decline in the release was the same in all of the hydrolysis tests. A phenomenological model was developed to describe the time profiles of krypton, xenon, and iodine isotopes; the model was in good agreement with the measurements.

7.1.3.2 DOE-HTGR-88506

In September 1990, Richards (GA) reviewed an early draft of ORNL-6610 (Myers 1991) and the preliminary HFR-B1 Capsule 3 gas release data (Conrad 1990) and issued a critique of the modeling work (DOE-HTGR-88506, Richards 1990). He concluded that initial evaluations of the HRB-17 and Petten hydrolysis data were probably misinterpreted and that these misinterpretations resulted from reporting the transient fission gas release data as R/B values rather than fractional release of the total inventory (stored inventory plus the instantaneous production rate. He converted the HFR-B1 data for six water-vapor injections to fractional release of inventory versus the elapsed time from water-vapor injection and obtained the results shown in Fig. 7-2. At high water-vapor pressures, the fractional release appears to level off at 20% to 30% of inventory for reaction times on the order of one day.[15] These values for fractional release correspond to measured peak R/B values that are in excess of 200%. He concluded that the use of (R/B) to report releases of stored fission gases can be misleading and may result in wrongful assessments of the impact of the experimental data on reactor design and safety.

Richards also argued that the HRB-17 data could not be arbitrarily extrapolated to the high water partial pressures characteristic of a large water ingress in a steam-cycle HTGR. During the HRB-17 experiments, measurements of fission-product release during fuel hydrolysis were obtained for water-vapor injections ranging from about 200 to 2,000 6 uatm (20 to 200 Pa). When integrated over the duration of the peak-release period, the observed fractional release of equilibrium inventory was found to be proportional to approximately the square of the water-vapor pressure. Figure 7-3 is taken from (Myers 1991) and shows this observed dependence of fractional release on water-vapor pressure. He superimposed the HFR-B1 data, converted to a fractional release basis, on the HRB-17 data and concluded that the fractional release was evidently independent of the water partial pressure at the two highest water pressures.

There is a sound theoretical basis for Richards's assertion if the interaction of the water vapor with the exposed fuel kernels behaves like a gas-solid chemical reaction that exhibits Langmuir-Hinshelwood kinetics (e.g., Thomson and Webb 1968). Most heterogeneous gas-solid reactions follow a Langmuir-type reaction mechanism. In its simplest form, a Langmuir-type reaction rate is given by:

[15] For large water ingress events in a steam-cycle MHTGR (PSID 1992), the reaction times are expected to be about 1 hour, and the observed fractional release (from Fig. 7-2) is less than 1%.

$$k = \frac{c_1 P}{1 + c_2 P} \tag{7-1}$$

where k is the reaction rate, P is the partial pressure of the reacting gas, and c_1 and c_2 are temperature-dependent rate constants for the adsorption and gasification steps in the reaction.

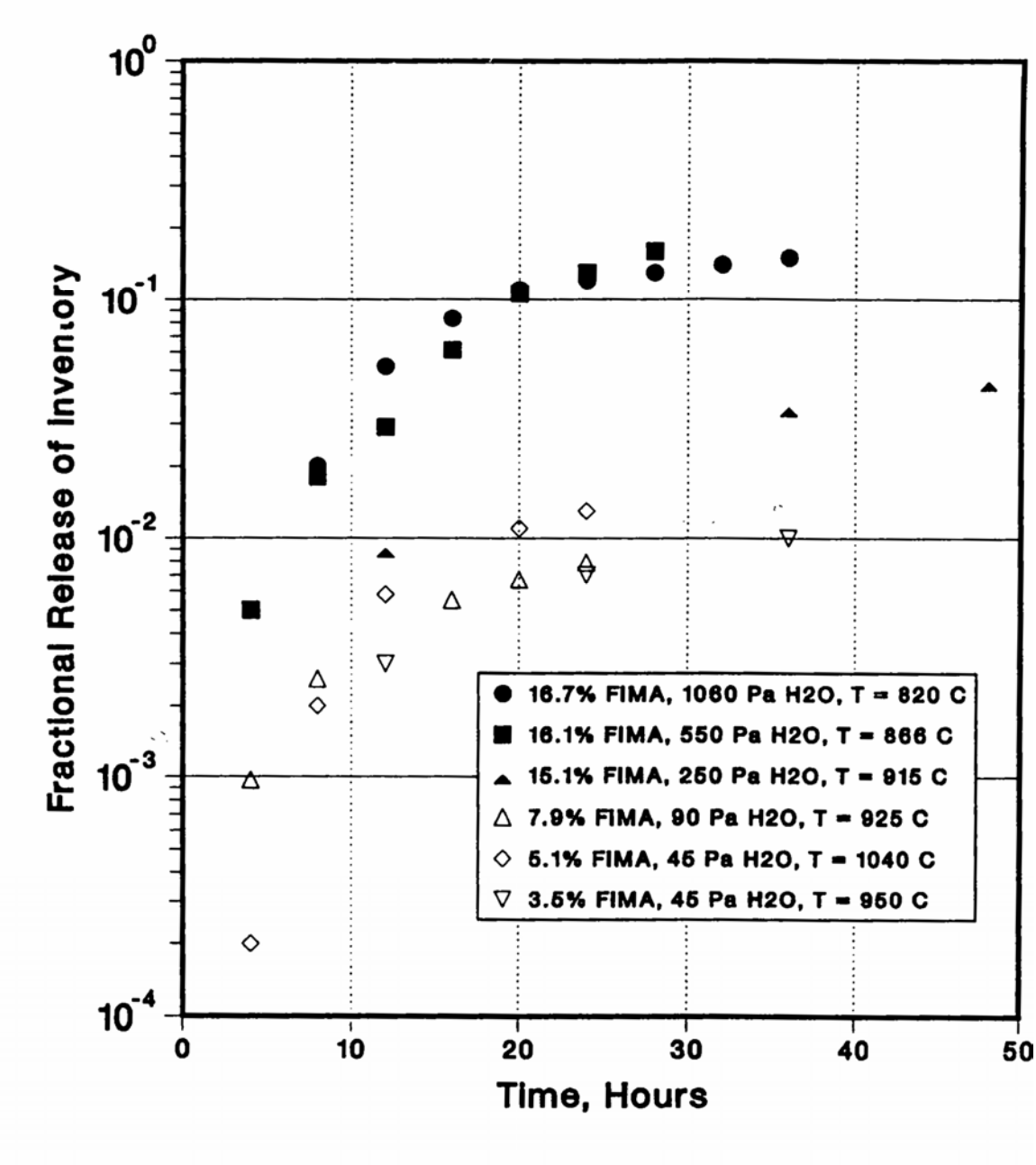

Fig. 7-2. Fractional release of Xe-133 during H_2O injection in HFR-B1

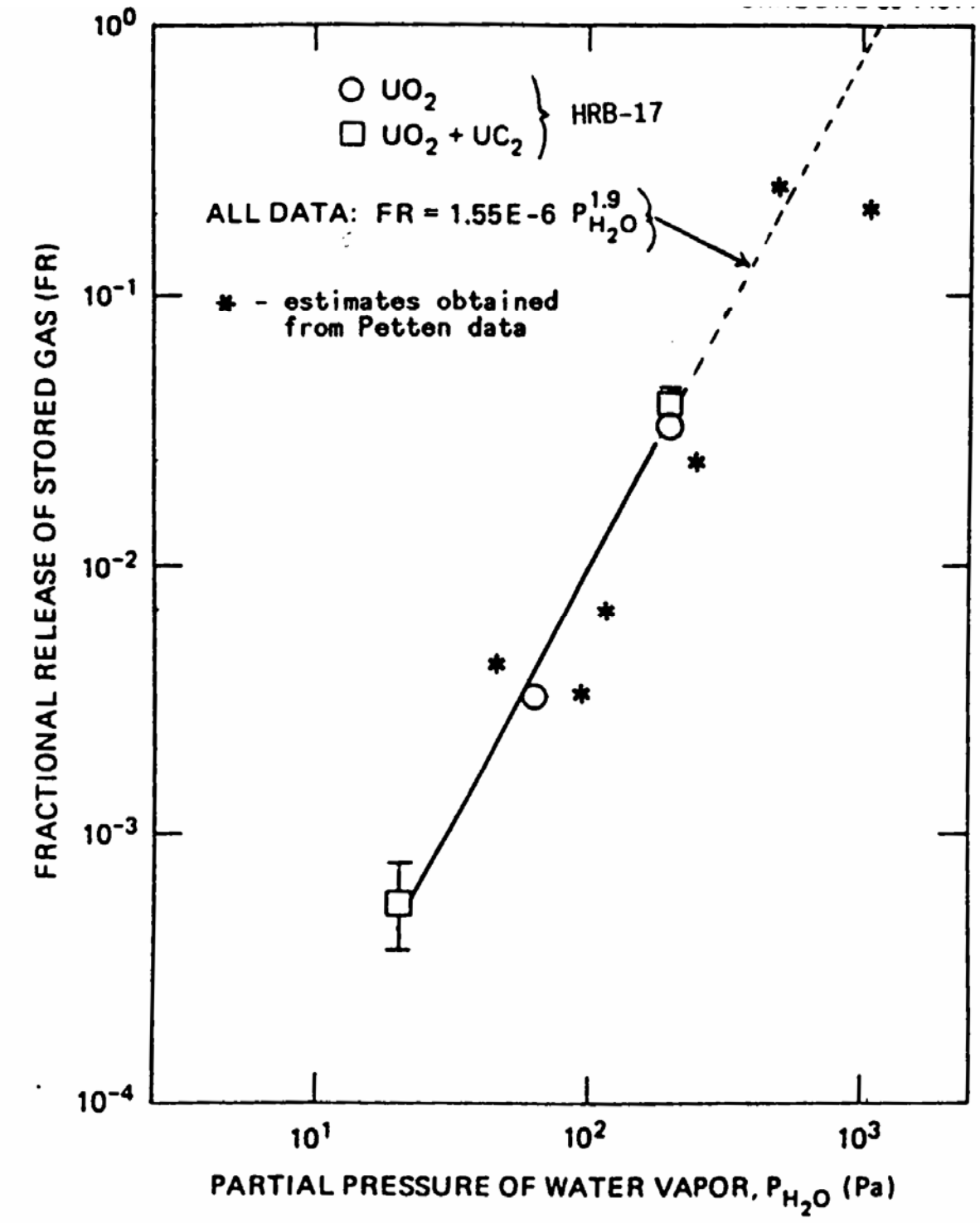

Fig. 7-3. Dependence of stored gas release on H_2O pressure

From Eqn. 7-1, it is apparent that the reaction rate is first order (i.e., linear) in reactant pressure at low reactant pressures and zero order in (i.e., independent of) reactant pressure at high reactant pressures. Of course, it is not a foregone conclusion that fuel hydrolysis would exhibit this reaction mechanism.

7.1.3.3 ORNL/TM-11846

In 1991, Myers issued a preliminary analysis of the Capsule 3 data in combination with the earlier HRB-17 data (ORNL/TM 11846, Myers 1991). He retained the same data interpretation and semi-empirical models developed earlier for HRB-17 (ORNL-6610, Myers 1991). In his modeling, he distinguished between the release of fission gas stored in bubbles and the diffusive release of fission-gas atoms. The dependence of the release of stored-fission gas on water-vapor pressure, P_{H20}, and temperature were established, taking into account the contributing mechanisms of gaseous release, the effect of graphite hydrolysis, and the requirement of consistency with experiment HRB-17 in which similar water-vapor injection tests were conducted. The dependence on P_{H20} becomes weaker as temperatures increase above 770 °C; the activation energy for release of stored-fission gas is 393 kJ/mol. Isorelease curves for the pressure-temperature plane were deduced from a derived functional relation. The stored-fission gas releases as a function of P_{H20} at a common temperature for experiments HFR-B1 and HRB-17 differ by a factor of 4. This discrepancy was attributed to the differences in fission-rate density and neutron flux between the two experiments. Diffusive release of fission gas occurred during and after the release of stored gas. The ratio of diffusive release during water-vapor injection to that prior to injection varied in contrast to the results from HRB-I7. The variation was attributed to the practice of injecting water vapor into HFR-B1 before sintering of the fuel, hydrolyzed in the previous test, was completed. The derived activation energy for diffusive release was 23.6 kJ/mol.

As shown in Fig. 7-4 (Myers 1991), Myers continued to maintain that there is a linear relation between the logarithms of the stored fission gas releases and the partial pressures of water vapor. This persists over at least three orders of magnitude in the partial pressure. Extrapolation of the calculated line in the figure would indicate complete release of the stored fission gas at a water vapor pressure of ~2 kPa, assuming the amount of stored fission gas to be a large fraction of the total gaseous inventory.

Myers acknowledged the earlier GA critique (Richards 1990) but largely dismissed it as being incomplete and overlooking too many important effects. He noted that Richards emphasized extrapolation of the gas release to water-vapor pressures beyond the experimental range (HRB-I7 and HFR-B1) and concluded that the present analysis did not provide any statistical justification for the extrapolation, which implies that the release of fission gas is independent of water-vapor pressure above 500 Pa. He stated that earlier work with UC_2 indicated that

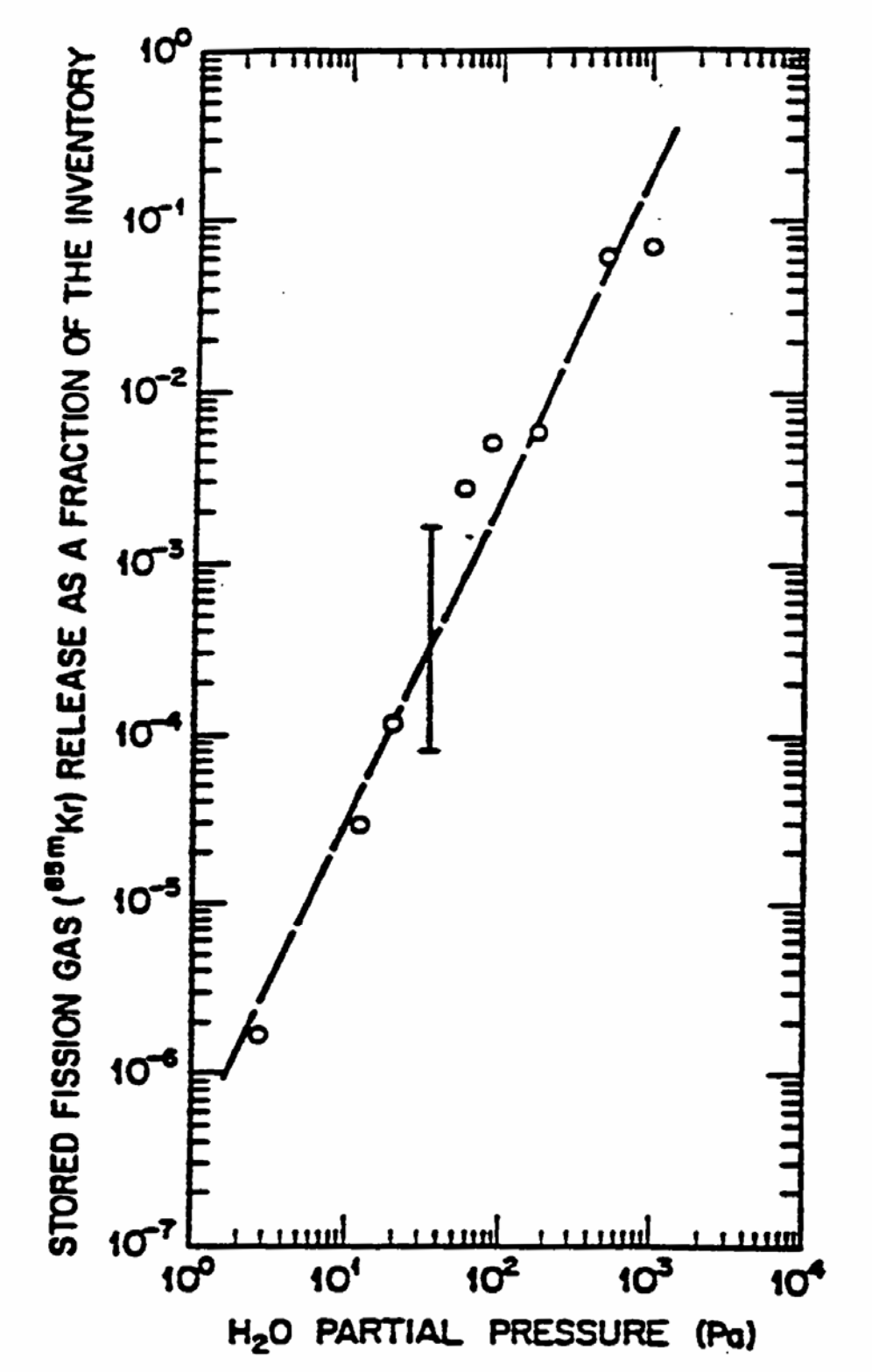

Fig. 7-4. Dependence of stored gas release on H_2O pressure (Myers 1991)

independence of the reaction rate with H_2O occurs between 1 and 10 kPa. If this result were to apply to the conditions of experiments HRB-I7 and HFR-B1, then additional experiments would be required to establish the dependence of fission gas release on water vapor pressure beyond 1 kPa.

7.1.3.4 ORNL/M-4294

In 1995, Myers issued a final evaluation of all the available hydrolysis data:

- During three irradiation experiments, HRB-17/18, HKF-K6 and HFR-B1, in which there were a known number of exposed kernels, water vapor was injected at partial pressures from 0.003 to 2.4 kPa.
- Post irradiation experiments were conducted in the KORA facility with compacts from HFR-B1, fuel spheres from irradiation in the AVR, and bare kernels from these configurations at pressures from 1 to 50 kPa.

His conclusions are largely consistent with his previous evaluations, and his earlier physical interpretations of the hydrolysis phenomena are retained. His conclusions are summarized below.

During irradiation, the general sequential response of the embedded, exposed fuel kernels to the injection of water vapor consisted of three stages: (1) a rapid transient release of fission gas with a concomitant increase in the steady-state release, (2) a period of constant steady-state release, and, upon cessation of water vapor injection, (3) a decline in the release to prehydrolysis values.

During postirradiation testing, the general sequential response was similar to that observed during irradiation but with the superposition of a general decline in release (corresponding to the decline in the fission gas inventory). The decline in release after the cessation of water vapor injection occurred much more rapidly under postirradiation than under irradiation conditions.

The primary and secondary sources of released fission gas were identified as collectives (gas bubbles) and interstitial gas atoms through evaluation of the quantity λ^{-n}~. Here λ is the decay constant and n is a measure of the relative concentrations of the isotopes of a given element. In stages 0 (prehydrolysis) and 2, n was small as observed innumerable times for diffusive release. In stage 1 where the transient release dominated, the n values were large. Large n values are associated with gas bubbles, as can be deduced by considering the net addition to and the decay of fission gas atoms within bubbles. In the postirradiation tests, such information could not be obtained because only one isotope ^{85}Kr was measurable.

The fractional transient release during irradiation was found to be the same for all isotopes of Kr and Xe (when ^{133}I was taken into account), to be dependent on a power of the water vapor pressure, the power being dependent on the temperature, and to have a large, associated

activation energy (393 kJ/mol). Transient releases were observed under post irradiation conditions, but the patterns were more complicated; these remain to be elucidated.

At 800 °C, a comparison of the irradiation and postirradiation data for the transient release shows a dependence of the release on the partial pressure of water vapor to the 1.7 power in the range 0.003 to 1 kPa and to the 0.07 power in the range 1 to 50 kPa.

The steady-state, fractional fission gas release in stage 2 is diffusive. The release can be characterized by the ratio, h_o, of the R/B during water vapor injection to that immediately preceding injection. This ratio, under irradiation conditions, is independent of the partial pressure of water vapor over the range 0.02 to 0.2 kPa and of isotopic variation. For the elements Kr and Xe, the ratio differs to the same extent as the atomic volumes of these elements differ. The ratio under postirradiation conditions has yet to be examined.

The temperature dependence of h_o differs before and during water vapor addition; the activation energy is *65.8* before and 23.6 kJ/mol during water vapor addition. By using these activation energies and the value of h_o at 680°C in experiment HFR-K6, the measured value of h_o at 767°C in experiment HFR-B1 is predicted.

During stage 3, which begins after the cessation of water vapor addition, the R/B declines. Under irradiation conditions, the characteristic time of the decline τ_c is inversely proportional to the neutron flux. Under postirradiation conditions, τ_c is much smaller than under irradiation conditions. Thermal energies govern the interaction of water-derived species under post irradiation conditions, whereas high energy depositions govern the interaction under irradiation conditions. The latter results in stronger binding and higher retentivity of the species than occurs in a thermal energy environment. Thus, it would be expected to be smaller in the thermal energy environment.

One noteworthy conclusion resulting from considering all of the hydrolysis data, including the postirradiation heating data from KORA, is not included in the above summary. As shown in Fig. 7-5, the fractional release of stored fission gases clearly becomes independent of water partial pressure above ~1 kPa as Richards had earlier argued (1990).

7.1.3.5 TECDOC-978

Section 5 of IAEA TECDOC-978, which was drafted in late 1996 and issued in 1997, provides a summary of the hydrolysis database that the more casual reader may prefer to the lengthy documents described in this section. However, the reader is advised that the 1990 critique by Richards is not cited in the TECDOC, and Fig. 7-5 does not appear in TECDOC (the other figures included here do appear) although the essential results shown in the figure are described.

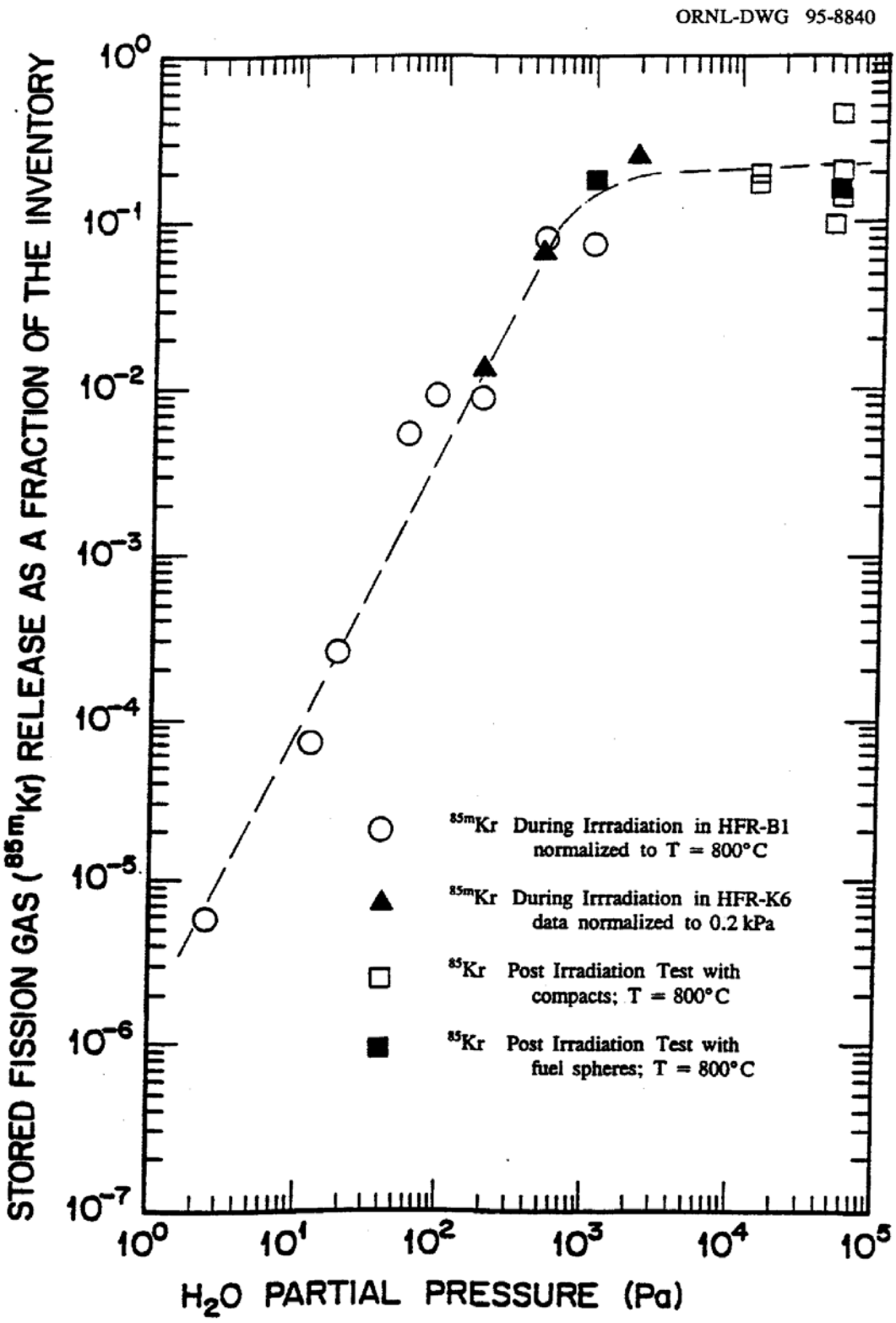

Fig. 7-5. Dependence of stored gas release on H_2O pressure (all data)

8 CONCLUSIONS

The major conclusions and recommendations resulting from a review of the HFR-B1 database in the process of preparing this summary report are listed below. The apparent "lessons learned" from the HFR-B1 experience for the planned AGR fission product transport tests (AGR-3, AGR-4, and AGR-8) are also enumerated.

8.1 Programmatic Conclusions

1. International cooperative programs for gas-cooled reactor development can be successful, but they can be programmatically challenging and need aggressive management oversight.
2. The HFR-B1 test was a major programmatic and technological success that yielded a wealth of data about fission gas release from UCO fuel particles.
3. Application of rigorous QA protocols to such cooperative programs is essential for proper test control and to assure that the test data will have the required pedigree for use in reactor design and licensing.
4. Proper archiving of test data is essential for future utilization of the test results for reactor design and licensing.
5. International shipment of irradiated nuclear materials, even in small quantities, can be subjected to prolonged delays.
6. A timely, well-planned PIE is essential for the success of fission product release (and fuel performance) experiments. The protracted delay in initiating the PIEs of the three HFR-B1 capsules caused valuable data loss, especially for 250-day Ag-110m.
7. Failure to complete and properly document the Capsule 1 PIE caused valuable data loss.
8. Failure to obtain a complete mass balance for Capsules 2 and 3, specifically, failure to leach the metal capsule components, compromised the data about fission metal transport.
9. Tomography is an acceptable analytical tool for characterizing fission product transport only if the results are properly calibrated by traditional, coring, sectioning, and counting methods.
10. Program closeouts should be expected to include responsible archiving and preservation of experimental data.

8.2 Technical Conclusions

1. Water vapor will react with the exposed UCO and UO_2 kernels in failed fuel particles and cause a significant transient increase in the fission gas release rates, including the release rates of radiologically important iodine isotopes.
2. The effect of hydrolysis on fission gas release from exposed kernels is largely reversible after the water is eliminated.
3. Large temperature increases under dry conditions also result in a transient release of stored fission gases, which has been termed an "enhanced" release. After a period of

time, this “enhanced” release diminishes, and a new steady-state release rate is established.

4. The use of a release rate-to-birth rate ratio (R/B) to characterize transient fission gas release as a result of hydrolysis or temperature increase can be misleading. These release phenomena are better characterized by the cumulative fractional release.
5. Fission gas release from LEU UCO fuel kernels is largely independent of burnup to at least 20% FIMA (despite the development of considerable macroscopic kernel porosity over that range of burnup).
6. The transport of volatile fission metals in core materials is complex, and its characterization is challenging.
7. The design of Capsule 1, while clever and imaginative, was too complex. Even if the tomography scans had been properly calibrated, it is doubtful that fundamental transport properties could have been reliably deduced from the complicated, three-dimensional concentration distributions.

8.3 Lessons Learned for the AGR FP Transport Tests

1. A well-defined fission product source is essential to characterize fission product transport in core materials. “Designed-to-fail” particles (standard fuel kernel with a thin pyrocarbon seal coat) serve that purpose well.
2. “Designed-to-fail” particles function as intended. They will fail early in the AGR irradiations based upon their behavior in HFR-B1 (and HRB-17/-18). The dtf particles can be fabricated with a thinner seal coat (10–15 μm versus the 23-μm seal used in HFR-B1 and HRB-17/-18).
3. A complete mass balance for each capsule is essential to characterize fission product transport in core materials.
4. A simple, one-dimensional test geometry is needed to characterize the transport of volatile fission metals in core materials.
5. The inclusion of a fertile particle in the AGR FP transport tests may be necessary to facilitate the maintenance of constant fuel temperatures to full burnup (i.e., >20% FIMA).
6. A timely, well-planned postirradiation examination will be essential for the success of the AGR fission product release experiments.
7. Adherence to rigorous QA protocols will be essential for proper test control; in particular, efficient protocols for disposition of inevitable nonconformances will be important.

8.4 Recommendations

1. Every effort should be made to determine the final disposition of the HFR-B1 electronic data files that were transmitted to ORNL. (At this writing, these data files have not been located.)
2. The fission-gas release data from Capsules 1 (burnup effects) and 2 (temperature effects) should be further analyzed, including a quantitative comparison of predicted gas release with the reference FDDM/F models to the measured data; and the results,

along with the other exisiting UCO gas release data, should be used to upgrade the current fission gas release models for LEU UCO particles as appropriate.

3. Further evaluation of the partial PIE data about fission metal release from Capsule 1 does not appear justified, given the limited information that has been recovered to date.

The “lessons learned” from the HFR-B1 should be factored into the design of the AGR-3, AGR-4, and AGR-8. These recommendations for the AGR tests have been made previously (Hanson 2005) and were strongly influenced by the HFR-B1 experience.

9 REFERENCES

Acharya, R., “Cesium and Silver Transport in R2-K13 Experiment,” DOE HTGR-88148, General Atomics, July 1987.

Acharya, R. T., et al., “Fuel Capsule HRB-21 Postirradiation Examination Data Report,” DOE-HTGR-100229, Oak Ridge National Laboratory, April 1995.

AGR “Technical Program Plan for the Advanced Gas Reactor Fuel Development and Qualification Program,” ORNL/TM-2002/262, Oak Ridge National Laboratory, April 2003.

Bueker, H. J., “HFR-B1 Capsule 1 Post Irradiation Examination, Progress Report 4, Subcontract No. 87X-SM415V,” IWE 1/HZ-TN-35/94, Forschungszentrum Juelich (KFA), August 1994.

Bueker, H. J., and H. Knauf, “Bohrprobennahme aus Grafitteilen der Kapsel 1 des Bestrahlungs-experimentes HFR-B1, Subcontract No. 87X-SM415V,” IWE 1/HZ-TN-12/95, Forschungszentrum Juelich (KFA), October 1995.

Burnette, R. D., Conrad, R., and T. Timke, “Quality Assurance for the HTGR Fuel Irradiation Experiment, D214.01/IHFR-BI,” Technical Memorandum, HFR/88/2478, Joint Research Centre, Petten, The Netherlands, April 1990.

Burnette, R. D., R. Conrad, and B. F. Myers, “The Operation of Experiment HFR-B1 in the Petten High Flux Reactor,” ORNL/TM-12740, Oak Ridge National Laboratory, September 1994.

Cadwallader, G. J., “SORS/NP1 Code Description and User’s Manual,” CEGA-002092, CEGA Corporation, September 1993.

Conrad, R. “Sweep Loops: System for Operation, Control and Analysis of HTR Fuel Irradiation Experiments, Project 406, Design and Safety Report,” P/10180/23, Joint Research Centre, Petten, The Netherlands, July 1980.

Conrad, R. “Irradiation Proposal for Irradiation of GA Fuel Rods-Project D214.01,” Technical Memorandum HFR/84/2194, Joint Research Centre, Petten, The Netherlands, May 20, 1985 (also GA Document 908423).

Conrad, R., R. D. Burnette, and Th. Timke, "Irradiation of GA HTGR Fuel Rods at Real Time Simulating Operating Conditions in the HFR Petten," Rev. 0, Technical Memorandum HFR/90/3082, Final Irradiation Report, Commission of the European Communities, Joint Research Center, Institute of Advanced Materials, HFR Division, Petten Establishment, The Netherlands, 1990.

Dassel, G., and H. A. Buurveld, “Gamma Spectrometry of Experiment 0214.01 GA Fuel Rods, ECN-CX-90-044,” Netherlands Energy Research Foundation ECN, Petten, The Netherlands, 1990.

De Zaaijer, D., “Kwaliteithandboek Hoge Flux Reactor," Rev. 0, ECN, Petten, The Netherlands, October 1989 *(in Dutch).*

Derz, H., and T. Flossdorf, “HFR-B1 Capsule 1, Ceramographic Examination of Coated-Particles in Fuel Rods,” Progress Report No. 5, Subcontract No. 87X-SM415V,” IWE 1/HZ-TN-37/94, Forschungszentrum Juelich (KFA), October 1994.

[Gen-IV] “A Technology Roadmap for Generation IV Nuclear Energy Systems,” GIF–002-00, Generation IV International Form, December 2002.

[GT-MHR] “Conceptual Design Report,” Int. GT-MHR 10025, Rev. 1, OKBM, November 1997.

[GT-MHR DDNs] “600 MW(t) Gas Turbine Modular Helium Reactor Design Data Needs,” DOE-GT-MHR-100217, Rev. 0, General Atomics, July 1996 (Draft).

Hanson, D. L., “A Review of Radionuclide Release from HTGR Cores during Normal Operation,” EPRI Report 1009382, Electric Power Research Institute, February 2004a.

Hanson, D. L., “The HFR-B1 Capsule 1 Data Base and Its Suitability for Use for Code Validation,” PC-000519, Rev. 0, General Atomics, May 2004b.

Hanson, D. L., Recommendations for Fission Product Transport Irradiation Tests,” PC-000527, Rev. 0, General Atomics, September 2005.

Ketema, D. J., and W. P. Voorbraak, “Neutron Metrology in the HFR, Irradiation of GA Fuel Rods, O2l4-01,” ECN-CX-91-081, Netherlands Energy Research Foundation ECN, Petten, October 1991.

Ketterer, J. W., “Capsule HFR-B1 Preirradiation Report,” HTGR-85-055, Rev. 1, GA Technologies, Inc., August 1985a.

Ketterer, J. W., “Capsule HFR-B1 Irradiation Proposal,” 908423, Rev. 0, GA Technologies, October 1985b *(proprietary information)*.

Ketterer, J. W., Capsule HFR BI Test Specification/Procedure, HTGR-86-084 (907480/N/C), GA Technologies, September 1986.

Ketterer, J. W., et al., “Capsules HRB-17/18 Final PIE Report,” 908945, Rev. N/C, GA Technologies, January 1987.

Martin, R. C., “Compilation of Fuel Performance and Fission Product Transport Models and Database for MHTGR Design,” ORNL/NPR-91/6, Oak Ridge National Laboratory, October 1993.

Medwid, W., “HFR-B1 Post-Irradiation Examination Capsule Test Specification,” DOE-HTGR-88556, Rev. A, General Atomics, May 1994.

Miller, C. M., “Background File for the FMB-3 Fuel Specification for Irradiation Experiments, 909630, Rev. N/C, General Atomics, September 1992 *(GA Proprietary Information)*.

Montgomery, F. C., and R. J. Precourt, “Test Status Report R/B Failed UCO Fuel,” 906427, Rev. 1, General Atomic Co., March 1982.

Morris, R. N., Email to D. L. Hanson, ORNL, April 20, 2006.

Myers, B. F., “Fission Gas Release,” Document No. 906555, Rev. 1, General Atomic Co., June 1982.

Myers, B. F., “HFR-B1: Proposal and Design Considerations,” GA Document No. 907551, GA Technologies, October 1984.

Myers, B. F. et al., “Capsule R2-K13; Final Report on Cells 2 and 3,” HTGR-85-068, GA Technologies Inc., September 1985.

Myers, B., The First Water Vapor Injection Tests in HFR-B1, Report ORNL/GCR-87/4, Oak Ridge National Laboratory, 1987a.

Myers, B. F., “Fuel Design Data Manual,” General Atomics Report 901866, Issue F, August 1987b *(GA Proprietary Information).*

Myers, B. F., “Experiment HFR-B1: A Preliminary Analysis of the Water Vapor Injection Experiments in Capsule 3,” Report ORNL/TM-11846, Oak Ridge National Laboratory, October 1991a.

Myers, B. F., “Plan for the Postirradiation Examination of the HFR-B1 Experiment,” ORNL/TM-11498, Oak Ridge National Laboratory, November 1991b.

Myers, B. F., “Effect of Water Vapor on the Release of Fission Gases from Uranium Oxycarbide in High-Temperature, Gas-Cooled Reactor Coated Fuel Particles,” *J. Am. Ceram, Soc*., 75 (1992) 686-693.

Myers, B. F., “Plan for the Postirradiation Examination Capsule 1 of the HFR-B1 Experiment,” ORNL/TM-12348, Oak Ridge National Laboratory, November 1993.

Myers, B. F., et al., “Interim Report on the Post Irradiation Examination of Capsules 2 and 3 of the HFR-B1 Experiment,” ORNL/M-3768, Oak Ridge National Laboratory, September 1994 (also GA Document 910828/0, June 1995).

Myers, B. F., “The Effect of Water Vapor on the Release of Fission Gas from the Fuel Elements of High-Temperature, Gas-Cooled Reactors: A Preliminary Assessment of Experiments HRB-17, HFR-B1, HFR-K6, and KORA,” Report ORNL/TM-4294, Oak Ridge National Laboratory, September 1995.

Nabielek, H., et al., Fuel Irradiation Experiments HFR-K6 and HFR-B 1 with Intermittent Water Vapor Injections, Response of Fuel, Fuel Elements and Gas-Cooled Reactor Cores Under Accidental Air and Water Ingress Conditions Proc. IAEA Technical Committee Meeting, Beijing, 1993, IAEA-TECDOC-784, Vienna, 1995, pp. 17-24.

Pfremmer, R.D., “Software Description and User’s Manual for GT-MHR Fuel Performance Code, SURVEY,” GA Document 911009/0, General Atomics, April 2002.

[PRPM] “Program Resource Procedures Manual,” 2nd ed., GA-A15466, February 2001.

[PSID] “Preliminary Safety Information Document for the Standard MHTGR,” Volumes 1-6, HTGR-84-024, Amendment B, August, 1992.

[QAM] “Quality Assurance Manual,” Rev. C, General Atomics, November 1993.

Richards, M. B., “HFR-B1 Post-Irradiation Examination Capsule Test Specification,” DOE-HTGR-88556, Rev. N/C, General Atomics, February 1994.

Richards, M. B., “Preliminary Evaluation of Petten Fuel-Hydrolysis Data” DOE-HTGR-88506, Rev. 0, September 1990.

Scheffel, W. J., and I. M. Tang, "Capsule HFR-B 1 Post-irradiation Examination Test Procedure," DOE-HTGR-88278 Issue N/C, GA Technologies Inc., March 1989.

Schenk, W., H. Kniauf, und D. Pitzer, "Spaltgasfreisetzung aus Brennstoffproben unter dem Einfluss von Feuchte," IRW-IB-6/93, Forschungszentrum Juelich GmbH (KFA), Heisse Zellen, Juni 1993 *(in German)*.

Schroeder, R., and H. Dahmen, “HFR Scan der Gammascandraehte,” IRW-TN-29/91, Forschungszentrum Juelich GmbH, October 1991.

Schroeder, R., “HFR-B1 Capsule 1 Post Irradiation Examination, Progress Report 2–15.12.1993 Subcontract No. 87X-SM415V,” IWE 1-TN-21/93, Forschungszentrum Juelich (KFA), December 1993.

Schroeder, R., I. Ruyter, and H. Dahmen, “HFR-B1 Capsule 1 Post Irradiation Examination, Progress Report 3 - 31.05.94, Subcontract No. 87X-SM415V,” IWE 1/HZ-TN-22/94, Forschungszentrum Juelich (KFA), May 1994a.

Schroeder, R., and H. Dahmen, “HFR-B1 Capsule 1, Inventory and Burnup of the Fuel Rods, Progress Report 6, Subcontract No. 87X-SM415V,” IWE 1/HZ-TN-44/94, Forschungszentrum Juelich (KFA), November 1994b.

Schroeder, R.,“HFR-B1 Capsule 1, Fission Products Outside of the Fuel Rods, Progress Report 7, Subcontract No. 87X-SM415V,” IWE 1/HZ-TN-10/95, Forschungszentrum Juelich (KFA), March 1995a.

Schroeder, R.,“HFR-B1 Capsule 1, Fission Products in the Matrix Material from the Surface of the Three Fuel Rods, Progress Report 8, Subcontract No. 87X-SM415V,” IWE 1/HZ-TN-8/95, Forschungszentrum Juelich (KFA), July 1995b.

Silady, F. A., “GT-MHR Program Closeout Packages,” PC-000466, Rev. 0, General Atomics, December 1996.

[TECDOC] “Fuel Performance and Fission Product Behavior in Gas Cooled Reactors,” IAEA-TECDOC-978, International Atomic Energy Agency, November 1997.

Tzung, F., “TRAFIC-FD, A Finite Difference Program to Compute Release of Metallic Fission Products from an HTGR Core: Code Theory and Users Manual,” CEGA-001904, CEGA Corporation, September 1992.

Tzung, F., “COPAR-FD, A Finite Difference Program to Compute Release of Metallic Fission Products from Coated Particles: Code Theory and Users Manual,” CEGA-002098, Rev. N/C, CEGA Corporation, September 1992.

Venneri, F., et al., “Deep Burn Transmutation,” GA Report No. FDO-EDO-N-TRT-X-000132, General Atomics, December 2001.

Schroeder, R., and H. Dahmen, “HFR-B1 Capsule 1, Inventory and Burnup of the Fuel Rods, Progress Report 6, Subcontract No. 87X-SM415V,” IWE 1/HZ-TN-44/94, Forschungszentrum Juelich (KFA), November 1994b.

Schroeder, R.,“HFR-B1 Capsule 1, Fission Products outside of the Fuel Rods, Progress Report 7, Subcontract No. 87X-SM415V,” IWE 1/HZ-TN-10/95, Forschungszentrum Juelich (KFA), March 1995a.

Schroeder, R.,“HFR-B1 Capsule 1, Fission Products in the Matrix Material from the Surface of the three Fuel Rods, Progress Report 8, Subcontract No. 87X-SM415V,” IWE 1/HZ-TN-8/95, Forschungszentrum Juelich (KFA), July 1995b.

Silady, F. A., “GT-MHR Program Closeout Packages,” PC-000466, Rev. 0, General Atomics, December, 1996.

[TECDOC] “Fuel Performance and Fission Product Behavior in Gas Cooled Reactors,” IAEA-TECDOC-978, International Atomic Energy Agency, November 1997.

Thomson, S. J., and G. Webb, *Heterogeneous Catalysis*, John Wiley & Sons, Inc., 1968.

Tzung, F., “TRAFIC-FD, A Finite Difference Program to Compute Release of Metallic Fission Products from an HTGR Core: Code Theory and Users Manual,” CEGA-001904, CEGA Corporation, September 1992.

Tzung, F., :COPAR-FD, A Finite Difference Program to Compute Release of Metallic Fission Products from Coated Particles: Code Theory and Users Manual,” CEGA-002098, Rev. N/C, CEGA Corporation, September 1992

Venneri, F., et al., “Deep Burn Transmutation,” GA Report No. FDO-EDO-N-TRT-X-000132, General Atomics, December 2001.

P.O. BOX 85608 SAN DIEGO, CA 92186-5608 (858) 455-3000